

Data inversion in coupled subsurface flow and geomechanics models

Marco A Iglesias¹ and Dennis McLaughlin²

¹ Mathematics Institute, University of Warwick, Coventry CV4 7AL, UK

² Department of Civil and Environmental Engineering, Massachusetts Institute of Technology, 15 Vassar St., Cambridge, MA 02139, USA

E-mail: m.a.iglesias-hernandez@warwick.ac.uk

Received 7 April 2012, in final form 23 July 2012

Published 8 October 2012

Online at stacks.iop.org/IP/28/115009

Abstract

We present an inverse modeling approach to estimate petrophysical and elastic properties of the subsurface. The aim is to use the fully coupled geomechanics-flow model of Girault *et al* (2011 *Math. Models Methods Appl. Sci.* **21** 169–213) to jointly invert surface deformation and pressure data from wells. We use a functional-analytic framework to construct a forward operator (parameter-to-output map) that arises from the geomechanics-flow model of Girault *et al*. Then, we follow a deterministic approach to pose the inverse problem of finding parameter estimates from measurements of the output of the forward operator. We prove that this inverse problem is ill-posed in the sense of stability. The inverse problem is then regularized with the implementation of the Newton-conjugate gradient (CG) algorithm of Hanke (1997 *Numer. Funct. Anal. Optim.* **18** 18–971). For a consistent application of the Newton-CG scheme, we establish the differentiability of the forward map and characterize the adjoint of its linearization. We provide assumptions under which the theory of Hanke ensures convergence and regularizing properties of the Newton-CG scheme. These properties are verified in our numerical experiments. In addition, our synthetic experiments display the capabilities of the proposed inverse approach to estimate parameters of the subsurface by means of data inversion. In particular, the added value of measurements of surface deformation in the estimation of absolute permeability is quantified with respect to the standard history matching approach of inverting production data with flow models. The proposed methodology can be potentially used to invert satellite geodetic data (e.g. InSAR and GPS) in combination with production data for optimal monitoring and characterization of the subsurface.

(Some figures may appear in colour only in the online journal)

1. Introduction

The consolidation of the subsurface due to pumping and withdrawal of fluids has been widely studied in the last few decades [10–12, 29]. It is well known, for example, that the production of oil and gas may cause subsidence of the ground surface above the reservoir wells [12]. Subsidence can potentially damage the infrastructure of wells and surrounding facilities. In order to prevent damage and to assess the environmental impact of hydrocarbon recovery, the surface deformation caused by a given production scenario must be accurately predicted. Modeling geomechanical effects coupled to subsurface flow is also essential for determining the environmental impact on applications such as groundwater withdrawal, CO₂ sequestration and underground gas storage. More recently [21, 20, 23], it has been recognized that efficient coupling between geomechanical effects and subsurface flow is also relevant for accurate flow predictions. In particular, for enhanced oil recovery, an accurate prediction of subsurface flow is required to develop optimal production strategies. Due to the environmental and economical relevance of the aforementioned applications, developing coupled geomechanics and subsurface flow models has become a priority for the geophysical community [37, 13, 33–35].

A model that couples geomechanics with subsurface flow can be thought as a mapping $F : \mathcal{K} \rightarrow \mathcal{O}$ defined on a set of admissible parameters \mathcal{K} that represent petrophysical and mechanical properties of the subsurface. The range of F is contained in the space of possible physical data \mathcal{O} . For a given parameter (subsurface properties) $\mathbf{Y} \in \mathcal{K}$, the corresponding $F(\mathbf{Y})$ is the model prediction of measurements that we may compare to real observations from the physical system. However, due to lack of direct information, it is not possible to assume that \mathbf{Y} can be given. More precisely, subsurface properties can only be measurements from core samples collected at a few locations. Simple interpolation of those measurements may not capture the highly heterogeneous structure inherent to subsurface properties. Then, unreliable predictions $F(\mathbf{Y})$ will be obtained from an inaccurate \mathbf{Y} . Fortunately, satellite and smart-well technology can provide accurate measurements of the geomechanical and flow dynamics. In other words, information about $F(\mathbf{Y})$ may be available from measurements. Therefore, given $F(\mathbf{Y})$, it is natural to pose the inverse problem (IP) of finding \mathbf{Y} . In this paper, we study this IP of estimating subsurface properties of given data from a coupled geomechanics-flow model.

1.1. Literature review

There is a vast literature on coupled geomechanics-flow models with the main focus on predicting land surface deformation due to subsurface fluid flow [9–12, 29]. These approaches are mainly based on the theory of poroelasticity [3, 38]. A general poroelasticity formulation yields a fully coupled three-dimensional PDE-based model whose numerical solution may be computationally burdensome. Several simplifications of poroelastic models of land deformation were proposed in the early work of [29, 9, 10]. In [29], for example, the reservoir is treated as an inclusion of an elastic half-space. In this approach, an analytical solution is utilized to evaluate the elastic response due to subsurface flow. In some poroelastic models such as [25, 33], the effect of the mechanical deformation of the rock is simplified so that a standard reservoir simulator can be utilized to model the reservoir variables (e.g. pressure). This in turn can be used as a source term in the elasticity equations for the reservoir/aquifer and its adjacent rock. However, ignoring or oversimplifying the full coupling between flow and geomechanics gives rise to lack of accuracy in reservoir modeling. The reservoir simulation community has therefore established ongoing efforts to develop efficient numerical methods

to solve coupled geomechanics-flow models. In particular, in this paper we consider the model introduced in [13] that describes the full coupling between the pore pressure p of a single-phase reservoir flow and the displacement \mathbf{u} caused by the mechanical deformation of the subsurface. This type of fully coupled model is therefore relevant for the subsurface applications described at the beginning of this section. Moreover, it provides a relatively simple yet realistic prototypical model that possesses theoretical and practical features of the standard coupling between geomechanics and flow. By using the coupled geomechanics-flow model of [13], the aim of our work is to construct the mapping F mentioned above, and develop the corresponding inversion to recover subsurface properties from pressure data p collected at wells and the deformation \mathbf{u} measured at the land surface.

While modeling coupled geomechanics-flow models has evolved significantly in the last years, the analysis and implementation of the corresponding inverse models are still in early stages. Recent progress of smart-well technology has led to numerous techniques capable of inverting production data from wells for estimating rock properties in reservoir models [26]. However, only a few attempts have been made to jointly invert data from wells and land surface deformation in coupled geomechanics-flow models. Clearly, the past absence of measurement technologies provided little motivation to develop data inversion techniques for geomechanics-flow models. Fortunately, the recent developments of the global positioning system (GPS) and the interferometric synthetic aperture radar (InSAR) technology provide accurate measurements of land deformation. Combining these types of geodetic measurements with production data from wells, motivated the approach of Vasco *et al* [37] for the estimation of permeability. To the best of our knowledge, [37] provides the basis for most recent approaches to data inversion for the estimation of subsurface properties in coupled geomechanics-flow models [34–36]. For this reason in the following lines we briefly describe the main aspects of their approach so the differences with our work become clear.

The model used in Vasco *et al* [37] is a semi-analytic coupled geomechanics-flow model where the elastic domain is a homogeneous half-space. Under this geometrical consideration, an analytical Green's function is available and the model simplifies considerably. The goal of [37] is to invert both pressure p from wells, and deformation \mathbf{u} at the surface, to estimate the absolute permeability K of a reservoir. Their approach considers a discretized system of equations of the form

$$F_{e,1}\mathbf{P} + F_{e,2}\mathbf{U} = 0, \quad (1)$$

$$F_{f,1}(\mathbf{P})\mathbf{K} + F_{f,2}\mathbf{U} = 0, \quad (2)$$

where $F_{e,i}$ and $F_{f,i}$ denote the matrices corresponding to the discretizations of the differential operators in the elasticity and the flow equations, respectively. \mathbf{P} , \mathbf{U} and \mathbf{K} denote the discretizations of p , \mathbf{u} and K , respectively. The discretized flow problem (2) is formulated as a system in terms of the absolute permeability \mathbf{K} with a matrix $F_{f,1}(\mathbf{P})$ that depends on \mathbf{P} . In other words, the standard Darcy's law term $-\nabla \cdot (K\nabla p)$ is discretized as $F_{f,1}(\mathbf{P})\mathbf{K}$. The strategy of [37] to estimate \mathbf{K} in (1) and (2) is the following. First, measurements of \mathbf{u} (at the land surface) and p (from wells) are 'inverted' to estimate \mathbf{P} at every location of the reservoir. In other words, \mathbf{P} in the elasticity equation (1) is treated as a parameter which is estimated through a least-squares approach. Then, the inverted \mathbf{P} is used back in (1) to compute \mathbf{U} . The resulting \mathbf{U} and the previously inverted \mathbf{P} are used to estimate the permeability \mathbf{K} in (2). The matrices $F_{e,i}$ and $F_{f,i}$ in (1) and (2) are ill-conditioned, and therefore the numerical implementation of the aforementioned two-step inversion procedure of Vasco *et al* [37] suffers from severe numerical instabilities. They proposed an *ad hoc* Tikhonov-type regularization to address the ill-posedness of the inversion in (1) and (2). Encouraging results for finding estimates of absolute permeability have been obtained with the implementation of the approach

of Vasco *et al* [37]. As we mentioned earlier, estimating unknown subsurface properties is a relevant task in geophysics applications. Therefore, [37] provides interesting ground for further investigations of the technique for estimating subsurface properties by means of data inversion in the coupled geomechanics-flow model. In this work, we take a step further by considering the more general geomechanics-flow model of [13] and developing a rigorous, robust and computationally efficient implementation of a data inversion technique for the estimation of subsurface properties.

1.2. Contribution of this work

We develop a mathematical framework and computational implementation for inverting data in the coupled geomechanics-flow model of [13]. Our approach consists of constructing a Hilbert space formulation of a differentiable forward operator F as above. In other words, F is the parameter-to-output operator that results from the coupled geomechanics-flow model of [13]. The IP of estimating subsurface properties \mathbf{Y} from data \mathbf{d} of surface deformation and well pressure is formulated as an equation $F(\mathbf{Y}) = \mathbf{d}$. By proving that the forward operator F is compact and weakly closed, the ill-posedness of the IP is exhibited. In order to regularize this IP, we propose the application of the truncated Newton-conjugate gradient (CG) algorithm proposed in [15]. Under assumptions of F , we use the theory of [15] to prove convergence and regularizing properties of the Newton-CG scheme. The differentiability of F and characterization of the corresponding adjoint operator are also proved. The theoretical results of this paper intend to expose the ill-posedness of the IP and promote the application of techniques that have been rigorously established for the solution of nonlinear ill-posed inverse problems.

We present numerical examples that show the numerical evidence of convergence and regularizing properties of the proposed application of the Newton-CG scheme. More precisely, the effect of the noise level and the parameters in the discrepancy principle are illustrated. Moreover, we display a set of experiments to show the practical relevance of the proposed approach to find estimates of subsurface properties by means of data inversion in coupled geomechanics-flow models. In particular, we focus on the estimation of the absolute permeability of reservoirs. Estimating this type of rock property is the typical IP addressed by the reservoir simulation community. However, in most techniques only measurements of the flow model (e.g. pressure from wells) are inverted. In our experiments, we show that the estimation of the absolute permeability can be significantly improved by inverting both pressure data from wells and surface deformation. Comparing the added value of inverting measurements of surface deformation for the estimation of the absolute permeability of reservoirs is a substantial contribution of our approach.

Our implementation and results differ from [37] in the following aspects. (1) We elaborate a general functional analytical framework of the IP. Then, in principle, any discretization can be considered including the one in [37]. (2) We consider the general case where no semi-analytical solution is utilized. While this approach is computationally more challenging, we promote computational efficiency by implementing state-of-the-art coupling techniques. (3) We propose a one-step inversion of the coupled geomechanics-flow model. In our framework, the artificial pressure estimation (first step of the inversion in [37]) is avoided. (4) Our approach allows the estimation of both petrophysical and elastic properties. In particular, we present the results for the estimation of absolute permeability and one of the moduli of elasticity. (5) We quantify the added value of measurements of surface deformation with respect to inverting only pressure data from wells.

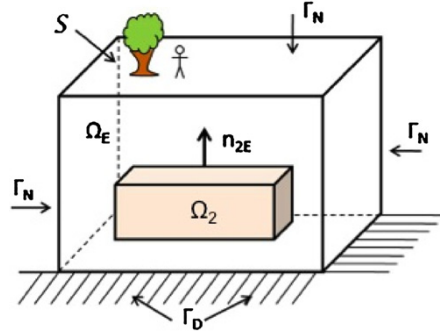


Figure 1. Geometry.

1.3. Outline

In section 2.1, we introduce the coupled geomechanics-flow model of [13]. Preliminary definitions are presented in section 2.2. The set of admissible parameters is defined in section 2.3. The forward operator and its differentiability are established in section 2.4. In section 3, the IP on F is formulated. In section 3.1, the ill-posedness of the IP is exposed. The Newton-CG algorithm utilized for the regularization of the IP is presented in section 3.1. The convergence and regularizing properties of this Newton-CG scheme are discussed in section 3.2. The characterization of the adjoint of the linearization of F is provided in section 3.3. In section 4.1, we discuss the numerical implementation of the inverse methodology. Numerical experiments are presented in section 4.2. Final conclusions are provided in section 4.3. The proofs of the theoretical results of this paper are displayed in the appendices of section 5.

2. The forward model

In the following section, we briefly describe the model following very closely the presentation of [13]. This model is then utilized in section 3 to construct the mapping F whose inversion is treated in the rest of this paper.

2.1. The geomechanics-flow prototypical model

The physical domain of the reservoir is a three-dimensional set denoted by Ω_2 . The reservoir is a poroelastic material whose dilation and shear moduli of elasticity are denoted by λ_R and μ_R , respectively. The absolute permeability of the reservoir is assumed diagonal $\mathbf{K} = K\mathbf{I}$. Single-phase Darcy's flow is considered through the reservoir. The fluid is considered slightly compressible and its viscosity is denoted by ν . As indicated in figure 1, the reservoir is surrounded by a non-reservoir elastic rock denoted by Ω_E . We denote by λ_E and μ_E the dilation and shear moduli of elasticity of Ω_E . We assume that Ω_2 and Ω_E are connected open bounded sets such that $\Omega_2 \cap \Omega_E = \emptyset$. We denote by b and M , the Biot's moduli and Biot's constant, respectively. We denote by $[0, T]$ the time window of interest for some final time $T > 0$. The model is the following interface problem [13]:

$$-\nabla \cdot [\lambda_R(\nabla \cdot \mathbf{u})\mathbf{I} + 2\mu_R\epsilon(\mathbf{u}) - bp\mathbf{I}] = 0, \quad \text{in } \Omega_2 \times (0, T], \quad (3)$$

$$\frac{1}{M} \frac{\partial p}{\partial t} - \nabla \cdot \nu^{-1} K \nabla p + b \frac{\partial}{\partial t} [\nabla \cdot \mathbf{u}] - q = 0, \quad \text{in } \Omega_2 \times (0, T], \quad (4)$$

$$-\nabla \cdot [\lambda_E(\nabla \cdot \mathbf{u})\mathbf{I} + 2\mu_E\boldsymbol{\epsilon}(\mathbf{u})] = \mathbf{f}, \quad \text{in } \Omega_E \times (0, T], \quad (5)$$

where q is the source/sink term, \mathbf{f} is a body force acting on Ω_E , $\mathbf{u} \in \mathbb{R}^n$ ($n = 2, 3$) is the displacement field and p is the pore pressure. In (3) and (5), the linearized strain tensor $\boldsymbol{\epsilon}$ is defined by

$$\boldsymbol{\epsilon}(\mathbf{u}) = \frac{1}{2}(\nabla\mathbf{u} + \nabla^T\mathbf{u}). \quad (6)$$

Problem (3)–(5) requires interface conditions between Ω_2 and Ω_E . For simplicity, we consider the case where the interface between Ω_2 and Ω_E coincides with $\partial\Omega_2$. The following interface conditions are then prescribed across $\partial\Omega_2$:

$$[\mathbf{u}] = 0, \quad [(\lambda(\nabla \cdot \mathbf{u})\mathbf{I} + 2\mu\boldsymbol{\epsilon}(\mathbf{u}))\mathbf{n}] = b p \mathbf{n}, \quad (7)$$

where \mathbf{n} is the outward normal vector to $\partial\Omega_2$ and the jump through $\partial\Omega_2$ of a function $w : \Omega_2 \cup \Omega_E \rightarrow \mathbb{R}$ is defined by $[w] = (w|_{\Omega_2} - w|_{\Omega_E})|_{\partial\Omega_2}$. We define

$$\Omega_1 = \Omega_E \cup \overline{\Omega_2} \quad (8)$$

and assume that $\partial\Omega_1 = \Gamma_D \cup \Gamma_N$, where Γ_D has positive measure. The problem is furnished with the following boundary conditions:

$$-v^{-1}K\nabla p \cdot \mathbf{n} = 0, \quad \text{on } \partial\Omega_2 \times (0, T], \quad (9)$$

$$\mathbf{u} = 0, \quad \text{on } \Gamma_D \times (0, T], \quad (10)$$

$$(\lambda_E(\nabla \cdot \mathbf{u})\mathbf{I} + 2\mu_E\boldsymbol{\epsilon}(\mathbf{u}))\mathbf{n} = \boldsymbol{\sigma}_N(x, t), \quad \text{on } \Gamma_N \times (0, T]. \quad (11)$$

For simplicity, no-flow boundary conditions (equation (9)) have been imposed on the reservoir domain Ω_2 . Initial conditions are also required:

$$p(x, 0) = p_0(x), \quad \text{in } \Omega_2, \quad (12)$$

$$\mathbf{u}(x, 0) = \mathbf{u}_0(x), \quad \text{in } \Omega_1. \quad (13)$$

Note that (3)–(13) is a fully coupled model between $p(x, t)$ and $\mathbf{u}(x, t)$. The solution to (3)–(13) yields the pore pressure field $p(x, t)$ defined on $\Omega_2 \times (0, T]$ and the displacement vector field $\mathbf{u}(x, t)$ on $\Omega_1 \times (0, T]$. These two predicted variables can be compared with observed quantities in the field. The dependent variable p can be typically measured at the locations of the injection/production wells. Analogously, \mathbf{u} is usually measured on the land surface that we denote by \mathcal{S} . Let us assume now that there are N injection/production wells located at $\{x_i\}_{i=1}^N$. Furthermore, we assume that fluid viscosity v is given. From the previous discussion, it follows that the physical problem defines the parameter-to-output mapping F :

$$(M, b, K, \lambda_R, \lambda_E, \mu_R, \mu_E) \xrightarrow{F} (\{p(x_i, t)\}_{i=1}^N, \mathbf{u}(x, t)|_{\mathcal{S}}), \quad (14)$$

where p and \mathbf{u} are the solutions to (3)–(13) for a given set of rock properties (b, M, K) and mechanical properties $(\lambda_R, \lambda_E, \mu_R, \mu_E)$. As we indicated earlier, the subsurface parameters $(b, M, K, \lambda_R, \lambda_E, \mu_R, \mu_E)$ may be difficult to characterize from direct measurements. In the rest of this section, we construct the analytical framework to properly define the forward operator F . Then, in section 3 we develop a mathematical and computational framework to find an ‘inverse’ of F . In other words, we propose a methodology for estimating rock and elastic properties from measurements of pressure from wells and deformations at the surface.

2.2. Preliminary definitions

We start with some preliminary definitions. For $i \in \{1, 2\}$, $[0, T]$ as before and any Hilbert space X , we define the following norms:

$$\|u\|_{H^k(\Omega_i)} \equiv \left(\sum_{|\alpha| \leq k} \int_{\Omega_i} |D^\alpha u|^2 \right)^{1/2}, \quad (15)$$

$$\|u\|_{H^k(0,T;X)} \equiv \left(\sum_{|\alpha| \leq k} \int_0^T \|D^\alpha u(t)\|_X^2 \right)^{1/2}, \quad (16)$$

$$\|u\|_{L^\infty(0,T;X)} \equiv \sup_{t \in [0,T]} \|u(t)\|_X, \quad (17)$$

where $k \in \mathbb{N}$, $k < \infty$. We consider the spaces $H^k(\Omega_i)$, $H^k(0, T; X)$ and $L^\infty(0, T; X)$ with the norms defined above (15)–(17) [8, chapter 5]. We additionally consider the space $C^k(\overline{\Omega}_i)$ as defined in [1], with norm

$$\|u\|_{C^k(\Omega_i)} \equiv \max_{|\alpha| \leq k} \sup_{x \in \Omega_i} |D^\alpha u|. \quad (18)$$

Let Γ be a subset of $\partial\Omega_1$. Let $\gamma_\Gamma : H^1(\Omega_1) \rightarrow L^2(\Gamma)$ be the trace operator on Γ , i.e. γ_Γ is the unique continuous linear operator such that $\gamma_\Gamma(v) = v|_\Gamma$ for all $v \in C^\infty(\Omega_1)$. Let us define $\mathcal{Y}_\Gamma(\mathbf{v}) \equiv (\gamma_\Gamma(v^1), \gamma_\Gamma(v^2), \gamma_\Gamma(v^3))$. From continuity of γ_Γ , there exists a positive constant C_Γ that depends only on Ω_1 , such that for every $\mathbf{v} \in H^1(\Omega_1)^3$,

$$\|\mathcal{Y}_\Gamma(\mathbf{v})\|_{L^2(\Gamma)^3} \leq C_\Gamma \|\mathbf{v}\|_{H^1(\Omega_1)^3}. \quad (19)$$

We furthermore define

$$\mathbf{H}_0 \equiv \{\mathbf{w} \in (H^1(\Omega_1))^3 : \mathcal{Y}_{\Gamma_D}(\mathbf{w}) = 0\}, \quad (20)$$

$$\mathcal{W} \equiv \mathbf{H}_0 \times H^1(\Omega_2), \quad (21)$$

and

$$\mathcal{H} \equiv H^1(0, T; \mathbf{H}_0) \times [H^1(0, T; L^2(\Omega_2)) \cap L^2(0, T; H^2(\Omega_2)) \cap L^\infty(0, T; H^1(\Omega_2))]. \quad (22)$$

The spaces \mathcal{W} and \mathcal{H} are equipped with the maximum norm, i.e.

$$\begin{aligned} \|(\mathbf{u}, p)\|_{\mathcal{H}} &\equiv \max \{ \|\mathbf{u}\|_{H^1(0,T;H^1(\Omega_1)^3)}, \|p\|_{H^{2,1}(\Omega_2 \times [0,T])}, \|p\|_{L^\infty(0,T;H^1(\Omega_2))} \}, \\ \|(\mathbf{w}, w)\|_{\mathcal{W}} &\equiv \max \{ \|\mathbf{w}\|_{H^1(\Omega_1)^3}, \|w\|_{H^1(\Omega_2)} \}, \end{aligned} \quad (23)$$

where

$$\|p\|_{H^{2,1}(\Omega_2 \times [0,T])} = \left(\|p\|_{L^2(0,T;H^2(\Omega_2))}^2 + \|p\|_{H^1(0,T;L^2(\Omega_2))}^2 \right)^{\frac{1}{2}}. \quad (24)$$

For any $\hat{\mathbf{Y}} \in \mathcal{K}$ and $r > 0$, we define $B(\hat{\mathbf{Y}}, r) \equiv \{\mathbf{Y} \in \mathcal{K} : \|\mathbf{Y} - \hat{\mathbf{Y}}\|_{\mathcal{K}} \leq r\}$. Finally, adopting a repeated index notation, we define the contraction operator of two second-order tensors \mathbf{a} and \mathbf{b} by $\mathbf{a} : \mathbf{b} \equiv a_{ij}b_{ij}$.

2.3. The admissible set of parameters

The main objective of this work is to implement a data inversion methodology for finding estimates of rock and mechanical properties of reservoirs. For the model defined in section 2.1 those properties are comprised of $\{b, M, K, \lambda, \mu\}$ where $\lambda : \Omega_1 \rightarrow \mathbb{R}^+$ and $\mu : \Omega_1 \rightarrow \mathbb{R}^+$ are defined by

$$\lambda \equiv \lambda_E + \chi_R(\lambda_R - \lambda_E), \quad \mu \equiv \mu_E + \chi_R(\mu_R - \mu_E), \quad (25)$$

and χ_R is the characteristic function of Ω_2 defined by

$$\chi_R \equiv \begin{cases} 1 & \text{if } x \in \Omega_2, \\ 0 & \text{if } x \in \Omega_1 - \Omega_2. \end{cases} \quad (26)$$

For simplicity, in the following we assume that b , M and μ are known and we consider only the estimation of K , the permeability of the reservoir (recall $K : \Omega_2 \rightarrow \mathbb{R}^+$), as well as the dilation modulus λ of elasticity. Due to the lack of direct measurements, the estimation of the absolute permeability of reservoirs constitutes the main focus of the literature in data inversion (data assimilation) for subsurface modeling [26]. However, the mechanical properties of the subsurface are also difficult to characterize from direct measurements. It is therefore relevant to consider a technique capable of providing estimates of both petrophysical (K) and mechanical (λ) properties. It is worth mentioning that the present framework can be extended to include also the estimation of b , M and μ .

Since λ and K are positive variables, we introduce the following parametrization:

$$\lambda = e^{\Upsilon_1}, \quad K = e^{\Upsilon_2}. \quad (27)$$

Available prior knowledge may now be utilized to define the set of admissible parameters where estimates (Υ_1, Υ_2) will be sought. Prior knowledge is typically available in terms of geostatistical information. For this reason, we assume that we are given covariance functions $\mathbf{C}_{\Upsilon_i} : \Omega_i \times \Omega_i \rightarrow \mathbb{R}$ ($i \in \{1, 2\}$). Even though this work is deterministic, the knowledge of these covariance functions can be used to enforce regularity of the admissible set of parameters. More precisely, consider covariance-based inner products

$$\langle \Upsilon_i, \tilde{\Upsilon}_i \rangle_{\mathcal{K}_i} \equiv \int_{\Omega_i} \int_{\Omega_i} \Upsilon_i(x) \mathbf{C}_{\Upsilon_i}^{-1}(x, x') \tilde{\Upsilon}_i(x') dx dx' \quad (28)$$

for $i \in \{1, 2\}$, where $\mathbf{C}_{\Upsilon_i}^{-1}$ is the formal inverse of \mathbf{C}_{Υ_i} defined by

$$\int_{\Omega_i} \int_{\Omega_i} \mathbf{C}_{\Upsilon_i}^{-1}(x, x') \mathbf{C}_{\Upsilon_i}(x', y) dx' = \delta(x - y). \quad (29)$$

Under certain assumptions on the covariance functions, inner products like (28) induce covariance-based norms equivalent to Sobolev norms (see [32, section 7.2.1] and [39]). For the present application, we require covariance functions such that the following equivalence is valid:

$$\|\cdot\|_{\mathcal{K}_1} \equiv |\langle \cdot, \cdot \rangle_{\mathcal{K}_1}|^{1/2} \cong \|\cdot\|_{H^2(\Omega_1)} \quad \text{and} \quad \|\cdot\|_{\mathcal{K}_2} \equiv |\langle \cdot, \cdot \rangle_{\mathcal{K}_2}|^{1/2} \cong \|\cdot\|_{H^3(\Omega_2)}. \quad (30)$$

Let \mathcal{K}_1 and \mathcal{K}_2 be the Sobolev spaces $H^2(\Omega_1)$ and $H^3(\Omega_2)$ equipped with the covariance-based norms defined in (28). We now define the admissible set of parameters

$$\mathcal{K} \equiv \mathcal{K}_1 \times \mathcal{K}_2 \quad (31)$$

with norm defined by

$$\|\cdot\|_{\mathcal{K}} \equiv \left[\|\cdot\|_{\mathcal{K}_1}^2 + \kappa \|\cdot\|_{\mathcal{K}_2}^2 \right]^{1/2}, \quad (32)$$

where $\kappa > 0$ is a factor that can be chosen to impose the relative weight of the subsurface properties based on prior knowledge. From standard Sobolev embeddings, it follows easily that $\mathcal{K}_1 \hookrightarrow C(\overline{\Omega_1})$ and $\mathcal{K}_2 \hookrightarrow C^1(\overline{\Omega_2})$. Therefore, there exists a constant $C_e > 0$ such that

$$\|\Upsilon_1\|_{C(\Omega_1)} \leq C_e \|\Upsilon_1\|_{\mathcal{K}_1}, \quad \|\Upsilon_2\|_{C^1(\Omega_2)} \leq C_e \|\Upsilon_2\|_{\mathcal{K}_2} \quad (33)$$

for all $(\Upsilon_1, \Upsilon_2) \in \mathcal{K}$ where C_e depends only on the geometry of Ω_1 and Ω_2 . Therefore, under the assumptions on the prior knowledge imposed with (30), the set of admissible parameters (31) enforces the regularity: $(\lambda, K) \in C(\overline{\Omega_1}) \times C^1(\overline{\Omega_2})$. This choice of regularity is required for the subsequent analysis of the forward operator. However, we recognize that rock properties are typically discontinuous due to the presence of multiple lithofacies. Nevertheless, this work, which corresponds to the single-lithofacie case, can be potentially combined with approaches for the inversion of multiple lithofacies such as the one presented in [18].

2.4. The forward operator

We now formally derive the variational form of the PDE interface problem (3)–(13). Equations (3) and (5) are multiplied by an arbitrary $\mathbf{w} \in \mathbf{H}_0$. Then, we integrate by parts, use (10)–(11), add the resulting equations and use (25) to find

$$\int_{\Omega_1} \lambda(\nabla \cdot \mathbf{u})(\nabla \cdot \mathbf{w}) + 2\mu\boldsymbol{\epsilon}(\mathbf{u}) : \boldsymbol{\epsilon}(\mathbf{w}) - \int_{\Omega_2} bp\nabla \cdot \mathbf{w} = \int_{\Gamma_N} \boldsymbol{\sigma}_N \cdot \mathbf{w} + \int_{\Omega_1} \mathbf{f} \cdot \mathbf{w}. \quad (34)$$

Multiplying (4) by a test function $w \in H^1(\Omega_2)$, integrating by parts and using (9) yields

$$\int_{\Omega_2} \frac{1}{M} \frac{\partial p}{\partial t} w + \int_{\Omega_2} v^{-1} K \nabla p \cdot \nabla w + \int_{\Omega_2} b \frac{\partial(\nabla \cdot \mathbf{u})}{\partial t} w = \int_{\Omega_2} qw. \quad (35)$$

It is important to ensure that the initial condition for the displacement \mathbf{u}_0 (13) is consistent with (12) and (34). We therefore assume that \mathbf{u}_0 is the solution to

$$\int_{\Omega_1} \lambda(\nabla \cdot \mathbf{u}_0)(\nabla \cdot \mathbf{w}) + 2\mu\boldsymbol{\epsilon}(\mathbf{u}_0) : \boldsymbol{\epsilon}(\mathbf{w}) - \int_{\Omega_2} bp_0\nabla \cdot \mathbf{w} = \int_{\Gamma_N} \boldsymbol{\sigma}_{N,0} \cdot \mathbf{w} + \int_{\Omega_1} \mathbf{f}_0 \cdot \mathbf{w}, \quad (36)$$

where $\boldsymbol{\sigma}_{N,0}(x) \equiv \boldsymbol{\sigma}_N(x, 0)$ and $\mathbf{f}_0(x) \equiv \mathbf{f}(x, 0)$. Let us define

$$\delta\mathbf{u} \equiv \mathbf{u} - \mathbf{u}_0, \quad \delta\mathbf{f} \equiv \mathbf{f} - \mathbf{f}_0, \quad \delta\boldsymbol{\sigma}_N \equiv \boldsymbol{\sigma}_N - \boldsymbol{\sigma}_{N,0}. \quad (37)$$

From (10), (34) and (36) it follows that $\delta\mathbf{u}$ satisfies

$$\delta\mathbf{u} = 0 \quad \text{in } \Omega_1 \times \{0\}, \quad \delta\mathbf{u} = 0 \quad \text{in } \Gamma_D \times (0, T], \quad (38)$$

and

$$\int_{\Omega_1} \lambda(\nabla \cdot \delta\mathbf{u})(\nabla \cdot \mathbf{w}) + 2\mu\boldsymbol{\epsilon}(\delta\mathbf{u}) : \boldsymbol{\epsilon}(\mathbf{w}) - \int_{\Omega_2} b[p - p_0]\nabla \cdot \mathbf{w} = \int_{\Gamma_N} \delta\boldsymbol{\sigma}_N \cdot \mathbf{w} + \int_{\Omega_1} \delta\mathbf{f} \cdot \mathbf{w}. \quad (39)$$

Since $\nabla \cdot \mathbf{u}_0$ is time independent, the equation for pressure remains the same with \mathbf{u} replaced by $\delta\mathbf{u}$. For ease in the notation, in the rest of the document we use \mathbf{u} instead of $\delta\mathbf{u}$ and \mathbf{f} instead of $\delta\mathbf{f}$. For simplicity, we consider $\boldsymbol{\sigma}_N$ time independent, i.e. $\boldsymbol{\sigma}_N - \boldsymbol{\sigma}_{N,0} = 0$. We define $L : \mathcal{K}_1 \times \mathcal{U} \times \mathbf{H}_0 \rightarrow \mathbb{R}$ by

$$L(\Upsilon_1, \mathbf{u}, \mathbf{w}) = \int_{\Omega_1} e^{\Upsilon_1} (\nabla \cdot \mathbf{u})(\nabla \cdot \mathbf{w}) + 2\mu\boldsymbol{\epsilon}(\mathbf{u}) : \boldsymbol{\epsilon}(\mathbf{w}). \quad (40)$$

The variational formulation of the models (35) and (39) can be posed as in the following definition.

Definition 2.1 (Variational model). *Given $\Upsilon \in \mathcal{K}$, find $\mathbf{h}(\Upsilon) \equiv (\mathbf{u}, p) \in \mathcal{H}$ such that $\mathbf{u}(\cdot, 0) = 0$, $p(\cdot, 0) = p_0$ and*

$$L(\Upsilon_1, \mathbf{u}, \mathbf{w}) - \int_{\Omega_2} b[p - p_0]\nabla \cdot \mathbf{w} = \int_{\Omega_1} \mathbf{f} \cdot \mathbf{w}, \quad (41)$$

$$\int_{\Omega_2} \frac{1}{M} \frac{\partial p}{\partial t} w + \int_{\Omega_2} v^{-1} e^{\Upsilon_2} \nabla p \cdot \nabla w + \int_{\Omega_2} b \frac{\partial(\nabla \cdot \mathbf{u})}{\partial t} w = \int_{\Omega_2} qw, \quad (42)$$

a.e. in $(0, t)$, for all $(\mathbf{w}, w) \in \mathcal{W}$.

Well-posedness of the variational model is a consequence of the subsequent proposition.

Proposition 2.1. *Let $p_0 \in H^1(\Omega_2)$, $\mathbf{f}_1 \in H^1(0, T; L^2(\Omega_1)^3)$, $f_2 \in H^1(0, T; L^2(\Omega_1))$ and $f_3 \in L^2(0, T; L^2(\Omega_2))$. For every $\Upsilon \in \mathcal{K}$, there exists a unique $(\mathbf{u}, p) \in \mathcal{H}$ such that $(\mathbf{u}(\cdot, 0), p(\cdot, 0)) = (0, p_0)$ and*

$$L(\Upsilon_1, \mathbf{u}, \mathbf{w}) - \int_{\Omega_2} bp\nabla \cdot \mathbf{w} = \int_{\Omega_1} \mathbf{f}_1 \cdot \mathbf{w} + \int_{\Omega_1} f_2 \nabla \cdot \mathbf{w}, \quad (43)$$

$$\int_{\Omega_2} \frac{1}{M} \frac{\partial p}{\partial t} w + \int_{\Omega_2} v^{-1} e^{\Upsilon_2} \nabla p \cdot \nabla w + \int_{\Omega_2} b \frac{\partial(\nabla \cdot \mathbf{u})}{\partial t} w = \int_{\Omega_2} f_3 w, \quad (44)$$

a.e. $t \in (0, T)$ for all $(\mathbf{w}, w) \in \mathcal{W}$. Moreover, for every $r > 0$ and $\hat{\Upsilon} \in \mathcal{K}$, there exists a positive constant C such that for all $\Upsilon \in B(\hat{\Upsilon}, r)$, the corresponding solution $\mathbf{h}(\Upsilon) \equiv (\mathbf{u}, p) \in \mathcal{H}$ of (43)–(44) satisfies

$$\|\mathbf{h}(\Upsilon)\|_{\mathcal{H}} \leq C[\|p_0\|_{H^1(\Omega_2)} + \|\mathbf{f}_1\|_{H^1(0,T;L^2(\Omega_1))} + \|f_2\|_{H^1(0,T;L^2(\Omega_1))} + \|f_3\|_{L^2(0,T;L^2(\Omega_2))}] \quad (45)$$

a.e. $t \in (0, T)$ for all $(\mathbf{w}, w) \in \mathbf{H}_0 \times L^2(\Omega_2)$. Additionally, C depends only on $b, v, M, \Omega, T, \|\hat{\Upsilon}\|, r$ and d .

Proof. See section 5.1. □

Remark 2.1. The proof of proposition 2.1 is primarily based on the work of [13]. There are, however, three main differences worth mentioning. First, in (43) we consider the case where Υ_1 is non-homogenous. Second, we require additional regularity for the pressure (i.e. $p \in H^{2,1}(\Omega \times [0, T])$). Third, we claim that the constant C from proposition 2.1 can be chosen uniformly in an arbitrary ball $B(\hat{\Upsilon}, r)$. The aforementioned regularity of p , as well as the property on C in (45), are key properties of the forward model which in turn ensure convergence of the proposed inverse methodology (see theorem 3.2).

Let us assume that measurements of pressure data are collected at each of the N well locations. We describe this measurement process with an operator $\mathcal{M}_p^l : \mathcal{P} \rightarrow L^2[0, T]$,

$$\mathcal{M}_p^l(p) = \int_{\Omega_2} p(x, t) \delta(x - x^l) dx, \quad (46)$$

where we abuse the standard notation and denote by $\delta(x - x^l)$ an L^2 -approximation to the Dirac delta function. The aim of expression (46) is to predict pressure measurements at the l th well. We then define

$$\mathcal{M}_p(p) = [\mathcal{M}_p^1(p), \dots, \mathcal{M}_p^N(p)]. \quad (47)$$

We recall that \mathcal{S} denotes the land surface (see figure 1). Measurements of changes in surface deformation are predicted with the operator $\mathcal{M}_u : L^2(0, T; H^1(\Omega_1)^3) \rightarrow L^2(0, T; L^2(\mathcal{S})^3)$ defined by

$$\mathcal{M}_u(\mathbf{u}) = \gamma_{\mathcal{S}}(\mathbf{u}) \quad (48)$$

with $\gamma_{\mathcal{S}}$ (the trace operator) defined in section 2.2. We define the observation space

$$\mathcal{O} \equiv L^2([0, T]; L^2(\mathcal{S})^3) \times (L^2[0, T])^N \quad (49)$$

with the inner product defined by

$$\langle \mathbf{d}_1, \mathbf{d}_2 \rangle_{L^2(\Omega_T)} = \frac{1}{\sigma_u} \int_0^T \int_{\mathcal{S}} \mathbf{d}_{u,1} \cdot \mathbf{d}_{u,2} d\sigma dt + \frac{1}{\sigma_p} \int_0^T \mathbf{d}_{p,1}^T \cdot \mathbf{d}_{p,2} dt \quad (50)$$

for all $\mathbf{d}_i = (\mathbf{d}_{u,i}, \mathbf{d}_{p,i}) \in \mathcal{O}$ ($i \in \{1, 2\}$) and for prescribed positive constants σ_p and σ_u . Consider the following definition.

Definition 2.2 (Forward operator). We define the forward operator $F : \Upsilon \rightarrow \mathcal{O}$ by

$$F(\Upsilon) \equiv (\mathcal{M}_u(\mathbf{u}), \mathcal{M}_p(p)), \quad (51)$$

where $\mathbf{h}(\Upsilon) = (\mathbf{u}, p)$ is the solution to the variational model (definition 2.1).

We recall that $\Upsilon_1 = \log \lambda$ and $\Upsilon_2 = \log K$ are the elastic and petrophysical parameters, respectively. For every pair of elastic-petrophysical parameters $\Upsilon = (\Upsilon_1, \Upsilon_2) \in \mathcal{K}$, $F(\Upsilon)$ in (51) is the prediction of pressure at wells (i.e. $\mathcal{M}_p(p)$) and deformation at the surface (i.e. $\mathcal{M}_u(\mathbf{u})$) obtained from the coupled geomechanics-flow model (41)–(42). Note that F is well defined due to the well-posedness of the variational problem (proposition 2.1) and the consistency of definitions (46)–(50).

We now state the differentiability of the forward operator.

Theorem 2.1 (Differentiability of F). *For every $\Upsilon \in \mathcal{K}$, the operator F is Frechet differentiable in \mathcal{K} . Moreover, its Frechet derivative $DF(\Upsilon) : \mathcal{K} \rightarrow \mathcal{O}$ is defined by*

$$DF(\Upsilon)\tilde{\Upsilon} = (\mathcal{M}_u(\tilde{\mathbf{u}}), \mathcal{M}_p(\tilde{p})), \quad (52)$$

where $\tilde{\mathbf{h}} \equiv (\tilde{\mathbf{u}}, \tilde{p})$ satisfies $(\tilde{\mathbf{u}}(x, 0), \tilde{p}(x, 0)) = (0, 0)$ and

$$L(\Upsilon_1, \tilde{\mathbf{u}}, \mathbf{w}) - \int_{\Omega_2} b\tilde{p}\nabla \cdot \mathbf{w} + \int_{\Omega_1} \tilde{\Upsilon}_1 e^{\Upsilon_1} (\nabla \cdot \mathbf{u})(\nabla \cdot \mathbf{w}) = 0, \quad (53)$$

$$\int_{\Omega_2} \frac{1}{M} \frac{\partial \tilde{p}}{\partial t} w + \int_{\Omega_2} v^{-1} e^{\Upsilon_2} \nabla \tilde{p} \cdot \nabla w + \int_{\Omega_2} b \frac{\partial \nabla \cdot \tilde{\mathbf{u}}}{\partial t} w + \int_{\Omega_2} v^{-1} \tilde{\Upsilon}_2 e^{\Upsilon_2} \nabla p \cdot \nabla w = 0 \quad (54)$$

a.e. in $(0, T)$, for all $\mathbf{W} \in \mathcal{W}$. In (53)–(54), $\mathbf{h}(\Upsilon) = (\mathbf{u}, p)$ is the solution to the variational model (41)–(42).

Proof. See section 5.2. □

3. The inverse problem

In the previous section we presented the geophysical problem of describing reservoir flow coupled to geomechanics for a prescribed elastic and petrophysical properties of the subsurface. We formulated this problem as forward operator F that maps the set of admissible (subsurface properties) parameters \mathcal{K} to the observation space \mathcal{O} . Let us now consider a specific physical problem and denote by $\Upsilon^\dagger = (\Upsilon_1^\dagger, \Upsilon_2^\dagger)$ the corresponding subsurface properties. Assuming that the model is perfect, if $\Upsilon^\dagger = (\Upsilon_1^\dagger, \Upsilon_2^\dagger)$ is known, then $(\mathbf{d}_u, \mathbf{d}_p) \equiv F(\Upsilon^\dagger)$ are the measurements that we collect if no error is made during the measurement process. However, as we stated before, knowledge of $\Upsilon^\dagger = (\Upsilon_1^\dagger, \Upsilon_2^\dagger)$ is very limited or even inexistent. However, $(\mathbf{d}_u, \mathbf{d}_p)$ (the observations) may be available from satellite observations and borehole measurements. We can then formulate the following IP.

Definition 3.1 (Inverse problem). *Given observations $(\mathbf{d}_u, \mathbf{d}_p) \in \mathcal{O}$, i.e. pressure data \mathbf{d}_p from wells and surface displacement data \mathbf{d}_u , find $\Upsilon = (\Upsilon_1, \Upsilon_2)$ such that*

$$F(\Upsilon) \equiv (\mathcal{M}_u(\mathbf{u}), \mathcal{M}_p(p)) = (\mathbf{d}_u, \mathbf{d}_p), \quad (55)$$

where $\mathbf{h}(\Upsilon) = (\mathbf{u}, p)$ is the solution to the variational model (definition 2.1).

In practice, the measurement process introduces error. Therefore, it is more realistic to assume that we are given data contaminated with noise \mathbf{d}^η . We additionally assume that we are provided with the knowledge of the noise level η , in the sense that

$$\|\mathbf{d} - \mathbf{d}^\eta\|_{\mathcal{O}} \leq \eta. \quad (56)$$

For the general case where $\eta \neq 0$, we understand the solution to the IP as an approximation when $\eta \rightarrow 0$ (see corollary 3.2 below).

3.1. Iterative regularization

The main goal now is to numerically solve the IP from definition 3.1. A straightforward approach is to consider a least-squares formulation of the form: find

$$\hat{\mathbf{Y}} \equiv \arg \min_{\mathbf{Y} \in \mathcal{K}} \|\mathbf{d}^\eta - F(\mathbf{Y})\|_{\mathcal{O}}^2. \quad (57)$$

One then may be tempted to implement a standard optimization technique to solve (57). However, as we explain below, solving the IP may result in numerical instabilities due to the compactness of the forward operator that we state in the following theorem.

Theorem 3.1. *F is compact and weakly (sequentially) closed in \mathcal{K} .*

Proof. See section 5.3. □

Corollary 3.1. *The IP of definition 3.1 is ill-posed in the following sense: there is a sequence $\mathbf{Y}^n \in \mathcal{K}$ for which $\mathbf{Y}^n \rightharpoonup \mathbf{Y}$ and $F(\mathbf{Y}^n) \rightarrow F(\mathbf{Y})$.*

Proof. Due to the compactness and the weak closeness of F , as well as the separability of the Hilbert spaces under consideration, the ill-posedness follows from standard arguments [7]. □

Corollary 3.1 implies that elements arbitrarily close in \mathcal{O} may not correspond to arbitrarily close preimages in \mathcal{K} . This ill-posedness may be reflected in the computational implementation for the solution to (57). For example, a standard gradient-descent technique typically provides a sequence of updates \mathbf{Y}^n that decrease the data misfit at each iteration (i.e. $\|\mathbf{d}^\eta - F(\mathbf{Y}^{n+1})\|_{\mathcal{O}} \leq \|\mathbf{d}^\eta - F(\mathbf{Y}^n)\|_{\mathcal{O}}$). One may expect this decrease to be accompanied with a reduction of the error with respect to a solution of the IP \mathbf{Y}^* (i.e. $\|\mathbf{Y}^n - \mathbf{Y}^*\|_{\mathcal{K}} \leq \|\mathbf{Y}^{n+1} - \mathbf{Y}^*\|_{\mathcal{K}}$). However, due to the aforementioned instability, after some iterations, the reduction of the data misfit may no longer correspond to decrease of the error. In fact, if the optimization technique is not properly stopped, this lack of stability may lead to large error in the estimate of the solution to the IP. It is therefore vital to alleviate this type of ill-posedness by means of regularization. In this work, we use a truncated Newton-CG algorithm introduced by Hanke in [15]. This is an iterative algorithm that consists of an outer loop where the IP is linearized around a previous estimate. At each iteration level, the update is given by computing, with a conjugate gradient (inner loop), a regularized approximation of the linearized problem. More precisely, if we denote by $DF(\mathbf{Y}^n)^*$ the adjoint operator of $DF(\mathbf{Y}^n)$, at each iteration level n , then the aim of the Newton-CG algorithm is to solve

$$DF(\mathbf{Y}^n)^* DF(\mathbf{Y}^n)(\mathbf{Y}^{n+1} - \mathbf{Y}^n) = DF(\mathbf{Y}^n)^* [\mathbf{d}^\eta - F(\mathbf{Y}^n)], \quad (58)$$

which are the normal equations of the linearized least-squares problem

$$\mathbf{Y}^{n+1} = \arg \min_{\mathbf{Y} \in \mathcal{K}} \|\mathbf{d}^\eta - F(\mathbf{Y}^n) - DF(\mathbf{Y}^n)(\mathbf{Y} - \mathbf{Y}^n)\|. \quad (59)$$

Since the linearization of a compact operator is compact [5, theorem 4.19], problem (59) inherits the ill-posedness of the nonlinear problem established in corollary 3.1. Under some conditions on F , the Newton-CG algorithm presented below alleviates the lack of stability that results from the compactness of the linearization in (59). In other words, this algorithm produces a stable solutions of the IP. However, the ill-posedness of the IP can be addressed by means of other regularization techniques (see the discussion after corollary 3.2). We refer the reader to [19] for a complete analysis of iterative regularization techniques for nonlinear ill-posed problems. We remark that the Newton-CG algorithm provides faster

convergence than gradient-based approaches (e.g. Landweber iteration [19, chapter 2]) at a reasonable computational cost. Nonetheless, other regularization techniques should be tested and compared for optimal computational performance. We now present the Newton-CG algorithm for the solution to the IP problem.

Algorithm 1 (Truncated Newton-CG).

Let $0 < \rho < 1$ and $\tau > 2/\rho^2$. For $n = 1, \dots$

- *Forward model. Evaluate the forward operator at the current estimate*

$$F(\Upsilon^n) = (\mathcal{M}_u(\mathbf{u}), \mathcal{M}_p(p)). \quad (60)$$

This implies computing $h(\Upsilon^n) \equiv (\mathbf{u}, p)$ by solving the variational model (definition 2.1).

- *Check for convergence (discrepancy principle). If*

$$\|\mathbf{d}^n - F(\Upsilon^n)\|_{\mathcal{O}} \leq \tau \eta \quad (61)$$

stop. Output: Υ^n .

- *CG inner loop. Define*

$$\mathbf{x}_1 = 0, \quad \mathbf{r}_1 = \mathbf{d}^n - F(\Upsilon^n), \quad \mathbf{s}_1 = \mathbf{d}^n - F(\Upsilon^n). \quad (62)$$

For $k = 1, \dots, k_{\max}$

- * *Check for convergence of the inner loop: if*

$$\|\mathbf{r}_k\|_{\mathcal{O}} \leq \rho \|\mathbf{d}^n - F(\Upsilon^n)\|_{\mathcal{O}} \quad (63)$$

stop. Output: \mathbf{x}^k .

- * *Update the inner loop iterate:*

$$\mathbf{x}^{k+1} = \mathbf{x}^k + \alpha^k DF(\Upsilon^n)^* \mathbf{s}_k, \quad (64)$$

where

$$\alpha^k = \frac{\|DF(\Upsilon^n)^* \mathbf{r}_k\|_{\mathcal{K}}^2}{\|DF(\Upsilon^n)DF(\Upsilon^n)^* \mathbf{s}_k\|_{\mathcal{O}}^2}. \quad (65)$$

- * *Update the conjugate directions:*

$$\mathbf{r}^{k+1} = \mathbf{r}^k - \alpha^k DF(\Upsilon^n)^* \mathbf{r}_k, \quad (66)$$

$$\mathbf{s}^{k+1} = \mathbf{r}^{k+1} + \left(\frac{\|DF(\Upsilon^n)^* \mathbf{r}_{k+1}\|_{\mathcal{K}}^2}{\|DF(\Upsilon^n)^* \mathbf{r}_k\|_{\mathcal{K}}^2} \right) \mathbf{s}^k. \quad (67)$$

- *Update. $\Upsilon^{n+1} = \Upsilon^n + \mathbf{x}^k$, set $n \rightarrow n + 1$ and repeat.*

Note that for each k , $DF(\Upsilon^n)^* \mathbf{r}_k$ can be stored and used in the subsequent iteration of the inner loop.

Remark 3.1. If $k_{\max} = 1$,

$$\Upsilon^{n+1} = \Upsilon^n + \frac{\|DF(\Upsilon^n)^*(\mathbf{d}^n - F(\Upsilon^n))\|_{\mathcal{K}}^2}{\|DF(\Upsilon^n)DF(\Upsilon^n)^*(\mathbf{d}^n - F(\Upsilon^n))\|_{\mathcal{O}}^2} DF(\Upsilon^n)^*(\mathbf{d}^n - F(\Upsilon^n)), \quad (68)$$

and then the Newton-CG algorithm becomes the steepest-descent method [19, chapter 3].

3.2. Convergence and regularizing properties

In this section, we present the conditions under which the Newton-CG algorithm provides stable solutions to the IP presented in definition 3.1. Consider the following assumption.

Assumption 3.1. For every $\hat{\mathbf{Y}}$ there exists constants $r > 0$ and $C > 0$ such that for all $\mathbf{Y}, \tilde{\mathbf{Y}} \in B(\hat{\mathbf{Y}}, r)$,

$$\|\mathbf{u} - \tilde{\mathbf{u}}\|_{H^1(\Omega_1)^3} \leq C \|\mathcal{M}_{\mathbf{u}}(\mathbf{u} - \tilde{\mathbf{u}})\|_{L^2(\mathcal{S})^3}, \quad (69)$$

$$\|p - \tilde{p}\|_{L^2(\Omega_2)} \leq C \|\mathcal{M}_p(p - \tilde{p})\|_{L^2[0,T]^N} \quad (70)$$

a.e. in $(0, T)$ where $\mathbf{h}(\mathbf{Y}) = (\mathbf{u}, p)$ and $\mathbf{h}(\tilde{\mathbf{Y}}) = (\tilde{\mathbf{u}}, \tilde{p})$ are the solutions to the variational model (41)–(42) with \mathbf{Y} and $\tilde{\mathbf{Y}}$, respectively.

Under the previous assumption we prove that the forward model satisfies a nonlinearity condition required for the convergence of the Newton-CG algorithm.

Theorem 3.2. Under assumption 3.1, for every $\hat{\mathbf{Y}}$ there exist constants $r > 0$ and $C > 0$ such that

$$\|F(\tilde{\mathbf{Y}}) - F(\mathbf{Y}) - DF(\mathbf{Y})(\tilde{\mathbf{Y}} - \mathbf{Y})\|_{\mathcal{O}} \leq C \|\tilde{\mathbf{Y}} - \mathbf{Y}\|_{\mathcal{K}} \|F(\tilde{\mathbf{Y}}) - F(\mathbf{Y})\|_{\mathcal{O}} \quad (71)$$

for all $\tilde{\mathbf{Y}}, \mathbf{Y} \in B(\hat{\mathbf{Y}}, r)$.

Proof. See section 5.4. □

Remark 3.2. Assumption 3.1 is key for the convergence result of theorem 3.2 and for the present problem is still an open problem. Note that the assumption is valid, for example, in the case where $\mathcal{M}_{\mathbf{u}}$ and \mathcal{M}_p are linear and coercive (i.e. $\|\mathbf{u}\|_{H^1(\Omega_1)^3} \leq C_{\mathbf{u}} \|\mathcal{M}_{\mathbf{u}}(\mathbf{u})\|_{L^2(\mathcal{S})^3}$ and $\|p\|_{L^2(\Omega_2)} \leq C_p \|\mathcal{M}_p(p)\|_{L^2[0,T]^N}$). In particular, if we consider the unrealistic case of having measurements of pressure and surface deformation everywhere on their corresponding domains, then $\mathcal{M}_{\mathbf{u}}$ and \mathcal{M}_p are the identity operators and the above property holds. Although our choices of $\mathcal{M}_{\mathbf{u}}$ and \mathcal{M}_p (46)–(48) are not coercive, assumption 3.1 may still be valid considering that the inequalities (69)–(70) must hold only for solutions to the variational problem (41)–(42) with parameters within a prescribed neighborhood.

The following result follows now from [15, theorem 5.3].

Corollary 3.2 (Hanke [15]). Consider assumption 3.1. Let $0 < \rho < 1$ and $\tau > 2/\rho^2$. Let \mathbf{Y} be a solution of the IP. There exists $r > 0$ such that if $\mathbf{Y}_0 \in B(\mathbf{Y}, r)$, then the Newton-CG algorithm is well defined and terminates after $m(\eta) < \infty$ outer iterations. Moreover, the estimate $\mathbf{Y}_{m(\eta)}^\eta$ converges to a solution of the IP as $\eta \rightarrow 0$.

This corollary ensures the termination of the Newton-CG algorithm after a finite number of iterations. The early termination of the scheme according to the discrepancy principle establishes the regularization property of the scheme. Indeed, the convergence of $\mathbf{Y}_{m(\eta)}^\eta$ to a solution of the IP as $\eta \rightarrow 0$ is the stability that we seek by means of regularization. It is worth mentioning that property (71) will ensure convergence of other iterative regularization techniques such as the Levenberg–Marquard and the Landweber technique [19].

3.3. Characterization of the adjoint

In the following, we provide the characterization of DF^* which is fundamental for the numerical implementation of the Newton-CG algorithm presented above. The following lemma is the basis for the adjoint characterization.

Lemma 3.1. *Let $\hat{\Upsilon} = (\hat{\Upsilon}_1, \hat{\Upsilon}_2) \in \mathcal{K}$ and $r > 0$. For all $\Upsilon = (\Upsilon_1, \Upsilon_2) \in B(\hat{\Upsilon}, r)$ there exists a unique $(\mathbf{w}_u, w_p) \in L^2(0, T; H^1(\Omega_1)^3) \times H^{2,1}(\Omega_2 \times [0, T])$ such that $w_p(x, T) = 0$ and*

$$L(\Upsilon_1, \mathbf{w}_u, \mathbf{h}_1) - \int_{\Omega_2} b \frac{\partial w_p}{\partial t} \nabla \cdot \mathbf{h}_1 = \int_S \mathbf{A}_1 \cdot \boldsymbol{\gamma}(\mathbf{h}_1), \quad (72)$$

$$\int_{\Omega_2} \left[-\frac{1}{M} \frac{\partial w_p}{\partial t} h_2 + v^{-1} e^{\Upsilon_2} \nabla w_p \cdot \nabla h_2 \right] - \int_{\Omega_2} b \nabla \cdot \mathbf{w}_u h_2 = \int_{\Omega_2} A_2 h_2 \quad (73)$$

a.e. in $[0, T]$ for all $(\mathbf{h}_1, h_2) \in \mathcal{W}$ and for all $(\mathbf{A}_1, A_2) \in L^2(0, T; L^2(\mathcal{S})^3) \times L^2(0, T; L^2(\Omega_2))$. Moreover,

$$\max \{ \|\mathbf{w}_u\|_{L^2(0, T; H^1(\Omega_1)^3)}, \|w\|_{H^{2,1}(\Omega_2 \times [0, T])} \} \leq C (\|\mathbf{A}_1\|_{L^2(0, T; L^2(\mathcal{S})^3)} + \|A_2\|_{L^2(0, T; L^2(\Omega_2))}), \quad (74)$$

where C depends only on $M, v, \mu, \Omega_1, \Omega_2, T, \hat{\Upsilon}$ and r .

Proof. See section 5.5. □

In the following proposition, we use the adjoint system (72)–(73) to characterize the adjoint of the Frechet derivative of the forward operator.

Proposition 3.1. *Let $\Upsilon \in \mathcal{K}$ and $\mathbf{h}(\Upsilon) = (\mathbf{u}, p)$ be the corresponding solution to the variational model (41)–(42). For every $\mathbf{d} \in \mathcal{O}$, the adjoint operator of $DF(\Upsilon)$ is the operator $DF(\Upsilon)^* : \mathcal{O} \rightarrow \mathcal{K}$ defined by*

$$DF(\Upsilon)^* \mathbf{d} = (f_1, f_2), \quad (75)$$

where

$$f_1(x) \equiv - \int_0^T \int_{\Omega_1} e^{\Upsilon_1} (\nabla \cdot \mathbf{u})(\nabla \cdot \mathbf{w}_u) C_1(x, x') dx', \quad (76)$$

$$f_2(x) \equiv - \int_0^T \int_{\Omega_2} v^{-1} e^{\Upsilon_2} \nabla p \cdot \nabla w_p C_2(x, x') dx', \quad (77)$$

and (\mathbf{w}_u, w_p) are the solutions to the adjoint problem (72)–(73) for

$$\mathbf{A}_1 = \frac{1}{\sigma_u} \mathbf{d}_u, \quad A_2 = \frac{1}{\sigma_p} \sum_{j=1}^N \mathbf{d}_p^j(t) \delta(x - x^j) dx. \quad (78)$$

Proof. See section 5.6. □

Table 1. Reservoir description.

Variable (units)	Nominal value
ν (Pas)	5×10^{-4}
M (Pa)	2.5×10^8
b	1
μ (Pa)	5×10^7
p_0 (Pa)	2.6×10^7
T (days)	500
^b Injection rate ($\text{m}^3 \text{s}^{-1}$)	1.25
^b Production rate ($\text{m}^3 \text{s}^{-1}$)	0.41

^a Constant on its domain of definition.

^b Constant on $[0, T]$.

4. Numerical implementation and examples

In this section, we present numerical examples that show the potential of the proposed inverse model for the estimation of petrophysical and elastic properties of the subsurface. In particular, we accomplish the following four goals. First, we show that inverting pressure and surface deformation data provide better estimates of the log-permeability (i.e. Υ_2) than the inversion of only pressure data. In other words, we display the advantage of inverting coupled flow-geomechanics models versus inverting standard flow models. Second, we show that the proposed technique is also capable of providing reasonable estimates of the elastic property $\log \lambda$ (i.e. Υ_1). The third goal of our numerical experiments is to expose issues of estimating both properties jointly (multi-parameter estimation). The fourth and final goal of this section is to provide the numerical evidence of regularization and convergence presented in previous sections. In section 4.1, we describe the numerical implementation of the proposed methodology. Then, numerical experiments are presented in section 4.2. For all experiments, the additional parameters in the model (41)–(42) (i.e. μ , q , M , b and ν) are assumed known. These parameters as well as pertinent information are displayed in table 1.

4.1. Implementation of the geomechanics-flow model

The first step of the Newton-CG scheme requires the evaluation of the forward operator. This in turn implies the solution to the variational problem (41)–(42). A direct approach to solve these types of fully coupled problems is to choose consistent discretizations for both the elasticity operator in (40) and the parabolic equation (42), respectively. One can then derive a fully coupled ODE system for the vector of pressure nodal values and the vector of nodal values of each component of the displacement field. The direct approach is then to solve the resulting ODE system with the standard solver of choice. However, this direct approach has two main disadvantages. First, for subsurface problems the size of the resulting ODE system is typically computationally prohibitive. Second, the direct approach may not be practical when previously developed software is utilized for the elasticity and/or the flow problem. In order to overcome those issues, several coupling techniques have been recently proposed [21, 20]. The aim of those techniques is to iteratively couple (maybe already existing) subsurface flow and geomechanical models so that the converged solution approximates the solution to the fully coupled problem. Convergence and stability properties of some of those techniques can also be found in [21, 20].

For the dimensions of the subsurface problem considered in this section, the fully coupled approach does not impose a significant computational challenge for solving the forward model. However, one realizes that computational savings are desirable when this type of model has

to be solved multiple times in an iterative scheme such as the utilized Newton-CG algorithm. In this case, computational efficiency and reasonable accuracy can be achieved by using an iterative coupling strategy. Moreover, iterative coupling enables us to utilize our existing independent codes for elasticity and subsurface flow. For these reasons, we implemented the fixed-stress coupling approach of Kim *et al* presented in [21]. Kim *et al* proved convergence and stability of the fixed-stress approach for problems similar to (41)–(42). We have additionally applied the aforementioned approach to solve the coupled problems (53)–(54) (linearization) and (72)–(73) (adjoint) that appear multiple times in the Newton-CG algorithm of section 3.

In our fixed-stress implementation for the solution to (41)–(42), we use the finite element (FE) method for the discretization of the elasticity operator (40). The domain Ω_1 is partitioned into a regular tetrahedral grid with linear elements. For this ‘elasticity part’, we follow the numerical approach and the MATLAB implementation of [2]. The nodal values of each coordinate of \mathbf{u} are evaluated on each vertex of the tetrahedral grid. On the other hand, since the parabolic equation (42) in p is a flow problem, the implementation of a locally mass conservative method is desirable. We therefore use the cell-center finite differences of [28]. In this case, Ω_2 is partitioned into hexahedral cells whose centers are the nodes of the pressure field p . On each cell, p is approximated with a constant function corresponding to the nodal value at that cell. The coupling term in (41) (second term on the left-hand side) is discretized by using the piecewise constant approximation of p . Due to the simple and regular geometry considered here, each hexahedron in the partition of Ω_2 has a unique partition into elements of Ω_1 . Therefore, p can be easily projected on Ω_1 to obtain a straightforward discretization of the coupling term in (41). For the discretization of the coupling term (third term on the left-hand side) in (42), we use the FE approximation for \mathbf{u} . Thus, $\nabla \cdot \mathbf{u}$ takes constant values on each element of Ω_1 . From the previous argument about the geometry, it follows that the projection of $\nabla \cdot \mathbf{u}$ in Ω_2 can be trivially obtained for the construction of the aforementioned coupling term. Finally, a backward-Euler discretization scheme is used for the time-discretization of (42). The resulting discretized systems are then iteratively coupled according to the fixed-stress approach of [21] which provides an approximate solution to the fully coupled model (41)–(42).

For the implementation of the Newton-CG algorithm, we take the ‘optimize-then-discretize’ approach that consists of implementing the numerical discretization of (60)–(68). More precisely, we use analogous procedures to the ones described above (based on the fixed-stress approach) to solve the discretized PDEs that define $DF(\Upsilon^n)$ (equations (53)–(54), theorem 2.1) and $DF(\Upsilon^n)^*$ (equations (72)–(73), proposition 3.1), respectively. Our ‘optimize-then-discretize’ implementation substantially differs from ‘discretize-then-optimize’, where the forward model (41)–(42) is first discretized and then the Newton-CG is applied to the derivative (and corresponding adjoint) of the discretized model. For the advantages and drawbacks of both approaches, we refer the reader to the discussion of [14, section 2.9]. For the computer code that we develop for the numerical implementation of (53)–(54) and (72)–(73), the ‘optimize-then-discretize’ approach provides a straightforward strategy. We recognize, however, that inconsistent gradients may appear and so the ‘discretize-then-optimize’ approach should also be considered. Nevertheless, our stopping criteria (discrepancy principle) does not involve the derivative of the forward map, and our experiments indicate that possible gradient inconsistencies do not affect the final outcome of the inversion.

4.2. Experiments

We now describe the geometry for the subsequent experiments. The domain Ω_1 is a rectangular box with a squared base of dimensions 4000 m \times 4000 m. The top of the box corresponds to

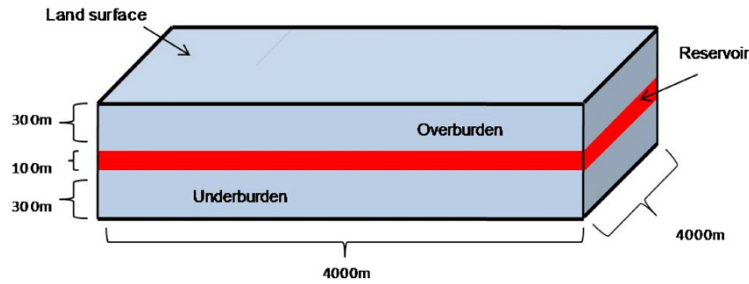


Figure 2. Experimental setup.

the ground surface \mathcal{S} where measurements of surface deformation are collected. The distance from \mathcal{S} to the base of Ω_1 is 700 m. The domain of the reservoir (i.e. Ω_2) is the rectangular box imbedded in Ω_1 as shown in figure 2. The dimensions of Ω_2 are 4000 m \times 4000 m \times 100 m. The faces of Ω_2 are parallel to the ones of Ω_1 . The underburden and the overburden consist of identical rectangular boxes, each of dimensions 4000 m \times 4000 m \times 300 m. Note that the top of the reservoir is at depth of 300 m with respect to the ground surface \mathcal{S} . We consider a well configuration that consists of two injection wells (red squares) and six production wells (black dots). The 2D view of the locations of those wells are displayed in figure 3 (top-right). Injection and production wells are operated under specified constant rates (see table 1).

For the validation of the Newton-CG algorithm we use synthetic data generated with our implementation for the solution to (41)–(42). To avoid inverse crimes, synthetic data are generated by solving (41)–(42) on a finer grid than the one used for the discretization of the variational problems in the data inversion scheme. For the fine simulation, Ω_1 is partitioned into 5×10^5 tetrahedral elements. The reservoir domain Ω_2 is discretized into $80 \times 80 \times 1$ cells. In contrast, for the implementation of the Newton-CG algorithm Ω_1 is partitioned into 1.25×10^5 elements while Ω_2 is partitioned into $40 \times 40 \times 1$ cells. Note that, for simplicity, we consider the case where Ω_2 is a thin reservoir which can be represented as one single layer in the vertical direction. Therefore, only two-dimensional flow takes place. Nevertheless, the full three-dimensional elasticity behavior is simulated on Ω_1 . For all the experiments of this paper, we consider $\kappa = 1$ in (32).

4.2.1. Estimation of $\Upsilon_2 = \log(K)$. Assuming that Υ_1 is known, in this subsection we consider only the estimation of the log-permeability Υ_2 . Note, however, that our formulation accounts for the joint estimation of Υ_1 and Υ_2 . In terms of the formulation of the previous section, the (single-parameter) estimation of Υ_2 simply consists of defining $\mathcal{K} = \mathcal{K}_2$. Additionally, since Υ_1 is known, the forward map is independent of Υ_1 and the last term on the right-hand side of (53) vanishes. In this case, it is not difficult to see that the adjoint operator (75) reduces to one component that corresponds to the adjoint of the derivative with respect to the (only unknown) Υ_2 .

To generate synthetic data, we first prescribe an isotropic spherical covariance model (see [6, chapter 4]) with range 1.7 km. This covariance model is used in the geostatistical software SGEMS [27] to generate a stochastic field by means of (unconditioned) sequential Gaussian simulation. The resulted field is denoted by Υ_2^\dagger and its plot is shown in figure 3 (top-left). We use this Υ_2^\dagger as the ‘true’ log-permeability field for the experiment in this section. In other words, we use Υ_2^\dagger in model (41)–(42) to find $\mathbf{u}(x, y, z, t)$ and $p(x, y, t)$. As an example, in figure 4 we show the three components of $\mathbf{u}(x, y, z, t = T)|_{\mathcal{S}}$, i.e. the change of displacement of

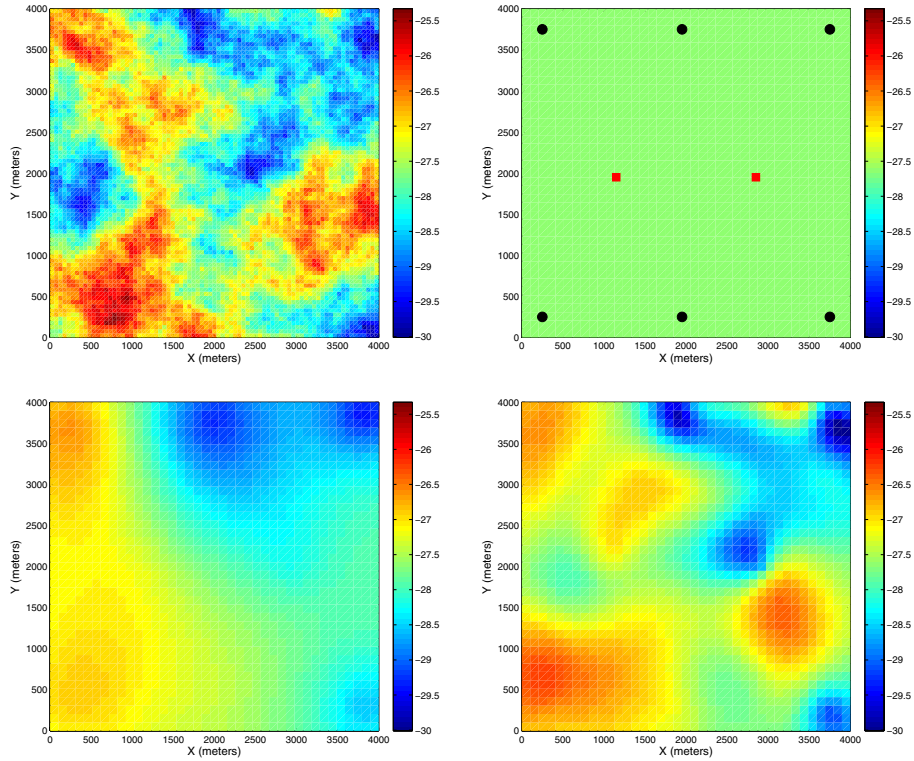


Figure 3. Estimation of $\Upsilon_2 = \log(K)$. Top-left: true log-perm Υ_2^\dagger ($\log(\text{m}^2)$). Top-right: prior log-perm ($\log(\text{m}^2)$) and well configuration. Bottom-left: estimate Υ_2 ($\log(\text{m}^2)$) from inverting $\mathbf{d} = \mathbf{d}_p$. Bottom-right: estimate Υ_2 ($\log(\text{m}^2)$) from inverting $\mathbf{d} = (\mathbf{d}_u, \mathbf{d}_p)$.

the ground surface \mathcal{S} at the final time. Similarly, in figure 4 (bottom-right) we plot the pressure field $p(x, y, t = T)$ at the final simulation time $t = T$. The solution $(\mathbf{u}(x, y, z, t), p(x, y, t))$ to (41)–(42) with the ‘true’ log-perm is now used to define synthetic data $(\mathbf{d}_u, \mathbf{d}_p)$ as follows:

$$\mathbf{d}_u(x, y, t) \equiv \mathbf{u}(x, y, z, t)|_{\mathcal{S}} + \epsilon_u(x, y, t), \quad \mathbf{d}_p(t) \equiv \{p(x^l, y^l, t) + \epsilon_p^l(t)\}_{l=1}^{13}, \quad (79)$$

where $\epsilon_u(x, y, t)$ is a field of Gaussian random noise defined on every point of \mathcal{S} , at each time of the discretization scheme. Analogously, for each well location (x^l, y^l) , $\epsilon_p^l(t)$ is Gaussian random noise defined at each time. For the experiment of this section, the variance of the noise in (79) is 1% of the observations. More precisely,

$$\|(\epsilon_u, \epsilon_p)\|_{\mathcal{O}} = 0.01\|(\mathbf{d}_u, \mathbf{d}_p)\|_{\mathcal{O}}. \quad (80)$$

For simplicity, the same time discretization is utilized for both, the generation of data and the implementation of the iterative scheme. Therefore, since the pressure data at each well is a function of time, it can be directly utilized for the evaluation of the data misfit in the second step of the Newton-CG algorithm. However, \mathbf{d}_u is defined on each nodal value of \mathcal{S} discretized on the finer grid (to avoid inverse crimes). Then, we need to project \mathbf{d}_u on the coarse grid utilized for the implementation of the Newton-CG algorithm. It is essential to emphasize that the true permeability Υ_2^\dagger is used only for the generation of synthetic data $(\mathbf{d}_u, \mathbf{d}_p)$. In

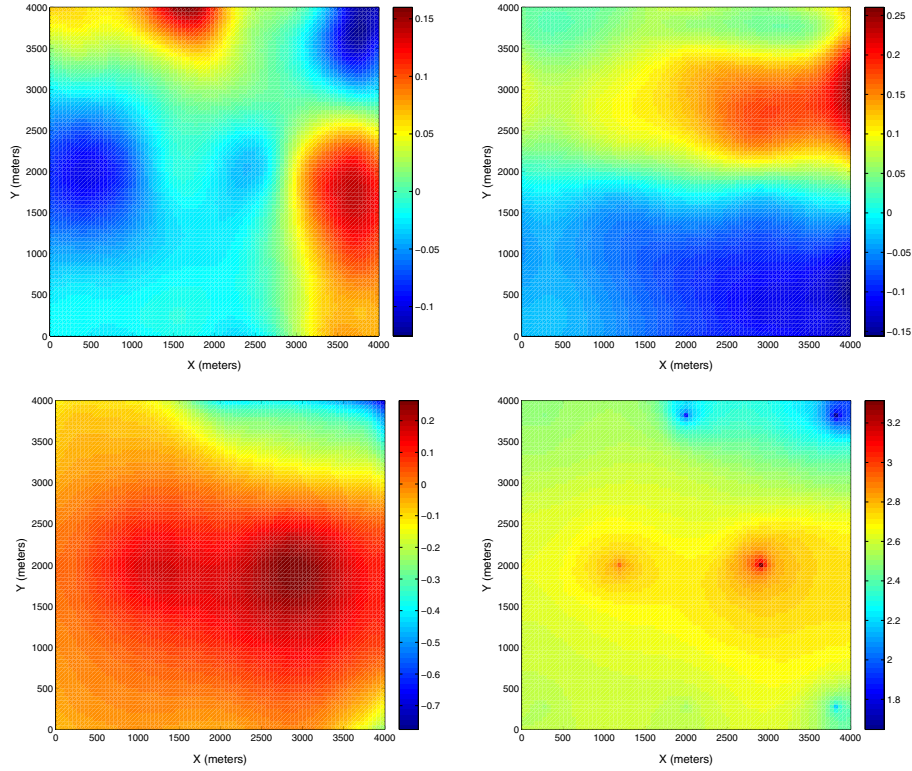


Figure 4. Solution to (41)–(42) for $\Upsilon_2 = \Upsilon_2^\dagger$ (i.e. ‘true’ log permeability). Top-left: $u_x(\mathbf{x}, t = T)|_S$ (m). Top-right: $u_y(\mathbf{x}, t = T)|_S$ (m). Bottom-left: $u_z(\mathbf{x}, t = T)|_S$ (m). Bottom-right: $p(x, y, t = T)$ ($\times 10^7$ Pa).

addition, the covariance expression that we used for the generation of Υ_2^\dagger , is also utilized for the definition of the space (28) (for $i = 2$). One can therefore think the covariance model as prior information incorporated into the inverse model. These prior information and synthetic data are used in our Newton-CG scheme to find an estimate Υ_2 of the log-permeability of the reservoir.

The experiment we present in this section (i.e. estimation of $\Upsilon_2 = \log(K)$ assuming Υ_1 known) is motivated by the interest of the reservoir modeling community in finding estimates of absolute permeability for improving the prediction of reservoir dynamics. However, most of the literature is focused on the estimation of permeability by inverting (or assimilation of) only production data from wells. In the present formulation, the assimilation of only production (pressure) data can be easily obtained by eliminating the second component of $\mathbf{d} = (\mathbf{d}_u, \mathbf{d}_p)$, and setting $\sigma_u \rightarrow \infty$ in (50). Thus, in this first set of experiments, we use our inversion approach to compute an estimate of log-permeability when we invert only pressure data (i.e. we use $\mathbf{d} = \mathbf{d}_p$). This estimate is shown in figure 3 (bottom-left). The same inversion approach is used to compute an estimate of log-perm when combined pressure and surface deformation data are inverted (i.e. when we use $\mathbf{d} = (\mathbf{d}_u, \mathbf{d}_p)$). In this case, the estimate is displayed in figure 3 (bottom-right). We recall that for this experiment, Υ_1 is known and so for simplicity we

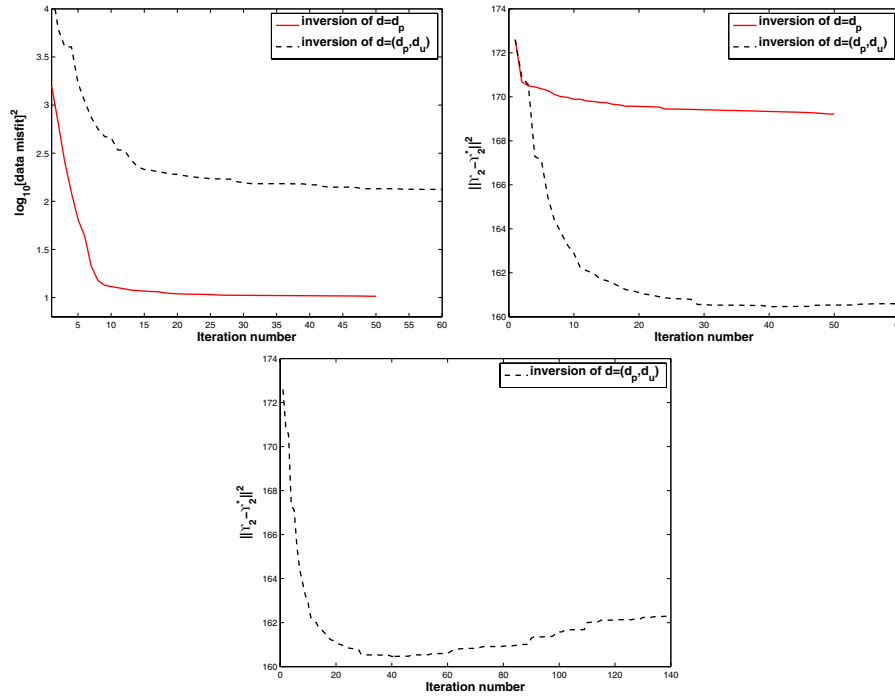


Figure 5. Performance of the procedure for the estimation of $\Upsilon_2 = \log(K)$. Top-left: \log_{10} of the squared data misfit. Top-right: squared error (expression (81)). The red solid line corresponds to the case where only pressure data are inverted. The dotted black line indicates the performance when pressure and surface deformation data are inverted. Bottom: same experiment corresponding to the dotted line of the top-right panel. In this case, however, the discrepancy principle is not enforced.

choose $\Upsilon_1(x, y) = 19.8 \log(\text{Pa})$ for all $(x, y) \in \Omega_1$. In both cases, we initialize the Newton-CG algorithm with the constant field shown in figure 3 (top-right). It comes as no surprise that the estimate computed by inverting only pressure data (from wells) recovers spatial features of the ‘true’ log-permeability Υ_2^\dagger at the regions close to the well locations (figure 3 (top-right)). From figure 3 (bottom-right), we can visually appreciate that the estimate computed with both pressure data and surface deformation has a better resemblance to Υ_2^\dagger in regions in-between the well locations. The performance of the estimation and the added value of the inversion of surface deformation is quantified with the errors defined by

$$\mathcal{E}_2(\Upsilon_2) = \|\Upsilon_2 - \Upsilon_2^\dagger\|_{\mathcal{K}_2}. \quad (81)$$

In figure 5 (top-right), we display the errors (81) as a function of iterations of the Newton-CG scheme. We clearly observe that the error with respect to the true log-permeability Υ_2^\dagger is smaller when both pressure and surface deformation are inverted. In both cases, we see that the data misfit, presented in figure 5 (top-left), decreases with the number of iterations. The Newton-CG scheme is stopped according to the discrepancy principle (61) with $\tau = 2.5$. In figure 5 (bottom), we display again the error when both types of data are inverted. However, in this case the Newton-CG scheme is not stopped according to the discrepancy principle. We then note

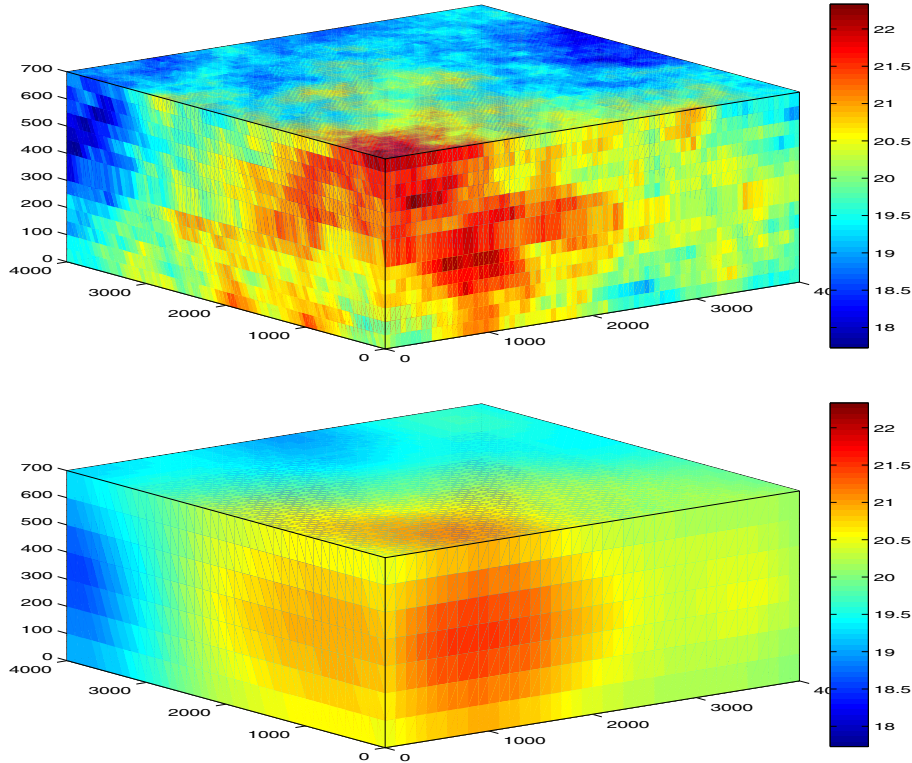


Figure 6. Estimation of $\Upsilon_1 = \log(\lambda)$. Top: true log-lambda Υ_1^\dagger (log(Pa)). Bottom: estimate Υ_1 (log(Pa)) from inverting $\mathbf{d} = (\mathbf{d}_u, \mathbf{d}_p)$.

an increase of the error after it reaches a minimum. This constitutes the numerical evidence of the ill-posedness predicted by corollary 3.1 due to the compactness of the forward operator. In other words, even though the current estimate predicts data close to the observations (in the observation space), the corresponding estimate diverges (in the parameter space) from the true log-permeability Υ_2^\dagger .

4.2.2. Estimation of $\Upsilon_1 = \log(\lambda)$. In this section, we assume that $\Upsilon_2 = \log(K)$ is known. For simplicity, we consider a constant field $\Upsilon_2(x, y) = -27.6 \log(\text{m}^2)$ for all $(x, y) \in \Omega_2$. The goal is now to test the inversion approach for finding an estimate $\Upsilon_1 = \log(\lambda)$ from synthetic data. Since λ is an elastic property, it is clear that data from surface deformation are more sensitive to changes in λ . Conversely, there is a low sensitivity in the pressure data with respect to λ . Due to this low sensitivity, very poor estimates (not shown) of λ are obtained when only pressure data are inverted. Therefore, for this experiment we consider the inversion of combined synthetic surface deformation and pressure data.

For the generation of synthetic data, we define a ‘true’ elastic parameter $\Upsilon_1 = \log(\lambda)$ statistically generated with sequential Gaussian simulation. We used a spherical covariance model with horizontal range of 3 km and vertical range of 1 km. The generated Gaussian field is denoted by Υ_1^\dagger and presented in figure 6 (top). We recall that the elastic property Υ_1^\dagger must be defined in Ω_1 . For reference, in figure 7 (top-left) we display the values of Υ_1^\dagger at Ω_2 , i.e.

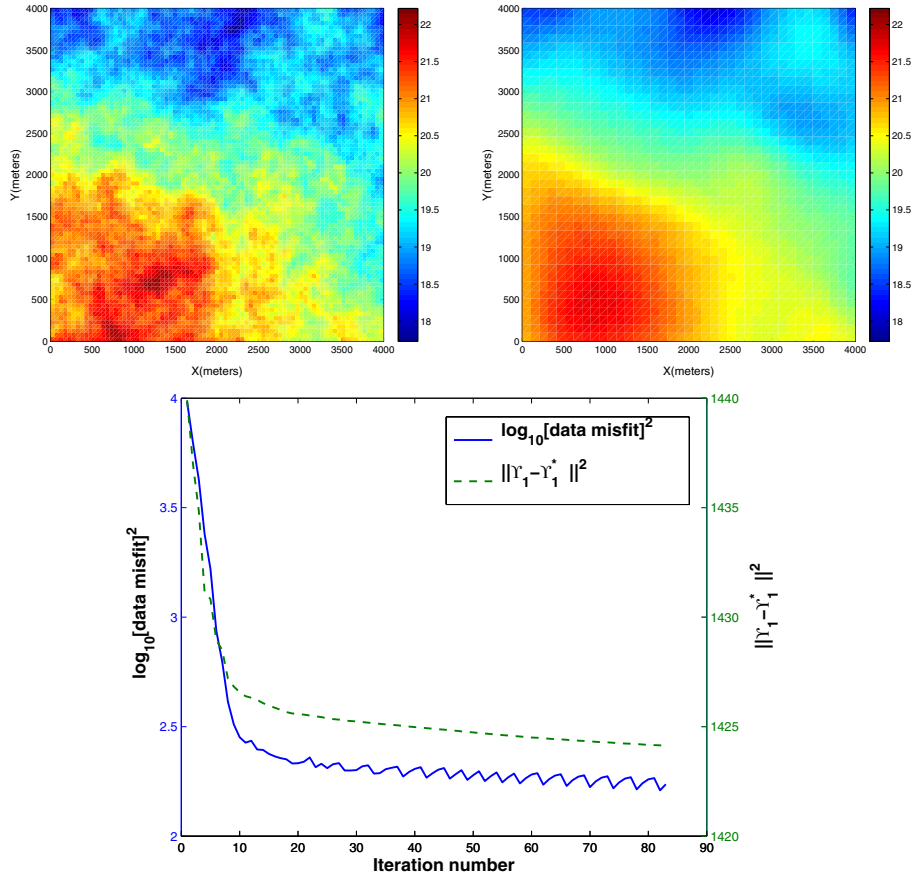


Figure 7. Estimation of $\Upsilon_1 = \log(\lambda)$. Top-left: true $\Upsilon_1^\dagger|_{\Omega_2}$ (log(Pa)). Top-right: estimate $\Upsilon_1|_{\Omega_2}$ (log(Pa)). Bottom (left axis): \log_{10} squared data misfit. Bottom (right axis) squared error.

$\Upsilon_1^\dagger(x, y, z = 300 \text{ m})$. The ‘true’ log-lambda is then used to solve the model equations (41)–(42). Then, synthetic data are generated by adding noise of 1% as described in the previous experiment. The initial guess for algorithm 1 is a constant field $\Upsilon_1(x, y) = 19.8 \log(\text{m}^2)$ for all $(x, y) \in \Omega_1$. In figure 6, (bottom) we present the estimate Υ_1 obtained after 80 iterations of the iterative scheme. After this number of iterations, the data misfit displayed in figure 7 (bottom) exhibits stagnation around a value that satisfies the discrepancy principle with $\tau = 3.6$. The corresponding values of the estimate at the reservoir $\Upsilon_1(x, y, z = 300 \text{ m})$ are shown in figure 7 (top-right). There is a clear visual agreement between the truth and the estimate. This agreement can be quantified by means of the error

$$\mathcal{E}_1(\Upsilon_1) = \|\Upsilon_1 - \Upsilon_1^\dagger\|_{\mathcal{K}_1}. \tag{82}$$

The square of this error as well as the performance of the squared data misfit is displayed in figure 7 (bottom). It is worth mentioning that the main agreement between Υ_1^\dagger and Υ_1 should

be expected at the reservoir Ω_2 . This can be easily understood by recalling that the only source for the elastic deformation of Ω_1 is the subsurface flow which is considered only within the reservoir Ω_2 . It is therefore not surprising that the estimate Υ_1 does not capture all the spatial features of Υ_1^\dagger . Nevertheless, in the norm of the parameter space \mathcal{K}_1 (defined in Ω_1), the error of the estimate Υ_1 decreases with the number of iterations (see figure 7 (bottom)).

4.2.3. Multiple-parameter estimation. We now present a final experiment where we test the capability of the Newton-CG algorithm to find joint estimates of Υ_1 and Υ_2 from combined synthetic pressure data and surface deformation (i.e. $\mathbf{d} = (\mathbf{d}_u, \mathbf{d}_p)$). In this experiment, we show the effect of the noise level on the estimation. Additionally, we numerically expose an apparent increase of the ill-posedness, in the sense of uniqueness, of the IP. Since the parameters $\Upsilon_1 = \log(K)$ and $\Upsilon_2 = \log(\lambda)$ are spatially varying functions, the lack of uniqueness is also experienced in the case of single-parameter estimation. In fact, nonuniqueness was observed in the experiments presented in sections 4.2.1 and 4.2.2. Indeed, both estimates and the truth are, within the noise level, solutions to the IP. Nevertheless, we are interested in recovering, at least partially, spatial features from the true properties. Intuitively, in the multiparameter estimation, one expects that ‘many more’ possible combinations of functions (Υ_1, Υ_2) can lead to the same data $\mathbf{d} = (\mathbf{d}_u, \mathbf{d}_p)$. In the experiment below, we show that completely inaccurate estimates can be obtained for large measurement errors.

The true log-perm Υ_2^\dagger and ‘true’ log-lambda Υ_1^\dagger are the fields displayed in figures 8 (top-left) and 9 (top), respectively. Synthetic data are generated with the same procedure as before. However, for this experiment we generated four sets of synthetic data corresponding to noise levels of 1%, 10%, 20% and 30% of the measurements. For all those sets, the CG algorithm is initialized with constant fields with values $\Upsilon_1(x, y) = 19.8 \log(\text{m}^2)$ ($(x, y) \in \Omega_1$) and $\Upsilon_2(x, y) = -27.6 \log(\text{m}^2)$ ($(x, y) \in \Omega_2$). For each set of data, the corresponding estimates (Υ_1, Υ_2) from the iterative scheme are presented from the second to fifth row of figures 8 and 9. In the second column of figure 8 we additionally present the restriction of Υ_1 to Ω_2 (the reservoir). The misfit between data and model predictions is displayed in figure 10 (left). The error of the estimates with respect to the truth is presented in figure 10 (right). The previous graph quantifies the detrimental effect of noise in the observations. In this case, the visual appreciation can be misleading. For example, one may argue that the permeability estimate obtained from data contaminated with 20% error provides a visually better estimate than the estimates obtained with smaller errors. However, in the joint estimation, one should expect a decrease in the total error which includes also the estimate of log-lambda. More precisely, the squared error in figure 10 (right) is defined by

$$\mathcal{E}(\Upsilon_1, \Upsilon_2)^2 = \mathcal{E}_1(\Upsilon_1)^2 + \mathcal{E}_2(\Upsilon_2)^2 \quad (83)$$

with \mathcal{E}_1 and \mathcal{E}_2 as defined in (82) and (81), respectively. It is also interesting to observe, from figure 10 (left), that the data misfit decreases and stagnates at a value which satisfies the discrepancy principle for $\tau = 2.6$ (1%), $\tau = 0.975$ (10%), $\tau = 0.98$ (20%), and $\tau = 0.97$ (30%). Similar values of τ were also found in [17, 18], where iterative regularization techniques were applied to parameter identification in reservoir models [17, 18]. Moreover, as indicated in [15], it is possible to obtain decrease of the error for τ s smaller than the ones predicted by the theory (see corollary 3.1).

We now compare the performance of the Newton-CG scheme for producing estimates in the case of multiparameter estimation against the single-parameter estimation case of the previous subsections. We emphasize that those single-parameter estimation examples differ substantially from multiparameter estimation. In other words, they are all different inverse problems. The aim here is to show the suboptimal performance of the multiparameter case. To

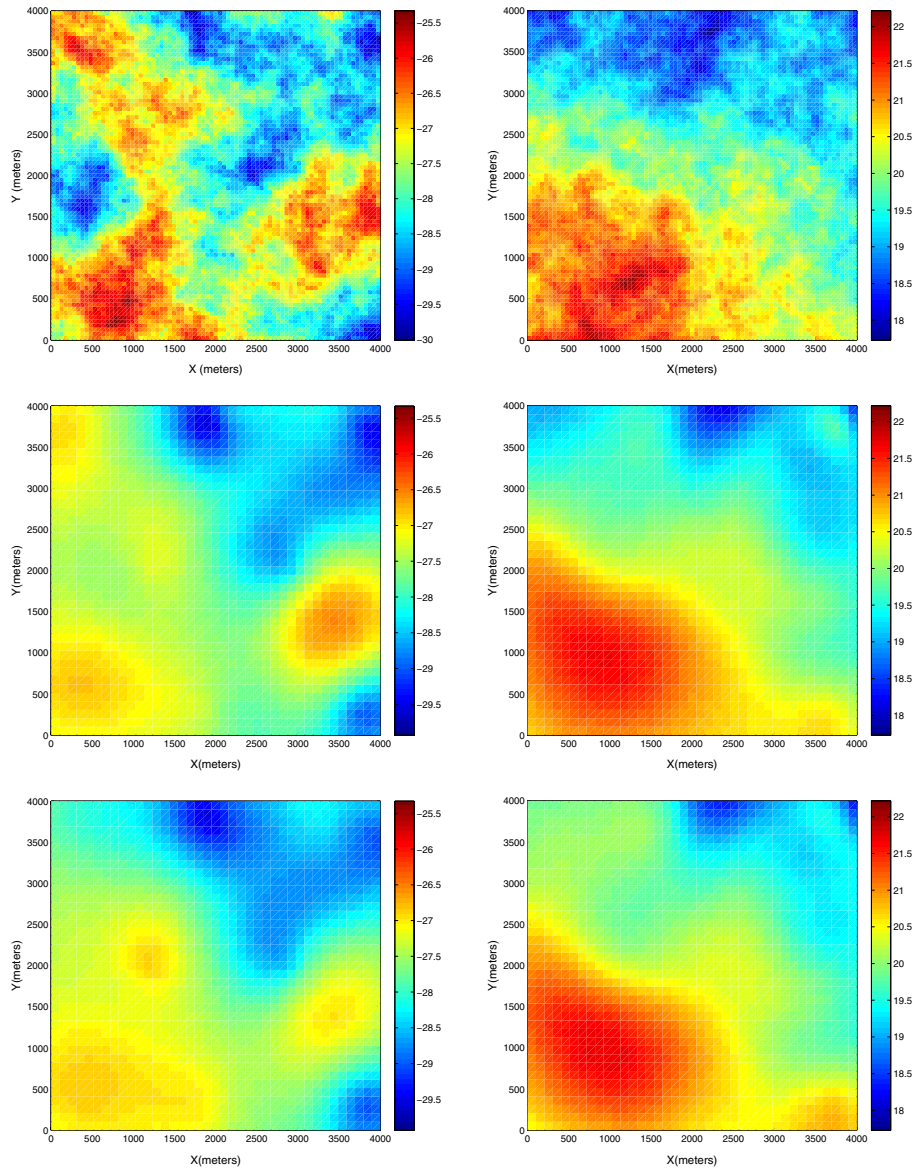


Figure 8. Estimation of $\Upsilon = (\Upsilon_1, \Upsilon_2) = (\log(\lambda), \log(K))$. Left column, from top to bottom: true log-perm (Υ_2^*) ($\log(\text{m}^2)$), estimates Υ_2 ($\log(\text{m}^2)$) obtained from inverting synthetic data contaminated with 1%, 10%, 20% and 30% of measurement error. Right column, from top to bottom: true log-lambda in Ω_2 ($\Upsilon_1^*|_{\Omega_2}$) ($\log(\text{Pa})$), estimates $\Upsilon_1|_{\Omega_2}$ ($\log(\text{Pa})$) obtained from inverting synthetic data contaminated with 1%, 10%, 20% and 30% of measurement error.

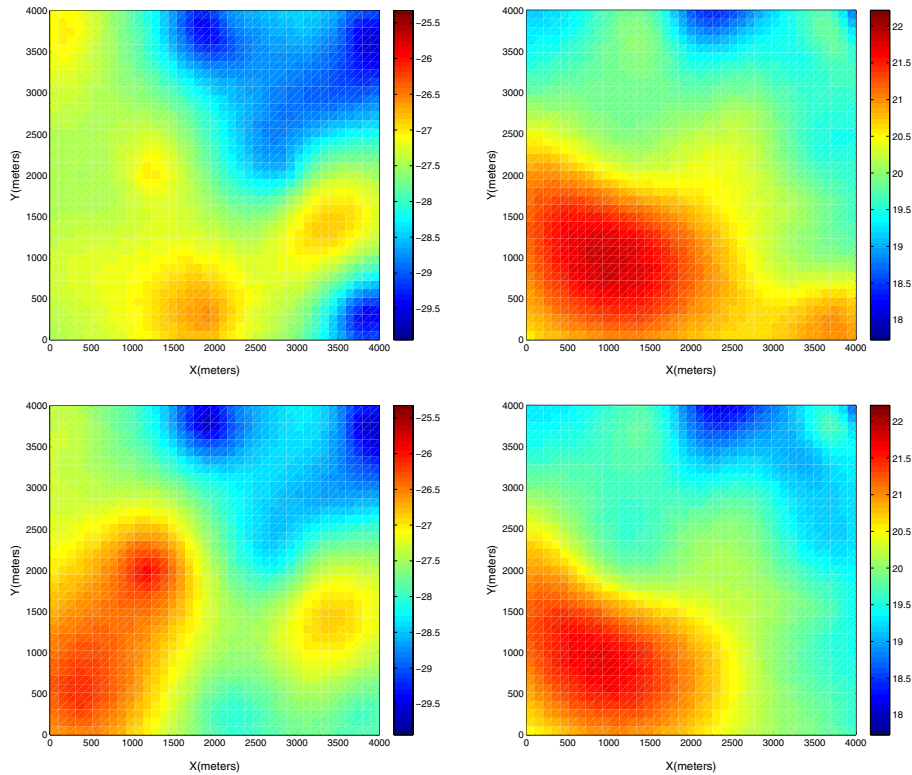


Figure 8. (Continued.)

the left (respectively right) of figure 11 we display the comparison in the norm (81) (respectively (82)) when multiparameter estimation is compared to single parameter-estimation for $\log(K)$ (respectively $\log(\lambda)$). Both, visually and quantitatively, the multiparameter estimate provides suboptimal results with respect to the single-parameter estimation case.

We finally remark that, for the multi-parameter case, the estimation of both parameters depends on the relative magnitudes of the norms in (32) (recall $\kappa = 1$ for this experiment). Then, by modifying κ in (32), more weight can be given to one or the other parameter based on the prior knowledge of the subsurface properties. To the best of our knowledge, in the context of inverting properties in geomechanics-flow model, the optimal choice of the weighting factor between the two subsurface properties is an open problem.

4.3. Conclusions and future work

Our synthetic experiments suggest that elastic and rock properties of the subsurface can be estimated via data inversion of coupled flow-geomechanics models. In the single-parameter estimation case, when both surface deformation and pressure data are inverted, more accurate estimates of permeability were obtained with respect to the ones obtained from only inverting pressure data. Furthermore, reasonable estimates of one of the elastic moduli were accomplished in the single-parameter case. In the multi-parameter case, suboptimal joint estimates of $\log(K)$ and $\log(\lambda)$ were obtained with respect to the single-parameter estimates.

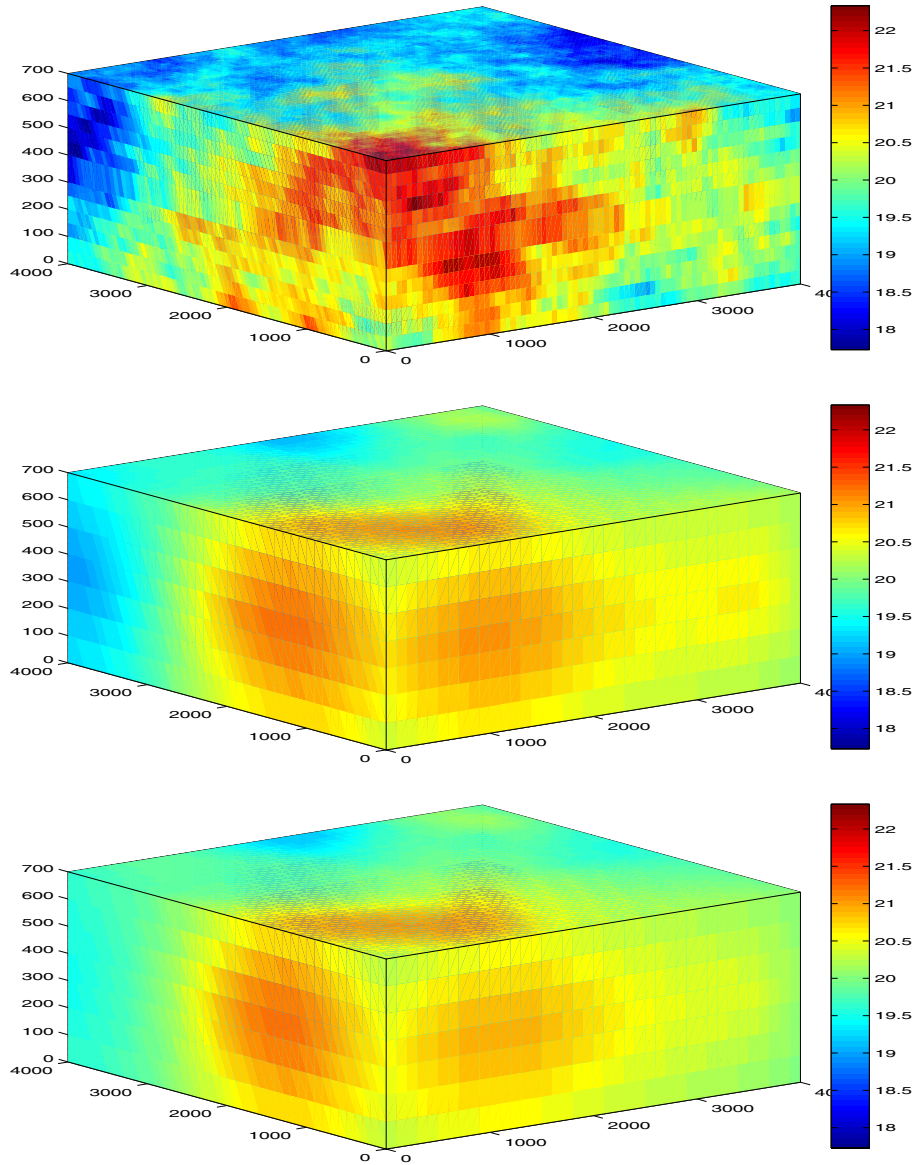


Figure 9. Estimation of $\Upsilon = (\Upsilon_1, \Upsilon_2) = (\log(\lambda), \log(K))$. From top to bottom: true log-lambda Υ_1^* (log(Pa)), and estimates Υ_1 (log(Pa)) obtained from inverting synthetic data contaminated with 1%, 10%, 20% and 30% of measurement error.

Nevertheless, those suboptimal estimates displayed some of the spatial features of the true properties. The lack of accuracy of the estimates in the multi-parameter case was presumably associated with the increase of ill-posedness (non-uniqueness) with respect to the single-parameter case.

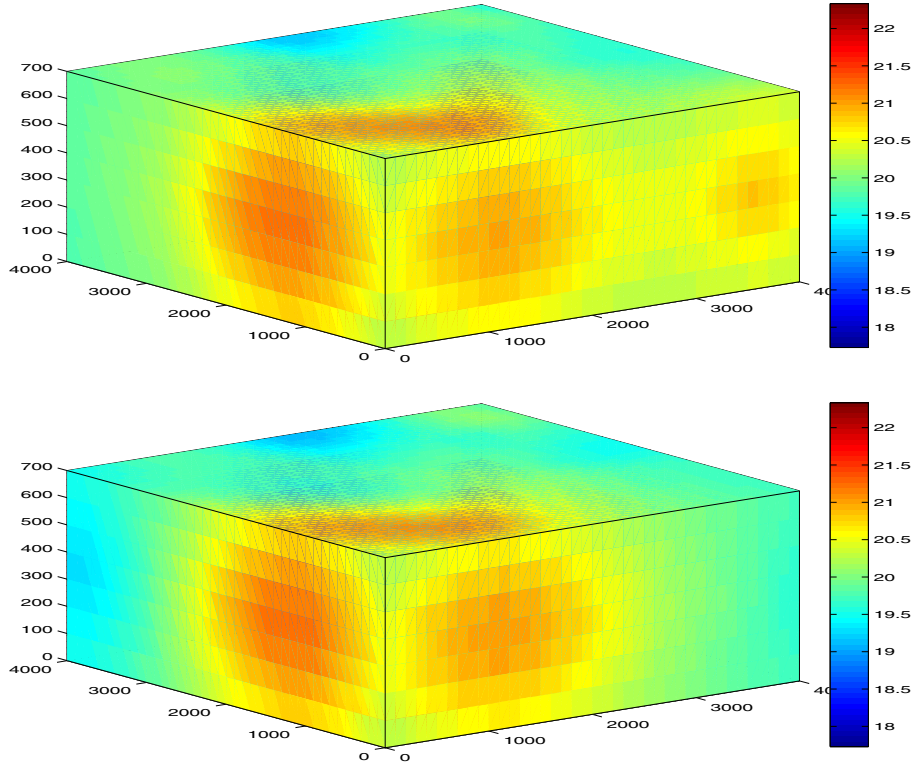


Figure 9. (Continued.)

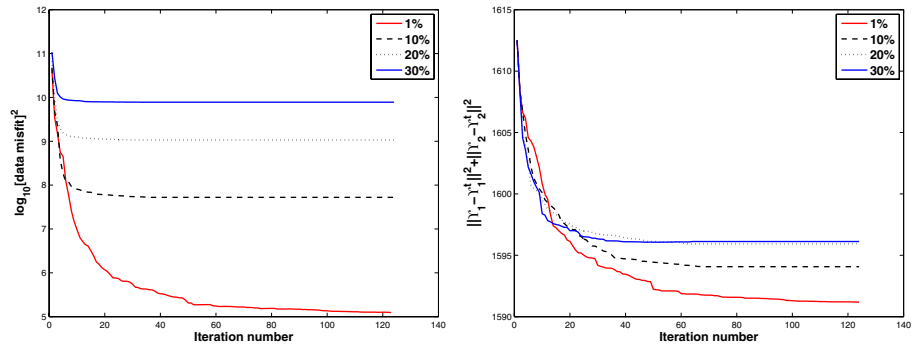


Figure 10. Performance of the estimation of $\Upsilon = (\Upsilon_1, \Upsilon_2) = (\log(\lambda), \log(K))$ for different noise levels. Left: \log_{10} squared data misfit. Right: error.

As we expect from the theoretical results of section 3, the utilized Newton-CG algorithm provided stable computational solutions of the IP. More precisely, the stopping criteria (discrepancy principle) of the scheme ensured that the decrease of the data misfit corresponded to a decrease in the error of the estimate with respect to the solution to the IP. Moreover, when

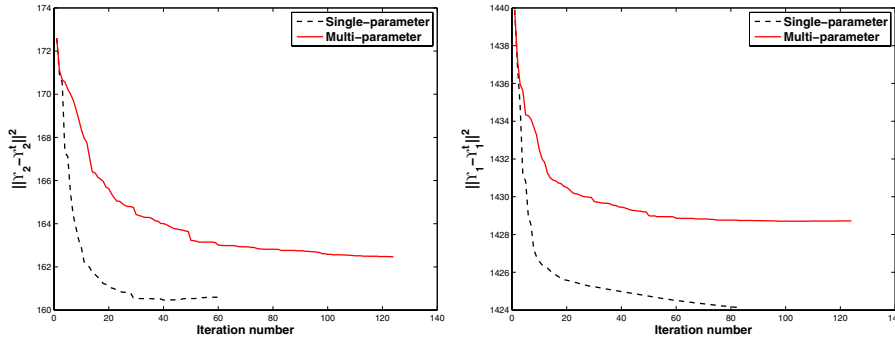


Figure 11. Performance comparison: multi-parameter versus single-parameter. Left: error \mathcal{E}_2 obtained from multiparameter estimation versus \mathcal{E}_2 obtained when only Υ_2 is estimated and Υ_1 is known. Right: error \mathcal{E}_1 obtained from multiparameter estimation versus \mathcal{E}_1 obtained when only Υ_1 is estimated and Υ_2 is known.

this criterion is not enforced, we observe divergence of the estimate from the solution to the IP. Finally, our experiments showed that the quality of the estimate improves for smaller noise levels. This constitutes the numerical evidence of the convergence with respect to the noise level predicted by corollary 3.1. In summary, our experiments show that the application of the Newton-CG algorithm of [15] provided the regularization required to find computational solutions to the IP. However, the properties of the forward operator studied in this work are suitable for the application of a broad spectrum of regularization techniques [19].

The model under consideration [13] provided valuable insight into the theoretical and computational aspects of inverting geodetic and production data to estimate subsurface properties. However, more challenging forward models are often encountered in applications where the interaction of multi-phase flow needs to be described. The research and development of simulators for such applications is advancing rapidly. It is therefore relevant to contribute with ideas toward the development of the corresponding inverse models.

5. Proofs

From Korn’s inequality [4] and Cauchy–Schwartz we know that there exist constants κ_1 and κ_2 such that

$$\kappa_1 \|\mathbf{w}\|_{H^1(\Omega_1)^3}^2 \leq \int_{\Omega} \boldsymbol{\epsilon}(\mathbf{w}) : \boldsymbol{\epsilon}(\mathbf{w}) \leq \kappa_2 \|\mathbf{w}\|_{H^1(\Omega_1)^3}^2 \tag{84}$$

for all $\mathbf{w} \in \{\mathbf{v} \in (H^1(\Omega_1))^3 : \boldsymbol{\gamma}_{\Gamma_D}(\mathbf{v}) = 0\}$.

For the sake of clarity, in the subsequent analysis, the notation for the norms of the spaces $H^k(0, T; H^j(\Omega_i))$ defined in section 2.2 will be simplified. More precisely, we define

$$\|p\|_{H^k(H^j(\Omega_i))} \equiv \|p\|_{H^k(0,T;H^j(\Omega_i))}. \tag{85}$$

We additionally define

$$\mathcal{A} \equiv \{\Omega_1, \Omega_2, \hat{\mathbf{Y}}, r, M, b, v, \mu, T\}. \tag{86}$$

In order to prove differentiability of the forward operator F , we first need the following proposition.

5.1. Proof of proposition 2.1

Let $\hat{\Upsilon} \in \mathcal{K}$ and $r > 0$. Let $\Upsilon = (\Upsilon_1, \Upsilon_2) \in B(\hat{\Upsilon}, r)$ and consider (43)–(44). The existence and uniqueness of $\mathbf{h}(\Upsilon) \equiv (\mathbf{u}, p) \in H^1(0, T; \mathbf{H}_0) \times (H^1(0, T; L^2(\Omega_2)) \cap L^\infty(0, T; H^1(\Omega_2)))$ that solves (43)–(44) follows directly from [13, theorem 2.1]. Note that $\lambda(x) = e^{\Upsilon_1(x)} > 0$ for all $x \in \Omega_1$, and (from our choice) $\lambda \in \mathcal{K}_1 \hookrightarrow C(\bar{\Omega})$. Then, coercivity and continuity of the bilinear form (43) can be established from standard arguments as for the case of constant λ of [13]. In addition, from our selection $\Upsilon_2 \in \mathcal{K}_2$, the embedding $\mathcal{K}_2 \hookrightarrow C^1(\bar{\Omega}_2)$ and the fact that $\mathbf{u} \in H^1(0, T; \mathbf{H}_0)$, it follows from [24] that $p \in H^{2,1}(\Omega_2 \times [0, T])$, where [24]

$$H^{2,1}(\Omega_2 \times [0, T]) \equiv L^2(0, T; H^2(\Omega_2)) \cap H^1(0, T; L^2(\Omega_2)) \tag{87}$$

with norm (24). Additionally, it can be shown [17, corollary 3.1] that

$$\begin{aligned} \|p\|_{H^{2,1}(\Omega_2 \times [0, T])} &\leq C \left\| \left| b \frac{\partial(\nabla \cdot \mathbf{u})}{\partial t} + f_3 \right| \right\|_{L^2(0, T; L^2(\Omega_2))} \\ &\leq C (b \|\mathbf{u}\|_{H^1(0, T; H^1(\Omega_1))} + \|f_3\|_{L^2(0, T; L^2(\Omega_2))}), \end{aligned} \tag{88}$$

where C may depend only on $\Omega_2, \hat{\Upsilon}, T$ and r . In other words, estimate (88) holds uniformly in $B(\hat{\Upsilon}, r)$.

The following proof consists of using the variational formulation (43)–(44) to find error estimates for p and \mathbf{u} that will lead to (45). Let us take $(\mathbf{w}, w) = (\frac{\partial \mathbf{u}}{\partial t}, p)$ in (43)–(44) to find

$$\begin{aligned} \frac{1}{2} \frac{d}{dt} \int_{\Omega_1} e^{\Upsilon_1} (\nabla \cdot \mathbf{u})^2 + \frac{1}{2} \frac{d}{dt} \int_{\Omega_1} \mu \boldsymbol{\epsilon}(\mathbf{u}) : \boldsymbol{\epsilon}(\mathbf{u}) - \int_{\Omega_2} b p \nabla \cdot \frac{\partial \mathbf{u}}{\partial t} \\ = \int_{\Omega_1} \mathbf{f}_1 \cdot \frac{\partial \mathbf{u}}{\partial t} + \int_{\Omega_1} f_2 \nabla \cdot \frac{\partial \mathbf{u}}{\partial t}, \end{aligned} \tag{89}$$

$$\frac{1}{M} \frac{1}{2} \frac{d}{dt} \int_{\Omega_2} p^2 + \int_{\Omega_2} v^{-1} e^{\Upsilon_2} |\nabla p|^2 + \int_{\Omega_2} b \frac{\partial(\nabla \cdot \mathbf{u})}{\partial t} p = \int_{\Omega_2} f_3 p. \tag{90}$$

We integrate the previous expressions from 0 to t and integrate by parts (with respect to time) the right-hand side of (89). We additionally use that $\mathbf{u}(\cdot, 0) = 0$ and add the resulting expressions to arrive at

$$\begin{aligned} \frac{1}{2} \int_{\Omega_1} e^{\Upsilon_1} (\nabla \cdot \mathbf{u})^2 + \frac{1}{2} \int_{\Omega_1} \mu \boldsymbol{\epsilon}(\mathbf{u}) : \boldsymbol{\epsilon}(\mathbf{u}) + \frac{1}{M} \frac{1}{2} \int_{\Omega_2} p^2 + \int_0^t \int_{\Omega_2} v^{-1} e^{\Upsilon_2} |\nabla p|^2 = \frac{1}{M} \frac{1}{2} \int_{\Omega_2} p_0^2 \\ + \int_0^t \int_{\Omega_2} f_3 p + \int_{\Omega_1} \mathbf{f}_1(t) \cdot \mathbf{u}(t) + \int_{\Omega_1} f_2(t) \nabla \cdot \mathbf{u}(t) \\ - \int_0^t \int_{\Omega_1} \frac{\partial \mathbf{f}_1}{\partial t} \cdot \mathbf{u} - \int_0^t \int_{\Omega_1} \frac{\partial f_2}{\partial t} \nabla \cdot \mathbf{u}. \end{aligned} \tag{91}$$

Therefore,

$$\begin{aligned} \frac{1}{2} \int_{\Omega_1} e^{\Upsilon_1} (\nabla \cdot \mathbf{u})^2 + \frac{1}{2} \int_{\Omega_1} \mu \boldsymbol{\epsilon}(\mathbf{u}) : \boldsymbol{\epsilon}(\mathbf{u}) + \frac{1}{M} \frac{1}{2} \int_{\Omega_2} p^2 + \int_0^t \int_{\Omega_2} v^{-1} e^{\Upsilon_2} |\nabla p|^2 \\ \leq \frac{1}{M} \frac{1}{2} \|p_0\|_{L^2(\Omega_2)}^2 + \int_0^t \|f_3\|_{L^2(\Omega_2)} \|p\|_{L^2(\Omega_2)} + \|\mathbf{f}_1(t)\|_{L^2(\Omega_1)} \|\mathbf{u}(t)\|_{L^2(\Omega_1)} \\ + \|f_2(t)\|_{L^2(\Omega_1)} \|\nabla \cdot \mathbf{u}(t)\|_{L^2(\Omega_1)} + \int_0^t \left\| \frac{\partial \mathbf{f}_1}{\partial t} \right\|_{L^2(\Omega_1)} \|\mathbf{u}\|_{L^2(\Omega_1)} \\ + \int_0^t \left\| \frac{\partial f_2}{\partial t} \right\|_{L^2(\Omega_1)} \|\nabla \cdot \mathbf{u}\|_{L^2(\Omega_1)}. \end{aligned}$$

From standard computations and (84), we have

$$\begin{aligned} \|\mathbf{u}(t)\|_{H^1(\Omega_1)} \leq & C \left(\|p_0\|_{H^1(\Omega_2)}^2 + \int_0^T \|f_3\|_{L^2(\Omega_2)} \|p\|_{L^2(\Omega_2)} + \|\mathbf{f}_1(t)\|_{L^2(\Omega_1)} \|\mathbf{u}(t)\|_{L^2(\Omega_1)} \right. \\ & + \|f_2(t)\|_{L^2(\Omega_1)} \|\nabla \cdot \mathbf{u}(t)\|_{L^2(\Omega_1)} + \int_0^T \left\| \frac{\partial \mathbf{f}_1}{\partial t} \right\|_{L^2(\Omega_1)} \|\mathbf{u}\|_{L^2(\Omega_1)} \\ & \left. + \int_0^T \left\| \frac{\partial f_2}{\partial t} \right\|_{L^2(\Omega_1)} \|\nabla \cdot \mathbf{u}\|_{L^2(\Omega_1)} \right), \end{aligned}$$

where C depends only on \mathcal{A} in (86). Integrating again and repeatedly applying Cauchy–Schwartz yields

$$\begin{aligned} \|\mathbf{u}\|_{L^2(H^1(\Omega_1))}^2 \leq & C (\|p_0\|_{H^1(\Omega_2)}^2 + \|f_3\|_{L^2(L^2(\Omega_2))} \|p\|_{L^2(L^2(\Omega_2))} \\ & + (\|\mathbf{f}_1\|_{H^1(L^2(\Omega_1))} + \|f_2\|_{H^1(L^2(\Omega_1))}) \|\mathbf{u}\|_{L^2(H^1(\Omega_1))}) \end{aligned}$$

which from (88) can be written as

$$\begin{aligned} \|\mathbf{u}\|_{L^2(H^1(\Omega_1))}^2 \leq & C (\|p_0\|_{H^1(\Omega_2)}^2 + \|f_3\|_{L^2(L^2(\Omega_2))}^2 \\ & + (\|\mathbf{f}_1\|_{H^1(L^2(\Omega_1))} + \|f_2\|_{H^1(L^2(\Omega_1))} + \|f_3\|_{L^2(L^2(\Omega_2))}) \|\mathbf{u}\|_{H^1(H^1(\Omega_1))}), \end{aligned} \tag{92}$$

where C depends only on \mathcal{A} . We now formally differentiate (43) with respect to time and take

$(\mathbf{w}, w) = \left(\frac{\partial \mathbf{u}}{\partial t}, \frac{\partial p}{\partial t}\right)$ to find

$$\begin{aligned} \int_{\Omega_1} e^{\gamma_1} \left(\nabla \cdot \frac{\partial \mathbf{u}}{\partial t}\right)^2 + \int_{\Omega_1} e^{\gamma_2} \epsilon \left(\frac{\partial \mathbf{u}}{\partial t}\right) : \epsilon \left(\frac{\partial \mathbf{u}}{\partial t}\right) - \int_{\Omega_2} b \frac{\partial p}{\partial t} \nabla \cdot \frac{\partial \mathbf{u}}{\partial t} \\ = \int_{\Omega_1} \frac{\partial \mathbf{f}_1}{\partial t} \cdot \frac{\partial \mathbf{u}}{\partial t} + \int_{\Omega_1} \frac{\partial f_2}{\partial t} \nabla \cdot \frac{\partial \mathbf{u}}{\partial t}, \\ \int_{\Omega_2} \frac{1}{M} \left[\frac{\partial p}{\partial t}\right]^2 + \frac{d}{dt} \int_{\Omega_2} \nu^{-1} e^{\gamma_2} |\nabla p|^2 + \int_{\Omega_2} b \frac{\partial \nabla \cdot \mathbf{u}}{\partial t} \frac{\partial p}{\partial t} = \int_{\Omega_2} f_3 \frac{\partial p}{\partial t}. \end{aligned}$$

Adding the equations above and integrating from 0 to t , we obtain

$$\begin{aligned} \int_0^t \int_{\Omega_1} e^{\gamma_1} \left[\nabla \cdot \frac{\partial \mathbf{u}}{\partial t}\right]^2 + \int_0^t \int_{\Omega_1} 2\mu \epsilon \left(\frac{\partial \mathbf{u}}{\partial t}\right) : \epsilon \left(\frac{\partial \mathbf{u}}{\partial t}\right) + \int_0^t \int_{\Omega_2} \frac{1}{M} \left[\frac{\partial p}{\partial t}\right]^2 + \int_{\Omega_2} \nu^{-1} e^{\gamma_2} |\nabla p|^2 \\ = \int_0^t \int_{\Omega_2} f_3 \frac{\partial p}{\partial t} + \int_{\Omega_2} \nu^{-1} e^{\gamma_2} |\nabla p_0|^2 + \int_0^t \int_{\Omega_1} \frac{\partial \mathbf{f}_1}{\partial t} \cdot \frac{\partial \mathbf{u}}{\partial t} + \int_0^t \int_{\Omega_1} \frac{\partial f_2}{\partial t} \nabla \cdot \frac{\partial \mathbf{u}}{\partial t}. \end{aligned} \tag{93}$$

We apply (84) and Cauchy–Schwartz in the previous expression (for $t = T$) to find

$$\begin{aligned} \left\| \frac{\partial \mathbf{u}}{\partial t} \right\|_{L^2(H^1(\Omega_1))}^2 \leq & C \left(\|f_3\|_{L^2(L^2(\Omega_2))} \left\| \frac{\partial p}{\partial t} \right\|_{L^2(L^2(\Omega_2))} + \|p_0\|_{H^1(\Omega_2)}^2 \right. \\ & \left. + (\|\mathbf{f}_1\|_{H^1(L^2(\Omega_1))} + \|f_2\|_{H^1(L^2(\Omega_1))}) \left\| \frac{\partial \mathbf{u}}{\partial t} \right\|_{L^2(H^1(\Omega_1))} \right), \end{aligned} \tag{94}$$

where C depends only on \mathcal{A} . From the previous inequality, it follows trivially that

$$\begin{aligned} \left\| \frac{\partial \mathbf{u}}{\partial t} \right\|_{L^2(H^1(\Omega_1))}^2 \leq & C (\|f_3\|_{L^2(L^2(\Omega_2))} \|p\|_{H^{2,1}(\Omega_2 \times [0,T])} + \|p_0\|_{H^1(\Omega_2)}^2 \\ & + (\|\mathbf{f}_1\|_{H^1(L^2(\Omega_1))} + \|f_2\|_{H^1(L^2(\Omega_1))}) \|\mathbf{u}\|_{H^1(H^1(\Omega_1))}) \end{aligned}$$

which from (88) becomes

$$\begin{aligned} \left\| \frac{\partial \mathbf{u}}{\partial t} \right\|_{L^2(H^1(\Omega_1))}^2 \leq & C (\|f_3\|_{L^2(L^2(\Omega_2))}^2 + \|p_0\|_{H^1(\Omega_2)}^2 \\ & + (\|\mathbf{f}_1\|_{H^1(L^2(\Omega_1))} + \|f_2\|_{H^1(L^2(\Omega_1))} + \|f_3\|_{L^2(L^2(\Omega_2))}) \|\mathbf{u}\|_{H^1(H^1(\Omega_1))}). \end{aligned}$$

By combining the previous inequality with (92) and applying Cauchy’s inequality, we find

$$\begin{aligned} \|\mathbf{u}\|_{H^1(H^1(\Omega_1))}^2 &\leq C \left(\|p_0\|_{H^1(\Omega_2)}^2 + \|f_3\|_{L^2(L^2(\Omega_2))}^2 \right. \\ &\quad \left. + \frac{1}{2\epsilon} [\|\mathbf{f}_1\|_{H^1(L^2(\Omega_1))}^2 + \|f_2\|_{H^1(L^2(\Omega_1))}^2 + \|f_3\|_{L^2(L^2(\Omega_2))}^2] + \frac{3}{2}\epsilon \|\mathbf{u}\|_{H^1(H^1(\Omega_1))}^2 \right), \end{aligned}$$

for all $\epsilon > 0$ and for some C that depends only on \mathcal{A} . Then, for ϵ sufficiently small we have

$$\|\mathbf{u}\|_{H^1(H^1(\Omega_1))}^2 \leq C(\|p_0\|_{H^1(\Omega_2)}^2 + \|f_3\|_{L^2(L^2(\Omega_2))}^2 + \|\mathbf{f}_1\|_{H^1(L^2(\Omega_1))}^2 + \|f_2\|_{H^1(L^2(\Omega_1))}^2), \tag{95}$$

where C depends only on \mathcal{A} .

From (33) and the fact that $\Upsilon \in B(\hat{\Upsilon}, r)$ it follows

$$\|\Upsilon_2 - \hat{\Upsilon}_2\|_{C^1(\bar{\Omega})} \leq C_e \|\Upsilon_2 - \hat{\Upsilon}_2\|_{\mathcal{K}_2} \leq C_e r.$$

In particular, $|\Upsilon_2(x) - \hat{\Upsilon}_2(x)| \leq C_e r$ for all $x \in \Omega_2$. Therefore, from (93) we find

$$\begin{aligned} v^{-1} e^{-C_e r} e^{\hat{\Upsilon}_2} \int_{\Omega_2} |\nabla p|^2 &\leq \int_{\Omega_2} v^{-1} e^{-C_e r} e^{\hat{\Upsilon}_2} |\nabla p|^2 \leq \int_{\Omega_2} v^{-1} e^{\Upsilon_2} |\nabla p|^2 \\ &\leq \int_0^t \int_{\Omega_2} f_3 \frac{\partial p}{\partial t} + \int_{\Omega_2} v^{-1} e^{\Upsilon_2} |\nabla p_0|^2 \\ &\quad + \int_0^t \int_{\Omega_1} \frac{\partial \mathbf{f}_1}{\partial t} \cdot \frac{\partial \mathbf{u}}{\partial t} + \int_0^t \int_{\Omega_1} \frac{\partial f_2}{\partial t} \nabla \cdot \frac{\partial \mathbf{u}}{\partial t}, \end{aligned} \tag{96}$$

where $\hat{\Upsilon}_{2,*} \equiv \min_{x \in \Omega_2} \{\hat{\Upsilon}_2(x)\}$. Then, from similar computations that led to (95), we arrive at

$$\int_{\Omega_2} |\nabla p(\cdot, t)|^2 \leq C(\|p_0\|_{H^1(\Omega_2)}^2 + \|f_3\|_{L^2(L^2(\Omega_2))}^2 + \|\mathbf{f}_1\|_{H^1(L^2(\Omega_1))}^2 + \|f_2\|_{H^1(L^2(\Omega_1))}^2)$$

a.e. in $[0, T]$ where C may depend only on \mathcal{A} . From (91) a similar estimate for $\int_{\Omega_2} |p(\cdot, t)|^2$ a.e. in $[0, T]$ can also be shown. Therefore,

$$\|p\|_{L^\infty(0,T;H^1(\Omega_2))} \leq C(\|p_0\|_{H^1(\Omega_2)}^2 + \|f_3\|_{L^2(L^2(\Omega_2))}^2 + \|\mathbf{f}_1\|_{H^1(L^2(\Omega_1))}^2 + \|f_2\|_{H^1(L^2(\Omega_1))}^2). \tag{97}$$

We combine (95) with (88) and (97) to finalize the proof .

5.2. Proof of theorem 2.1

Consider the following observation.

Observation 1. *It is straightforward to show that the exponential operators $e^{\Upsilon_1} : C(\bar{\Omega}) \rightarrow C(\bar{\Omega})$ and $e^{\Upsilon_2} : C^1(\bar{\Omega}_2) \rightarrow C^1(\bar{\Omega}_2)$ are continuously Frechet differentiable. From the assumed embedding $\mathcal{K}_1 \hookrightarrow C(\bar{\Omega})$ and $\mathcal{K}_2 \hookrightarrow C^1(\bar{\Omega}_2)$, it follows easily that $e^{\Upsilon_1} : \mathcal{K}_1 \rightarrow C(\bar{\Omega}_1)$ and $e^{\Upsilon_2} : \mathcal{K}_2 \rightarrow C^1(\bar{\Omega}_2)$ are also continuously Frechet differentiable.*

We now prove the following lemma.

Lemma 5.1. *Let $G : \mathcal{K} \rightarrow \mathcal{H}$ be the mapping $G(\Upsilon) = \mathbf{h} \equiv (\mathbf{u}, p)$ given by the solution to the variational model (41)–(42). G is continuous in \mathcal{K} .*

Proof. Let $\Upsilon \in \mathcal{K}$ and $\epsilon > 0$. Let $\mathbf{h} = (\mathbf{u}, p)$ as above. Let $C > 0$ be the constant granted by proposition 2.1 applied to $B(\Upsilon, 1)$. Define

$$A \equiv C^2(1 + 2v^{-1})(\|p_0\|_{H^1(\Omega_2)} + \|q\|_{L^2(L^2(\Omega_2))} + \|\mathbf{f}\|_{H^1(L^2(\Omega_1))}). \tag{98}$$

From observation 1, we take $\tilde{\delta} > 0$ such that

$$\|e^{\tilde{\Upsilon}_1} - e^{\Upsilon_1}\|_{C(\bar{\Omega}_1)} + \|e^{\tilde{\Upsilon}_2} - e^{\Upsilon_2}\|_{C^1(\bar{\Omega}_2)} \leq \frac{\epsilon}{A}, \tag{99}$$

provided that

$$\|\tilde{\Upsilon}_1 - \Upsilon_1\|_{\mathcal{K}_1} + \|\tilde{\Upsilon}_2 - \Upsilon_2\|_{\mathcal{K}_2} < \tilde{\delta}. \tag{100}$$

Let $\delta \equiv \min\{1, \tilde{\delta}\}$. Proposition 2.1 ensures that for every $\tilde{\Upsilon} \in \mathcal{K}$ with $\|\Upsilon - \tilde{\Upsilon}\|_{\mathcal{K}} \leq \delta$,

$$\|\tilde{\mathbf{h}}\|_{\mathcal{H}} \leq C\left(\|p_0\|_{H^1(\Omega_2)} + \|q\|_{L^2(L^2(\Omega_2))} + \|\mathbf{f}\|_{H^1(L^2(\Omega_1))}\right), \tag{101}$$

where $\tilde{\mathbf{h}}(\tilde{\Upsilon}) = (\tilde{\mathbf{u}}, \tilde{p})$ is the solution to (41)–(42) for $\tilde{\Upsilon}$. Moreover, from (41)–(42) it is not difficult to see that $\mathbf{h} - \tilde{\mathbf{h}}$ satisfies

$$L(\Upsilon_1, \mathbf{u} - \tilde{\mathbf{u}}, \mathbf{w}) - \int_{\Omega_2} b[p - \tilde{p}]\nabla \cdot \mathbf{w} = \int_{\Omega_1} \left[(e^{\tilde{\Upsilon}_1} - e^{\Upsilon_1})(\nabla \cdot \tilde{\mathbf{u}})(\nabla \cdot \mathbf{w}), \tag{102}$$

$$\begin{aligned} & \int_{\Omega_2} \frac{1}{M} \frac{\partial [p - \tilde{p}]}{\partial t} w + \int_{\Omega_2} v^{-1} e^{\Upsilon_2} \nabla \cdot [p - \tilde{p}] \cdot \nabla w + \int_{\Omega_2} b \frac{\partial \nabla \cdot [\mathbf{u} - \tilde{\mathbf{u}}]}{\partial t} w \\ & = - \int_{\Omega_2} v^{-1} w \nabla \cdot (e^{\tilde{\Upsilon}_2} - e^{\Upsilon_2}) \nabla \tilde{p}, \end{aligned} \tag{103}$$

for all $(\mathbf{w}, w) \in \mathcal{W}$. The right-hand side of (103) has been obtained after integrating by parts and using the boundary condition (9). Proposition 2.1 can be now applied to (102)–(103). Therefore,

$$\|\mathbf{h} - \tilde{\mathbf{h}}\|_{\mathcal{H}} \leq C\left(\|f_2\|_{H^1(L^2(\Omega_1))} + \|\mathbf{f}_3\|_{L^2(L^2(\Omega_2))}\right), \tag{104}$$

where

$$f_2 = (e^{\tilde{\Upsilon}_1} - e^{\Upsilon_1}) \nabla \cdot \tilde{\mathbf{u}}, \quad \mathbf{f}_3 = -v^{-1} \nabla \cdot (e^{\tilde{\Upsilon}_2} - e^{\Upsilon_2}) \nabla \tilde{p}. \tag{105}$$

From (105) and some simple computations, we find

$$\|\mathbf{h} - \tilde{\mathbf{h}}\|_{\mathcal{H}} \leq C\left(\|e^{\tilde{\Upsilon}_1} - e^{\Upsilon_1}\|_{C(\bar{\Omega}_1)} \|\tilde{\mathbf{u}}\|_{H^1(H^1(\Omega_1))} + 2v^{-1} \|e^{\tilde{\Upsilon}_2} - e^{\Upsilon_2}\|_{C^1(\bar{\Omega}_2)} \|\tilde{p}\|_{L^2(H^2(\Omega_2))}\right). \tag{106}$$

Note that, from proposition 2.1, the constant C in (104) (and therefore in (106)) is the same as in (101). We finally combined (106) with (98), (99) and (101) to obtain

$$\|\mathbf{h} - \tilde{\mathbf{h}}\|_{\mathcal{H}} \leq C \frac{\epsilon}{A} (1 + 2v^{-1}) \|\tilde{\mathbf{h}}\|_{\mathcal{H}} \leq \epsilon, \tag{107}$$

which proves the continuity of G at an arbitrary $\Upsilon \in \mathcal{K}$. □

For $\Upsilon_i, \tilde{\Upsilon}_i \in \mathcal{K}_i$ ($i \in \{1, 2\}$). Let us define the residuals

$$R(\Upsilon_i, \tilde{\Upsilon}_i) \equiv e^{\tilde{\Upsilon}_i} - e^{\Upsilon_i} - (\tilde{\Upsilon}_i - \Upsilon_i) e^{\Upsilon_i}. \tag{108}$$

Lemma 5.2. *Let $\Upsilon, \tilde{\Upsilon} \in \mathcal{K}$ and $\mathbf{h}(\Upsilon) = (\mathbf{u}, p)$, $\tilde{\mathbf{h}}(\tilde{\Upsilon}) = (\tilde{\mathbf{u}}, \tilde{p})$ be the corresponding solutions to (41)–(42). Let $\xi = (\xi_{\mathbf{u}}, \xi_p)$ be the solution to*

$$L_1(\Upsilon_1, \xi_{\mathbf{u}}, \mathbf{w}) - \int_{\Omega_2} b \xi_p \nabla \cdot \mathbf{w} + \int_{\Omega_1} (\tilde{\Upsilon}_1 - \Upsilon_1) e^{\Upsilon_1} (\nabla \cdot \mathbf{u})(\nabla \cdot \mathbf{w}) = 0, \tag{109}$$

$$\begin{aligned} & \int_{\Omega_2} \frac{1}{M} \frac{\partial \xi_p}{\partial t} w + \int_{\Omega_2} v^{-1} e^{\Upsilon_2} \nabla \xi_p \cdot \nabla w + \int_{\Omega_2} b \frac{\partial \nabla \cdot \xi_{\mathbf{u}}}{\partial t} w \\ & + \int_{\Omega_2} v^{-1} (\tilde{\Upsilon}_2 - \Upsilon_2) e^{\Upsilon_2} \nabla p \cdot \nabla w = 0, \end{aligned} \tag{110}$$

for all $(\mathbf{w}, w) \in \mathcal{W}$. Then, the residuals

$$\mathbf{r}_u \equiv \tilde{\mathbf{u}} - \mathbf{u} - \xi_u, \quad r_p \equiv \tilde{p} - p - \xi_p, \quad (111)$$

are the solutions to the following variational problem

$$\begin{aligned} L_1(\Upsilon_1, \mathbf{r}_u, \mathbf{w}) - \int_{\Omega_2} b r_p \nabla \cdot \mathbf{w} &= - \int_{\Omega_1} R(\Upsilon_1, \tilde{\Upsilon}_1) (\nabla \cdot \tilde{\mathbf{u}}) (\nabla \cdot \mathbf{w}) \\ &+ \int_{\Omega_1} (\Upsilon_1 - \tilde{\Upsilon}_1) e^{\Upsilon_1} (\nabla \cdot (\tilde{\mathbf{u}} - \mathbf{u})) (\nabla \cdot \mathbf{w}), \end{aligned} \quad (112)$$

$$\begin{aligned} \int_{\Omega_2} \frac{1}{M} \frac{\partial r_p}{\partial t} w + \int_{\Omega_2} v^{-1} e^{\Upsilon_2} \nabla r_p \cdot \nabla w + \int_{\Omega_2} b \frac{\partial \nabla \cdot \mathbf{r}_u}{\partial t} w &= - \int_{\Omega_2} v^{-1} R(\Upsilon_2, \tilde{\Upsilon}_2) \nabla \tilde{p} \cdot \nabla w \\ &+ \int_{\Omega_2} v^{-1} e^{\Upsilon_2} (\Upsilon_2 - \tilde{\Upsilon}_2) (\nabla \tilde{p} - \nabla p) \cdot \nabla w, \end{aligned} \quad (113)$$

a.e. in $(0, T]$ for all $(\mathbf{w}, w) \in \mathcal{W}$.

Proof. The proof is straightforward from (40), (41)–(42) and (53)–(54). \square

Proof of theorem 2.1. Let $\Upsilon \in \mathcal{K}$ be arbitrary but fixed and $\epsilon > 0$. Let $\mathbf{h} \equiv (\mathbf{u}, p)$ be the solution to (41)–(42) for all $\mathbf{W} \in \mathcal{W}$ a.e. $t \in (0, T]$. Let $\tilde{\Upsilon} \in \mathcal{K}$ be arbitrary and let $\tilde{\mathbf{h}} \equiv (\tilde{\mathbf{u}}, \tilde{p})$ be the corresponding solution to (41)–(42), for all $\mathbf{W} \in \mathcal{H}$ a.e. in $(0, T]$. Let C_e and C_S be given by (33) and (19), respectively. Define

$$\omega \equiv \max\{\|e^{\Upsilon_2}\|_{C^1(\bar{\Omega}_2)}, \|e^{\Upsilon_1}\|_{C(\bar{\Omega}_1)}\}, \quad (114)$$

and

$$A \equiv \left(\frac{1}{\sigma_p} \sum_{j=1}^N \|\delta(x - x^j)\|_{L^2(\Omega_2)}^2 dt + \frac{1}{\sigma_u} C_S \right)^{1/2} C(2v^{-1} + 1)(\|\mathbf{h}\|_{\mathcal{H}} + C_e \omega). \quad (115)$$

From the lemma 5.1, we take $\delta_1 > 0$ such that

$$\|\mathbf{h} - \tilde{\mathbf{h}}\|_{\mathcal{H}} \leq \frac{\epsilon}{A}, \quad (116)$$

provided $\|\tilde{\Upsilon} - \Upsilon\|_{\mathcal{K}} \leq \delta_1$. Consider the residuals defined in (108). From observation 1 let $\delta_2 > 0$ be such that

$$\|R(\Upsilon_1, \tilde{\Upsilon}_1)\|_{C(\bar{\Omega}_1)} \leq \frac{\epsilon}{A} \|[\tilde{\Upsilon}_1 - \Upsilon_1]\|_{\mathcal{K}_1} \quad (117)$$

$$\|R(\Upsilon_2, \tilde{\Upsilon}_2)\|_{C^1(\bar{\Omega}_2)} \leq \frac{\epsilon}{A} \|[\tilde{\Upsilon}_2 - \Upsilon_2]\|_{\mathcal{K}_2}, \quad (118)$$

provided that $\|\tilde{\Upsilon}_i - \Upsilon_i\|_{\mathcal{K}_i} \leq \delta_2$ ($i = 1, 2$). Let $C > 0$ be the constant from proposition 2.1 applied to $B(\Upsilon, \min\{\delta_1, \delta_2\})$. Then,

$$\|\tilde{\mathbf{h}}\|_{\mathcal{H}} \leq C(\|p_0\|_{H^1(\Omega_2)} + \|q\|_{L^2(L^2(\Omega_2))} + \|\mathbf{f}\|_{H^1(L^2(\Omega_1))}), \quad (119)$$

provided $\|\tilde{\Upsilon} - \Upsilon\|_{\mathcal{K}} \leq \min\{\delta_1, \delta_2\}$. Let $\xi = (\xi_u, \xi_p)$ be the solution to (109)–(110) that exists due to proposition 2.1. We now show that $DF(\Upsilon)(\tilde{\Upsilon} - \Upsilon) = (\mathcal{M}_u(\xi_u), \mathcal{M}_p(\xi_p))$. We first define the residuals $\mathbf{r} = (\mathbf{r}_u, r_p)$ (111), and note that

$$F(\tilde{\Upsilon}) - F(\Upsilon) - DF(\Upsilon)(\tilde{\Upsilon} - \Upsilon) = (\mathcal{M}_u(\mathbf{r}_u), \mathcal{M}_p(r_p)), \quad (120)$$

which from (46)–(50) becomes

$$\begin{aligned} \|F(\tilde{\Upsilon}) - F(\Upsilon) - DF(\Upsilon)(\tilde{\Upsilon} - \Upsilon)\|_{\mathcal{O}}^2 &= \frac{1}{\sigma_p} \int_0^T |\mathcal{M}_p(r_p)|^2 dt + \frac{1}{\sigma_u} \int_0^T \int_S |\mathcal{Y}_S(\mathbf{r}_u)|^2 d\sigma dt \\ &\leq \frac{1}{\sigma_p} \int_0^T \|r_p\|_{L^2(\Omega_2)}^2 \sum_{j=1}^N \|\delta(x - x^j)\|_{L^2(\Omega_2)}^2 dt + \frac{1}{\sigma_u} \int_0^T C_S \|\mathbf{r}_u\|_{H^1(\Omega_1)}^2 dt \\ &\leq \left(\frac{1}{\sigma_p} \sum_{j=1}^N \|\delta(x - x^j)\|_{L^2(\Omega_2)}^2 dt + \frac{1}{\sigma_u} C_S \right) \|\mathbf{r}\|_{\mathcal{H}}^2. \end{aligned} \tag{121}$$

The rest of the proof consist of finding a bound for $\|\mathbf{r}\|_{\mathcal{H}}^2$ so that the differentiability can be established. From lemma 5.2 we know that $\mathbf{r} = (\mathbf{r}_u, r_p)$ satisfy (112)–(113). So, we integrate by parts the right-hand side of (113) and apply the boundary condition (9) to find

$$\begin{aligned} \int_{\Omega_2} \frac{1}{M} \frac{\partial r_p}{\partial t} w + \int_{\Omega_2} v^{-1} e^{\Upsilon_2} \nabla r_p \cdot \nabla w + \int_{\Omega_2} b \frac{\partial(\nabla \cdot \mathbf{r}_u)}{\partial t} w &= \int_{\Omega_2} v^{-1} \nabla \cdot (R(\Upsilon_2, \tilde{\Upsilon}_2) \nabla \tilde{p}) w \\ &\quad - \int_{\Omega_2} v^{-1} \nabla \cdot (e^{\Upsilon_2} (\Upsilon_2 - \tilde{\Upsilon}_2) (\nabla \tilde{p} - \nabla p)) w. \end{aligned} \tag{122}$$

It is not difficult to see that (112) and (122) can be written as (43)–(44) for $\mathbf{f}_1 = 0$ and

$$f_2 = -R(\Upsilon_1, \tilde{\Upsilon}_1) (\nabla \cdot \tilde{\mathbf{u}}) + (\Upsilon_1 - \tilde{\Upsilon}_1) e^{\Upsilon_1} (\nabla \cdot (\tilde{\mathbf{u}} - \mathbf{u})), \tag{123}$$

$$\mathbf{f}_3 = v^{-1} \nabla \cdot (R(\Upsilon_2, \tilde{\Upsilon}_2) \nabla \tilde{p}) - v^{-1} \nabla \cdot (e^{\Upsilon_2} (\Upsilon_2 - \tilde{\Upsilon}_2) (\nabla \tilde{p} - \nabla p)). \tag{124}$$

From proposition (2.1), it follows that

$$\|\mathbf{r}\|_{\mathcal{H}} \leq C(\|f_2\|_{H^1(L^2(\Omega_1))} + \|f_3\|_{L^2(L^2(\Omega_2))}), \tag{125}$$

where the constant C can be chosen to be the same as in (119). Some straightforward computations show now that

$$\begin{aligned} \|\mathbf{r}\|_{\mathcal{H}} &\leq 2Cv^{-1} \|R(\Upsilon_2, \tilde{\Upsilon}_2)\|_{C^1(\bar{\Omega}_2)} \|p\|_{L^2(H^2(\Omega_2))} + C \|R(\Upsilon_1, \tilde{\Upsilon}_1)\|_{C(\bar{\Omega}_1)} \|\tilde{\mathbf{u}}\|_{H^1(H^1(\Omega_1))} \\ &\quad + 2Cv^{-1} \|\Upsilon_2 - \tilde{\Upsilon}_2\|_{C^1(\bar{\Omega}_2)} \|e^{\Upsilon_2}\|_{C^1(\bar{\Omega}_2)} \|p - \tilde{p}\|_{L^2(H^2(\Omega_2))} \\ &\quad + C \|\Upsilon_1 - \tilde{\Upsilon}_1\|_{C(\bar{\Omega}_1)} \|e^{\Upsilon_1}\|_{C(\bar{\Omega}_1)} \|\mathbf{u} - \tilde{\mathbf{u}}\|_{H^1(H^1(\Omega_1))}. \end{aligned}$$

From (114), and (116), (117)–(118) we obtain

$$\begin{aligned} \|\mathbf{r}\|_{\mathcal{H}} &\leq C \left(2v^{-1} \frac{\epsilon}{A} \|\Upsilon_2 - \tilde{\Upsilon}_2\|_{\mathcal{K}_2} + \frac{\epsilon}{A} \|\Upsilon_1 - \tilde{\Upsilon}_1\|_{\mathcal{K}_1} \right) \|\mathbf{h}\|_{\mathcal{H}} \\ &\quad + C\omega(2v^{-1} \|\Upsilon_2 - \tilde{\Upsilon}_2\|_{C^1(\bar{\Omega}_2)} + \|\Upsilon_1 - \tilde{\Upsilon}_1\|_{C(\bar{\Omega}_1)}) \frac{\epsilon}{A}. \end{aligned} \tag{126}$$

Then, from (33) and the definition of the corresponding norms

$$\begin{aligned} \|\mathbf{r}\|_{\mathcal{H}} &\leq C(2v^{-1} + 1) \|\Upsilon - \tilde{\Upsilon}\|_{\mathcal{K}} \frac{\epsilon}{A} \|\mathbf{h}\|_{\mathcal{H}} + \omega C_e C(2v^{-1} + 1) C \|\Upsilon - \tilde{\Upsilon}\|_{\mathcal{K}} \frac{\epsilon}{A} \\ &\leq C(2v^{-1} + 1) (\|\mathbf{h}\|_{\mathcal{H}} + C_e \omega) \|\Upsilon - \tilde{\Upsilon}\|_{\mathcal{K}} \frac{\epsilon}{A}. \end{aligned} \tag{127}$$

From (115) we arrive at

$$\|\mathbf{r}\|_{\mathcal{H}} \leq \epsilon \left(\frac{1}{\sigma_p} \sum_{j=1}^N \|\delta(x - x^j)\|_{L^2(\Omega_2)}^2 dt + \frac{1}{\sigma_u} C_S \right)^{-1/2} \|\Upsilon - \tilde{\Upsilon}\|_{\mathcal{K}}. \tag{128}$$

We combine the previous expression with (121) to obtain

$$\|F(\tilde{\Upsilon}) - F(\Upsilon) - DF(\Upsilon)(\tilde{\Upsilon} - \Upsilon)\|_{\mathcal{O}} \leq \epsilon \|\Upsilon - \tilde{\Upsilon}\|_{\mathcal{K}}, \tag{129}$$

which proves differentiability of F . □

5.3. Proof of theorem 3.1

Let \mathcal{B} be a bounded set in \mathcal{K} . We prove that $F(\mathcal{B})$ is a relatively compact set in \mathcal{O} . Note that $F(\mathcal{B}) = \{(\mathcal{M}_{\mathbf{u}}(\mathbf{u}), \mathcal{M}_p(p)) \in \mathcal{O} \mid \mathbf{h}(\Upsilon) = (\mathbf{u}, p) \text{ is the solution to (41)–(42) for } \Upsilon \in \mathcal{B}\}$.

Therefore, $F(\mathcal{B}) = F_1(\mathcal{B}) \times F_2(\mathcal{B})$ where

$$F_1(\mathcal{B}) = \{\mathcal{M}_{\mathbf{u}}(\mathbf{u}) \in L^2(0; T, L^2(\mathcal{S})^3) \mid \mathbf{u} \text{ is the first component of } \mathbf{h}(\Upsilon) = (\mathbf{u}, p) \text{ with } \Upsilon \in \mathcal{B}\},$$

$$F_2(\mathcal{B}) = \{\mathcal{M}_p(p) \in L^2[0; T]^N \mid p \text{ is the second component of } \mathbf{h}(\Upsilon) = (\mathbf{u}, p) \text{ with } \Upsilon \in \mathcal{B}\}.$$

We first prove that F_2 is relatively compact in $L^2(0; T, L^2(\mathcal{S})^3)$. We do so by verifying that the hypotheses of [31, theorem 1] are satisfied. In other words, we show that

- (1) $\{\int_{t_1}^{t_2} \xi(t) dt : \xi \in F_2(\mathcal{B})\}$ is relatively compact in $L^2(\mathcal{S})^3$ for all $0 < t_1 \leq t_2 < T$.
- (2) $\|\xi(t+h) - \xi(t)\|_{L^2(0, T-h; L^2(\mathcal{S})^3)} \rightarrow 0$ as $h \rightarrow 0$ uniformly in $F_2(\mathcal{B})$.

To show (1), we consider an arbitrary sequence in $\{\int_{t_1}^{t_2} \xi(t) dt : \xi \in F_2(\mathcal{B})\}$. In other words, we consider

$$\left\{ \int_{t_1}^{t_2} \mathcal{M}_{\mathbf{u}}(\mathbf{u}^n(t)) dt : \mathbf{u}^n \text{ is the first component of } \mathbf{h}(\Upsilon^n) = (\mathbf{u}, p) \text{ with } \Upsilon^n \in \mathcal{B} \right\}, \quad (130)$$

for an arbitrary sequence $\Upsilon^n \in \mathcal{B}$. Then, $\|\Upsilon^n\|_{\mathcal{K}} \leq C_1$ for all $n \in \mathbb{N}$. From proposition 2.1 and (45), it follows that

$$\|\mathbf{u}^n\|_{H^1(0, T; H^1(\Omega_1)^3)} \leq \|\mathbf{h}^n\|_{\mathcal{H}} \leq C[\|p_0\|_{H^1(\Omega_2)} + \|q\|_{L^2(L^2(\Omega_2))} + \|\mathbf{f}\|_{H^1(L^2(\Omega_1))}] \equiv Q, \quad (131)$$

where C depends on C_1 . From the Sobolev embedding $H^1(0, T; H^1(\Omega_1)^3) \hookrightarrow C(0, T; H^1(\Omega_1)^3)$ [8, theorem 2, 5.9.2], we have

$$\|\mathbf{u}^n(\cdot, t)\|_{H^1(\Omega_1)^3} \leq \|\mathbf{u}^n\|_{C(0, T; H^1(\Omega_1)^3)} \leq \tilde{C}\|\mathbf{u}^n\|_{H^1(0, T; H^1(\Omega_1)^3)} \leq \tilde{C}Q, \quad (132)$$

for all $t \in [0, T]$ and for some constant $\tilde{C} > 0$ that depends on T . Then, (132) implies that the sequence $\|\mathbf{u}^n(\cdot, t)\|_{H^1(\Omega_1)^3}$ is bounded for all $t \in [0, T]$. Since the trace $\gamma_{\mathcal{S}} : H^1(\Omega_1)^3 \rightarrow L^2(\mathcal{S})^3$ is a compact operator [22, theorem 6.10.5], there exists a subsequence also denoted by $\gamma_{\mathcal{S}}(\mathbf{u}^n(\cdot, t))$ and $\kappa_t^* \in L^2(\mathcal{S})^3$ such that

$$\gamma_{\mathcal{S}}(\mathbf{u}^n(\cdot, t)) \rightarrow \kappa_t^* \text{ strongly in } L^2(\mathcal{S})^3, \quad (133)$$

as $n \rightarrow \infty$, for all $t \in [0, T]$. Let us define $\kappa : [0, T] \rightarrow L^2(\mathcal{S})^3$ by $\kappa(t) \equiv \kappa_t^*$. Since κ is the pointwise limit of strongly measurable functions, κ itself is strongly measurable [16, theorem 3.5.4(3)]. We then have that

$$\|\gamma_{\mathcal{S}}(\mathbf{u}^n(\cdot, t)) - \kappa(t)\|_{L^2(\mathcal{S})^3} \rightarrow 0, \quad (134)$$

for every $t \in [0, T]$. In addition, from (19) and (132) we know that

$$\|\gamma_{\mathcal{S}}(\mathbf{u}^n(t))\|_{L^2(\mathcal{S})} \leq C_S \tilde{C}Q,$$

which after passing the limit yields,

$$\|\kappa(t)\|_{L^2(\mathcal{S})} \leq C_S \tilde{C}Q.$$

From the two previous estimates we obtain

$$\|\gamma_{\mathcal{S}}(\mathbf{u}^n(\cdot, t)) - \kappa(t)\|_{L^2(\mathcal{S})^3} \leq 2C_S \tilde{C}Q, \quad (135)$$

for all $t \in [0, T]$ and for all $n \in \mathbb{N}$. Let $t_1, t_2 \in (0, T)$ such that $t_1 \leq t_2$. Define $g_n : \mathbb{R} \rightarrow \mathbb{R}$ by

$$g_n(t) \equiv \begin{cases} \chi_{[t_1, t_2]} \|\gamma_{\mathcal{S}}(\mathbf{u}^n(\cdot, t)) - \kappa(t)\|_{L^2(\mathcal{S})^3} & t \in [0, T] \\ 0 & t \notin [0, T], \end{cases} \quad (136)$$

where $\chi_{[t_1, t_2]}$ is the characteristic function of $[t_1, t_2]$. Then, from (135) and (134) we observe that

$$|g_n(t)| \leq 2C_S \tilde{C}B, \quad \lim_{n \rightarrow \infty} g_n(t) = 0, \tag{137}$$

for all $t \in \mathbb{R}$. Then, from the dominated convergence theorem [8, theorem 2, 5.9.2], it follows that

$$\lim_{n \rightarrow \infty} \int_{t_1}^{t_2} \|\gamma_S(\mathbf{u}^n(\cdot, t)) - \kappa(t)\|_{L^2(\mathcal{S})^3} dt = \lim_{n \rightarrow \infty} \int_{\mathbb{R}} g_n(t) dt = \int_{\mathbb{R}} \lim_{n \rightarrow \infty} g_n(t) dt = 0. \tag{138}$$

On the other hand, from [8, theorem 8, E.5],

$$\left\| \int_{t_1}^{t_2} (\gamma_S(\mathbf{u}^n(\cdot, t)) - \kappa(t)) dt \right\|_{L^2(\mathcal{S})^3} \leq \int_{t_1}^{t_2} \|\gamma_S(\mathbf{u}^n(\cdot, t)) - \kappa(t)\|_{L^2(\mathcal{S})^3} dt,$$

which combined with (138) yields,

$$\int_{t_1}^{t_2} \mathcal{M}_{\mathbf{u}}(\mathbf{u}^n(t)) dt \equiv \int_{t_1}^{t_2} \gamma_S(\mathbf{u}^n(t)) dt \rightarrow \int_{t_1}^{t_2} \kappa(t) dt \quad \text{in } L^2(\mathcal{S})^3, \tag{139}$$

for arbitrary $0 < t_1 \leq t_2 < T$. We have shown that an arbitrary sequence $\left\{ \int_{t_1}^{t_2} \mathcal{M}_{\mathbf{u}}(\mathbf{u}^n(t)) dt \right\}$ has a convergent subsequence for all $0 < t_1 \leq t_2 < T$. Then, the set $\left\{ \int_{t_1}^{t_2} \xi(t) dt : \xi \in F_2(\mathcal{B}) \right\}$ is relatively compact in $L^2(\mathcal{S})^3$ for all $0 < t_1 \leq t_2 < T$ which proves (1). On the other hand, from [8, theorem 2, 5.9.2] we have that

$$\mathbf{u}^n(t+h) - \mathbf{u}^n(t) = \int_t^{t+h} \frac{d\mathbf{u}^n}{dt} dt, \tag{140}$$

for all $h > 0$. Then, for all $t \in [0, T-h]$, [8, theorem 8, E.5] and Cauchy–Schwarz yield

$$\begin{aligned} \|\mathbf{u}^n(t+h) - \mathbf{u}^n(t)\|_{H^1(\Omega_1)^3} &\leq \int_t^{t+h} \left\| \frac{d\mathbf{u}^n}{dt} \right\|_{H^1(\Omega_1)^3} dt \\ &\leq h^{1/2} \|\mathbf{u}^n\|_{H^1(0, T; H^1(\Omega_1)^3)}. \end{aligned} \tag{141}$$

We use (19) and (131) to find

$$\|\gamma_S(\mathbf{u}^n(t+h)) - \gamma_S(\mathbf{u}^n(t))\|_{L^2(0, T-h; L^2(\mathcal{S})^3)} \leq h^{1/2} C_S Q(T-h), \tag{142}$$

which implies $\|\gamma(\mathbf{u}^n(t+h)) - \gamma(\mathbf{u}^n(t))\|_{L^2(0, T-h; L^2(\mathcal{S})^3)} \rightarrow 0$ as $h \rightarrow 0$ for all $n \in \mathbb{N}$ which establishes (2). Then $F_2(\mathcal{B})$ is relatively compact in $L^2(0, T; L^2(\mathcal{S})^3)$.

To prove that $F_1(\mathcal{B})$ is relatively compact in $L^2[0, T]^N$, we take a sequence $\mathbf{Y}^n \in \mathcal{B}$. From the same argument as before, we have

$$\|p^n\|_{H^{2,1}(\Omega_2 \times [0, T])} \leq \|h^n\|_{\mathcal{H}} \leq C(\|p_0\|_{H^1(\Omega_2)} + \|q\|_{L^2(L^2(\Omega_2))} + \|f\|_{H^1(L^2(\Omega_1))}) \equiv Q,$$

where C depends on C_1 . Then p^n is a bounded sequence in $H^{2,1}(\Omega_2 \times [0, T])$. From the Lions–Aubin theorem [30, proposition III, 1.3] we know that $H^{2,1}(\Omega_2 \times [0, T])$ is compactly imbedded in $L^2(0, T; L^2(\Omega_2))$. Therefore, for some subsequence (also denoted by p^n) we have that $p^n \rightarrow p^*$ (strongly) in $L^2(0, T; L^2(\Omega_2))$ for some $p^* \in L^2(0, T; L^2(\Omega_2))$. From the continuity of \mathcal{M}_p it follows that

$$\mathcal{M}_p(p^n) \rightarrow \mathcal{M}_p(p^*) \text{ strongly in } L^2(0, T)^N, \tag{143}$$

which proves that $F_1(\mathcal{B})$ is relatively compact in $L^2(0, T)^N$. Since $F_1(\mathcal{B})$ and $F_2(\mathcal{B})$ are relatively compact in $L^2(0, T; L^2(\mathcal{S})^3)$ and $L^2(0, T)^N$, respectively, then $F(\mathcal{B})$ is relatively compact in \mathcal{O} which establishes the compactness of F .

We now prove that F is weakly sequentially closed. Let us take an arbitrary sequence $\mathbf{Y}^n \rightharpoonup \mathbf{Y} \in \mathcal{K}$. Let us assume that $F(\mathbf{Y}^n) \rightharpoonup (\mathbf{y}_u, \mathbf{y}_p)$ in \mathcal{O} . First we note that the embeddings in (33) are compact. Then, there exist $\mathbf{Y} \equiv (\Upsilon_1, \Upsilon_2) \in C(\bar{\Omega}_1) \times C^1(\bar{\Omega}_2)$ such

that $\Upsilon_1^n \rightarrow \Upsilon_1$ strongly in $C(\overline{\Omega}_1)$ and $\Upsilon_2^n \rightarrow \Upsilon_2$ strongly in $C^1(\overline{\Omega}_2)$. Let $\mathbf{h}^n(\Upsilon^n) \equiv (\mathbf{u}^n, p^n)$ and $\mathbf{h}(\Upsilon) \equiv (\mathbf{u}, p)$ be the solutions to (41)–(42) for Υ^n and Υ , respectively. It is not difficult to see that $\mathbf{h}^n - \mathbf{h} = (\mathbf{u}^n - \mathbf{u}, p^n - p)$ satisfies

$$L(\Upsilon_1^n, \mathbf{u}^n - \mathbf{u}, \mathbf{w}) - \int_{\Omega_2} b[p^n - p]\nabla \cdot \mathbf{w} = \int_{\Omega_1} [(e^{\Upsilon_1} - e^{\Upsilon_1^n})(\nabla \cdot \mathbf{u})(\nabla \cdot \mathbf{w})], \tag{144}$$

$$\begin{aligned} & \int_{\Omega_2} \frac{1}{M} \frac{\partial [p^n - p]}{\partial t} w + \int_{\Omega_2} v^{-1} e^{\Upsilon_2^n} \nabla \cdot [p^n - p] \cdot \nabla w + \int_{\Omega_2} b \frac{\partial \nabla \cdot [\mathbf{u}^n - \mathbf{u}]}{\partial t} w, \\ & = - \int_{\Omega_2} v^{-1} w \nabla \cdot (e^{\Upsilon_2} - e^{\Upsilon_2^n}) \nabla p \end{aligned} \tag{145}$$

for all $(\mathbf{w}, w) \in \mathcal{W}$. We now prove that $\mathbf{h}^n \rightarrow \mathbf{h} \in \mathcal{H}$. Let $\epsilon > 0$. From continuity of the exponential function, let $\delta > 0$ such that

$$\|e^{\Upsilon_1} - e^{\tilde{\Upsilon}_1}\|_{C(\overline{\Omega}_1)} \leq \frac{\epsilon}{A}, \quad \|e^{\tilde{\Upsilon}_2} - e^{\Upsilon_2}\|_{C^1(\overline{\Omega}_2)} \leq \frac{\epsilon}{A}, \tag{146}$$

with

$$A \equiv C^{-1} (\|\mathbf{u}\|_{H^1(H^1(\Omega_1))} + 2v^{-1}\|p\|_{L^2(H^2(\Omega_2))})^{-1}, \tag{147}$$

provided that $\|\tilde{\Upsilon}_1 - \Upsilon_1\|_{C(\overline{\Omega}_1)} \leq \delta$ and $\|\tilde{\Upsilon}_2 - \Upsilon_2\|_{C^1(\overline{\Omega}_2)} \leq \delta$. Let $N \in \mathbb{N}$ such that $\|\Upsilon_1^n - \Upsilon_1\|_{C(\overline{\Omega}_1)} \leq \delta$ and $\|\Upsilon_2^n - \Upsilon_2\|_{C^1(\overline{\Omega}_2)} \leq \delta$ for every $n \geq N$. From proposition 2.1 applied to $B(\Upsilon, \delta)$, there is $C > 0$ such that

$$\|\mathbf{h}^n - \mathbf{h}\|_{\mathcal{H}} \leq C (\|e^{\Upsilon_1} - e^{\Upsilon_1^n}\|_{C(\overline{\Omega}_1)} \|\mathbf{u}\|_{H^1(H^1(\Omega_1))} + 2v^{-1} \|e^{\Upsilon_2} - e^{\Upsilon_2^n}\|_{C^1(\overline{\Omega}_2)} \|p\|_{L^2(H^2(\Omega_2))}), \tag{148}$$

for all $n > N$. Therefore, from (146)–(147)

$$\|\mathbf{h}^n - \mathbf{h}\|_{\mathcal{H}} \leq C \left(\|\mathbf{u}\|_{H^1(H^1(\Omega_1))} + 2v^{-1} \|p\|_{L^2(H^2(\Omega_2))} \right) \frac{\epsilon}{A} = \epsilon, \tag{149}$$

which implies that $\mathbf{h}^n \rightarrow \mathbf{h} \in \mathcal{H}$. From the continuity of \mathcal{M}_p and \mathcal{M}_u , it follows that $F(\Upsilon^n) \rightarrow F(\Upsilon)$ (strongly) in \mathcal{O} . Therefore, $F(\Upsilon^n) \rightarrow F(\Upsilon)$. From uniqueness of the limit of a weak convergent sequence, we find $F(\Upsilon) = (\mathbf{y}_u, \mathbf{y}_p)$ which proves that F is weakly (sequentially) closed.

5.4. Proof of theorem 3.2

The proof of 3.2 requires the following analysis. For $i \in \{1, 2\}$ we define

$$\Omega_i^> \equiv \{x \in \Omega_i : |\Upsilon_i - \tilde{\Upsilon}_i| > 0\} \tag{150}$$

and

$$W(\tilde{\Upsilon}_i, \Upsilon_i) = \begin{cases} \frac{R(\Upsilon_i, \tilde{\Upsilon}_i)}{e^{\tilde{\Upsilon}_i} - e^{\Upsilon_i}} & \text{if } x \in \Omega_i^> \\ 0 & \text{if } x \in \Omega - \Omega_i^> \end{cases} \tag{151}$$

where the residuals are defined in (108) The following proposition is needed.

Lemma 5.3. *For all $\Upsilon, \tilde{\Upsilon} \in \mathcal{K}$, $W(\tilde{\Upsilon}_1, \Upsilon_1) \in L^\infty(\Omega_1)$, $W(\tilde{\Upsilon}_2, \Upsilon_2) \in W^{1,\infty}(\Omega_2)$. Additionally, for every $\hat{\Upsilon} \in \mathcal{K}$, there exists $r > 0$ such that for all $\Upsilon, \tilde{\Upsilon} \in B(\hat{\Upsilon}, r)$*

$$\|W(\tilde{\Upsilon}_1, \Upsilon_1)\|_{L^\infty(\Omega_1)} \leq C \|\tilde{\Upsilon}_1 - \Upsilon_1\|_{C(\overline{\Omega}_1)} \tag{152}$$

$$\|W(\tilde{\Upsilon}_2, \Upsilon_2)\|_{H^1(\Omega_2)} \leq C \|\tilde{\Upsilon}_2 - \Upsilon_2\|_{C^1(\overline{\Omega}_2)} \tag{153}$$

where C may depend only on $\Omega_1, \Omega_2, \hat{\Upsilon}$ and r .

Proof. The proof is very similar to the one of proposition 3.1 in [17] and so we omit it. \square

Lemma 5.4. For every $\hat{\Upsilon} \in \mathcal{K}$, there exists $r > 0$ such that for all $\Upsilon, \tilde{\Upsilon} \in B(\hat{\Upsilon}, r)$ and all $(v_{\mathbf{u}}, v_p) \in L^2(0, T; L^2(\Omega_1)) \times H^{2,1}(\Omega_2 \times [0, T])$ there exist functions $\eta_{\mathbf{u}} \in L^2(0, T; \mathbf{H}_0(\Omega_1))$ and $\eta_p \in H^1(0, T; L^2(\Omega_2))$ such that

$$\nabla \cdot \eta_{\mathbf{u}} = W(\tilde{\Upsilon}_1, \Upsilon_1)v_{\mathbf{u}} \quad \text{in } \Omega_1, \quad (154)$$

$$\nabla \eta_p = W(\tilde{\Upsilon}_2, \Upsilon_2)\nabla v_p \quad \text{in } \Omega_2, \quad (155)$$

a.e. in $[0, T]$. Moreover,

$$\|\eta_{\mathbf{u}}\|_{L^2(H^1(\Omega_1)^3)} \leq C\|\tilde{\Upsilon}_1 - \Upsilon_1\|_C\|v_{\mathbf{u}}\|_{L^2(L^2(\Omega_1))}, \quad (156)$$

$$\left\| \frac{\partial \eta_p}{\partial t} \right\|_{L^2(L^2(\Omega_2))} \leq C\|\Upsilon_2 - \tilde{\Upsilon}_2\|_{C^1} \left\| \frac{\partial v_p}{\partial t} \right\|_{L^2(L^2(\Omega_2))}, \quad (157)$$

where $C > 0$ depends only on $\Omega_1, \Omega_2, \hat{\Upsilon}$ and r .

Proof. For almost every t in $[0, T]$, let $\phi(\cdot, t)$ be the solution to the following problem:

$$\nabla \cdot \nabla \phi(\cdot, t) = W(\tilde{\Upsilon}_1, \Upsilon_1)v_{\mathbf{u}} \quad \text{in } \Omega_1, \quad (158)$$

$$\phi(\cdot, t) = 0 \quad \text{on } \partial\Omega_1, \quad (159)$$

The existence of a unique solution $\phi(\cdot, t) \in H^1(\Omega_1)$ to (158)–(159) follows from standard PDE theory. Furthermore, from elliptic regularity we know that $\phi(\cdot, t) \in H^2(\Omega_1)$ and

$$\|\phi(\cdot, t)\|_{H^2(\Omega_1)} \leq C\|W(\tilde{\Upsilon}_1, \Upsilon_1)v_{\mathbf{u}}\|_{L^2(\Omega_1)}, \quad (160)$$

where C may possibly depend on Ω_1 . Similar arguments to the ones used in the proof of lemma 3.3 in [17] can be applied here to show that $\phi : [0, T] \rightarrow H^2(\Omega_1)$ is strongly measurable. Then, from (160) and the previous proposition, it follows easily that $\phi \in L^2(0, T; H^2(\Omega_1))$. We define $\eta_{\mathbf{u}} \equiv \nabla \phi \in L^2(0, T; H^1(\Omega_1)^3)$ and note that (158) implies that $\eta_{\mathbf{u}}$ satisfies (154) a.e. in $[0, T]$. Moreover, from (160)

$$\|\eta_{\mathbf{u}}(\cdot, t)\|_{H^1(\Omega_1)^3} \leq C\|W(\tilde{\Upsilon}_1, \Upsilon_1)\|_{L^\infty(\Omega_1)}\|v_{\mathbf{u}}(\cdot, t)\|_{L^2(\Omega)}, \quad (161)$$

which from the previous proposition implies (156). The existence of η_p in (155) and estimate (157) follows directly from lemma 3.3 in [17]. \square

Proof of theorem 3.2. Let $r > 0$ be such that the results of lemma 5.4 and assumption 3.1 hold on $B(\hat{\Upsilon}, r)$. Let $C > 0$ be the maximum of the corresponding C s in (156)–(157) and (69)–(70). Let $\Upsilon, \tilde{\Upsilon} \in B(\hat{\Upsilon}, r)$. Let $\xi = (\xi_{\mathbf{u}}, \xi_p)$ be the solution to (109)–(110) which exist from proposition 2.1. Let $\mathbf{r} = (\mathbf{r}_{\mathbf{u}}, r_p)$ be the residuals defined as in (111) of lemma 5.2. Note that, in terms of these residuals, the left-hand side of (71) can be written as

$$\|F(\tilde{\Upsilon}) - F(\Upsilon) - DF(\Upsilon)(\tilde{\Upsilon} - \Upsilon)\|_{\mathcal{O}}^2 = \frac{1}{\sigma_p} \int_0^T |\mathcal{M}_p(r_p)|^2 dt + \frac{1}{\sigma_{\mathbf{u}}} \int_0^T \int_S |\mathcal{M}_{\mathbf{u}}(\mathbf{r}_{\mathbf{u}})|^2. \quad (162)$$

From lemma 5.2, $\mathbf{r} = (\mathbf{r}_u, r_p)$ satisfies (112)–(113) which after adding and using (151) becomes

$$\begin{aligned} L(\Upsilon_1, \mathbf{r}_u, \mathbf{w}) &= \int_{\Omega_2} br_p \nabla \cdot \mathbf{w} + \int_{\Omega_2} \frac{1}{M} \frac{\partial r_p}{\partial t} w + \int_{\Omega_2} b \frac{\partial \nabla \cdot \mathbf{r}_u}{\partial t} w + \int_{\Omega_2} v^{-1} e^{\Upsilon_2} \nabla r_p \cdot \nabla w \\ &= - \int_{\Omega_1} W(\tilde{\Upsilon}_1, \Upsilon_1)(e^{\tilde{\Upsilon}_1} - e^{\Upsilon_1})(\nabla \cdot \tilde{\mathbf{u}})(\nabla \cdot \mathbf{w}) \\ &\quad + \int_{\Omega_1} (\Upsilon_1 - \tilde{\Upsilon}_1) e^{\Upsilon_1} (\nabla \cdot (\tilde{\mathbf{u}} - \mathbf{u}))(\nabla \cdot \mathbf{w}) \\ &\quad - \int_{\Omega_2} v^{-1} W(\tilde{\Upsilon}_2, \Upsilon_2)(e^{\tilde{\Upsilon}_2} - e^{\Upsilon_2}) \nabla \tilde{p} \cdot \nabla w \\ &\quad + \int_{\Omega_2} (v^{-1} e^{\Upsilon_2} (\Upsilon_2 - \tilde{\Upsilon}_2) \nabla (p - \tilde{p}) \cdot \nabla w) \end{aligned}$$

for all $(\mathbf{w}, w) \in \mathcal{W}$. In particular, the previous expression holds (a.e. in $(0, T)$) for $(\mathbf{w}, w) \equiv (\mathbf{w}_u^j(\cdot, t), w_p^j(\cdot, t))$ where $\mathbf{W} = (\mathbf{w}_u^j(x, t), w_p^j(x, t))$ is the solution to the adjoint problem (72)–(73) with

$$\mathbf{A}_1 \equiv \frac{1}{N\sigma_{\mathbf{u}}} \mathcal{Y}_{\mathcal{S}}(\mathbf{r}_u), \quad A_2^j \equiv \frac{1}{\sigma_p} \delta(x - x^j) \int_{\Omega_2} r_p(\xi, t) \delta(\xi - x^j) d\xi, \quad (163)$$

for some $j \in \{1, \dots, N\}$. Therefore,

$$\begin{aligned} \int_0^T L(\Upsilon_1, \mathbf{r}_u, \mathbf{w}_u^j) &- \int_0^T \int_{\Omega_2} br_p \nabla \cdot \mathbf{w}_u^j + \int_0^T \int_{\Omega_2} \frac{1}{M} \frac{\partial r_p}{\partial t} w_p^j + \int_0^T \int_{\Omega_2} b \frac{\partial \nabla \cdot \mathbf{r}_u}{\partial t} w_p^j \\ &+ \int_0^T \int_{\Omega_2} v^{-1} e^{\Upsilon_2} \nabla r_p \cdot \nabla w_p^j = \int_0^T (D_1^j + D_2^j) dt, \end{aligned} \quad (164)$$

where

$$\begin{aligned} D_1^j &\equiv - \int_{\Omega_1} (W(\tilde{\Upsilon}_1, \Upsilon_1)(e^{\tilde{\Upsilon}_1} - e^{\Upsilon_1})(\nabla \cdot \tilde{\mathbf{u}})(\nabla \cdot \mathbf{w}_u^j) \\ &\quad + \int_{\Omega_1} (\Upsilon_1 - \tilde{\Upsilon}_1) e^{\Upsilon_1} (\nabla \cdot (\tilde{\mathbf{u}} - \mathbf{u}))(\nabla \cdot \mathbf{w}_u^j), \end{aligned} \quad (165)$$

$$D_2^j \equiv \int_{\Omega_2} v^{-1} W(\tilde{\Upsilon}_2, \Upsilon_2)(e^{\tilde{\Upsilon}_2} - e^{\Upsilon_2}) \nabla \tilde{p} \cdot \nabla w_p^j + \int_{\Omega_2} (v^{-1} e^{\Upsilon_2} (\Upsilon_2 - \tilde{\Upsilon}_2) \nabla (p - \tilde{p}) \cdot \nabla w_p^j). \quad (166)$$

On the other hand, since $\mathbf{W} = (\mathbf{w}_u^j(x, t), w_p^j(x, t))$ satisfies (72)–(73) a.e. in $(0, T)$ for all $(\mathbf{h}_1, \mathbf{h}_2) \in \mathcal{W}$, in particular, for $\mathbf{h}_1 = \mathbf{r}_u(\cdot, t)$ and $h_2 = r_p(\cdot, t)$, (72)–(73) become

$$\begin{aligned} L(\Upsilon_1, \mathbf{r}_u, \mathbf{w}_u^j) &- \int_{\Omega_2} b \frac{\partial w_p^j}{\partial t} \nabla \cdot \mathbf{r}_u = \frac{1}{N\sigma_{\mathbf{u}}} \int_{\mathcal{S}} |\mathcal{Y}_{\mathcal{S}}(\mathbf{r}_u)|^2, \\ \int_{\Omega_2} \left(-br_p \nabla \cdot \mathbf{w}_u^j - r_p \frac{1}{M} \frac{\partial w_p^j}{\partial t} - v^{-1} e^{\Upsilon_2} \nabla w_p^j \cdot \nabla r_p \right) &= \frac{1}{\sigma_p} \left(\int_{\Omega_2} r_p \delta(x - x^j) \right)^2. \end{aligned}$$

We add the resulting equations, use (46), (48), integrate in $(0, T)$, integrate by parts some of the terms and use the fact that $w_p^j(\cdot, T) = \mathbf{r}_u(\cdot, 0) = r_p(\cdot, 0) = 0$ to find

$$\begin{aligned} \int_0^T L(\Upsilon_1, \mathbf{r}_u, \mathbf{w}_u^j) &+ \int_{\Omega_2} b \frac{\partial \nabla \cdot \mathbf{r}_u}{\partial t} w_p^j \\ &+ \int_0^T \int_{\Omega_2} \left(-br_p \nabla \cdot \mathbf{w}_u^j + w_p^j \frac{1}{M} \frac{\partial r_p}{\partial t} - v^{-1} e^{\Upsilon_2} \nabla w_p^j \cdot \nabla r_p \right) \\ &= \frac{1}{\sigma_p} \int_0^T (\mathcal{M}_p^j(r_p))^2 + \frac{1}{N\sigma_{\mathbf{u}}} \int_0^T \|\mathcal{M}_{\mathbf{u}}(\mathbf{r}_u)\|_{L^2(\mathcal{S})}^2. \end{aligned}$$

Combining the previous expression with (164) yields

$$\frac{1}{\sigma_p} \int_0^T (\mathcal{M}_p^j(r_p))^2 + \frac{1}{N\sigma_u} \int_0^T \|\mathcal{M}_u(\mathbf{r}_u)\|_{L^2(\mathcal{S})}^2 = \int_0^T (D_1^j + D_2^j) dt. \quad (167)$$

From (162) and (167), we have that

$$\begin{aligned} \|F(\tilde{\Upsilon}) - F(\Upsilon) - DF(\Upsilon)(\tilde{\Upsilon} - \Upsilon)\|_{\mathcal{O}}^2 &= \frac{1}{\sigma_p} \int_0^T |\mathcal{M}_p(r_p)|^2 dt + \frac{1}{\sigma_u} \int_0^T \int_{\mathcal{S}} |\mathcal{M}_u(\mathbf{r}_u)|^2 \\ &= \frac{1}{\sigma_p} \sum_{j=1}^N \int_0^T |\mathcal{M}_p(r_p)|^2 dt + \frac{1}{\sigma_u} \int_0^T \int_{\mathcal{S}} |\mathcal{M}_u(\mathbf{r}_u)|^2 \\ &= \sum_{j=1}^N \left(\int_0^T (D_1^j + D_2^j) dt \right). \end{aligned} \quad (168)$$

The rest of the proof consists of using (69)–(70) to find an estimate of D_1^j and D_2^j (165)–(166) in terms of the right-hand side of (71) as required.

Note from lemma 3.1 that $\mathbf{W}^j = (\mathbf{w}_u^j, w_p^j)$ satisfies the following estimate:

$$\begin{aligned} \max \left\{ \left\| \frac{\partial w_p^j}{\partial t} \right\|_{L^2(L^2(\Omega_2))}, \|\mathbf{w}_u^j\|_{L^2(H^1(\Omega_1)^3)} \right\} &\leq C_1 \left(\frac{1}{N\sigma_u} \|\mathcal{Y}_{\mathcal{S}}(\mathbf{r}_u)\|_{L^2(L^2(\mathcal{S}))} \right. \\ &\quad \left. + \frac{1}{\sigma_p} \|\delta(x - x^j)\|_{L^2(\Omega_2)} \left(\int_0^T \left(\int_{\Omega_2} r_p(\xi, t) \delta(\xi - x^j) d\xi \right) dt \right)^{1/2} \right), \end{aligned} \quad (169)$$

where C_1 may depend on \mathcal{A} . From definitions (46) and (48), the previous expression becomes

$$\begin{aligned} \max \left\{ \left\| \frac{\partial w_p^j}{\partial t} \right\|_{L^2(L^2(\Omega_2))}, \|\mathbf{w}_u^j\|_{L^2(H^1(\Omega_1)^3)} \right\} \\ \leq C_1 \left(\frac{1}{N\sigma_u} \|\mathcal{M}_u(\mathbf{r}_u)\|_{L^2(L^2(\mathcal{S}))} + \frac{1}{\sigma_p} \|\delta(x - x^j)\|_{L^2} \|\mathcal{M}_p^j(r_p)\|_{L^2(0,T)} \right). \end{aligned} \quad (170)$$

From lemma 5.4 we know the existence of $\eta_p \in H^{2,1}(\Omega_2 \times (0, T))$ and $\eta_u \in L^2(0, T; \mathbf{H}_0(\Omega_1))$ that satisfies (154)–(157) for all $(v_u, v_p) \in L^2(0, T; L^2(\Omega_1)) \times H^{2,1}(\Omega_2 \times (0, T))$. In particular, $(v_u, v_p) = (\nabla \cdot \mathbf{w}_u^j, w_p^j)$, where (\mathbf{w}_u^j, w_p^j) is the solution to the adjoint problem defined above. In other words,

$$\nabla \cdot \eta_u^j = W(\tilde{\Upsilon}_1, \Upsilon_1) \nabla \cdot \mathbf{w}_u^j \quad \text{in } \Omega_1, \quad (171)$$

$$\nabla \eta_p^j = W(\tilde{\Upsilon}_2, \Upsilon_2) \nabla w_p^j \quad \text{in } \Omega_2, \quad (172)$$

a.e. in $(0, T)$. Lemma 5.4 also ensures that

$$\|\eta_u^j\|_{L^2(H^1(\Omega_1)^3)} \leq C \|\tilde{\Upsilon}_1 - \Upsilon_1\|_C \|\nabla \cdot \mathbf{w}_u^j\|_{L^2(L^2(\Omega_1))}, \quad (173)$$

$$\left\| \frac{\partial \eta_p^j}{\partial t} \right\|_{L^2(L^2(\Omega_2))} \leq C \|\Upsilon_2 - \tilde{\Upsilon}_2\|_C \left\| \frac{\partial w_p^j}{\partial t} \right\|_{L^2(L^2(\Omega_2))}, \quad (174)$$

where $C > 0$ depends only on \mathcal{A} . Then, we combine (173)–(174), (169) and the embedding (19) to find

$$\begin{aligned} \max \left\{ \left\| \frac{\partial \eta_p^j}{\partial t} \right\|_{L^2(L^2)}, \|\eta_u^j\|_{L^2(H^1)} \right\} &\leq C \|\tilde{\Upsilon} - \Upsilon\|_{\mathcal{K}} \left(\frac{1}{N\sigma_u} \|\mathcal{M}_u(\mathbf{r}_u)\|_{L^2(L^2(\mathcal{S}))} \right. \\ &\quad \left. + \frac{1}{\sigma_p} \|\delta(x - x^j)\|_{L^2} \|\mathcal{M}_p^j(r_p)\|_{L^2(0,T)} \right), \end{aligned} \quad (175)$$

where C depends only on \mathcal{A} . Note that we can use (171)–(172) to rewrite (165)–(166) as follows:

$$\begin{aligned} D_1^j &\equiv \int_{\Omega} \left(W(\tilde{\Upsilon}_1, \Upsilon_1)(e^{\tilde{\Upsilon}_1} - e^{\Upsilon_1})(\nabla \cdot \tilde{\mathbf{u}})(\nabla \cdot \mathbf{w}_u^j) + \int_{\Omega} (\Upsilon_1 - \tilde{\Upsilon}_1) e^{\Upsilon_1} (\nabla \cdot (\tilde{\mathbf{u}} - \mathbf{u}))(\nabla \cdot \mathbf{w}_u^j) \right. \\ &= - \int_{\Omega} \left(W(\tilde{\Upsilon}_1, \Upsilon_1) e^{\Upsilon_1} (\nabla \cdot (\tilde{\mathbf{u}} - \mathbf{u}))(\nabla \cdot \mathbf{w}_u^j) \right. \\ &\quad + \int_{\Omega} (e^{\tilde{\Upsilon}_1} (\nabla \cdot \tilde{\mathbf{u}})(\nabla \cdot \eta_u^j) - (e^{\Upsilon_1} (\nabla \cdot \mathbf{u}))(\nabla \cdot \eta_u^j)) \\ &\quad \left. + \int_{\Omega} (\Upsilon_1 - \tilde{\Upsilon}_1) e^{\Upsilon_1} (\nabla \cdot (\tilde{\mathbf{u}} - \mathbf{u}))(\nabla \cdot \mathbf{w}_u^j), \right. \end{aligned} \quad (176)$$

$$\begin{aligned} D_2^j &\equiv \int_{\Omega_2} \nabla \tilde{p} \cdot v^{-1} W(\tilde{\Upsilon}_2, \Upsilon_2)(e^{\tilde{\Upsilon}_2} - e^{\Upsilon_2}) \nabla w_p^j + \int_{\Omega_2} (v^{-1} e^{\Upsilon_2} (\Upsilon_2 - \tilde{\Upsilon}_2) \nabla(p - \tilde{p}) \cdot \nabla w_p^j) \\ &= - \int_{\Omega_2} \nabla(\tilde{p} - p) \cdot v^{-1} W(\tilde{\Upsilon}_2, \Upsilon_2) e^{\Upsilon_2} \nabla w_p^j \\ &\quad + \int_{\Omega_2} \nabla \tilde{p} \cdot v^{-1} e^{\tilde{\Upsilon}_2} \nabla \eta_p^j - \int_{\Omega_2} \nabla p \cdot v^{-1} e^{\Upsilon_2} \nabla \eta_p^j \\ &\quad + \int_{\Omega_2} (v^{-1} e^{\Upsilon_2} (\Upsilon_2 - \tilde{\Upsilon}_2) \nabla(p - \tilde{p}) \cdot \nabla w_p^j). \end{aligned} \quad (177)$$

We now consider the equations satisfied by $\mathbf{h} - \tilde{\mathbf{h}}$ tested against (η_u^j, η_p^j) , i.e.

$$\begin{aligned} \int_{\Omega_2} \frac{1}{M} \frac{\partial(\tilde{p} - p)}{\partial t} \eta_p^j - \int_{\Omega_2} v^{-1} e^{\Upsilon_2} \nabla p \cdot \nabla \eta_p^j \\ + \int_{\Omega_2} v^{-1} e^{\tilde{\Upsilon}_2} \nabla \tilde{p} \cdot \nabla \eta_p^j + \int_{\Omega_2} b \frac{\partial \nabla \cdot (\tilde{\mathbf{u}} - \mathbf{u})}{\partial t} \eta_p^j = 0, \end{aligned} \quad (178)$$

and

$$\begin{aligned} \int_{\Omega} (2\mu \epsilon((\mathbf{u} - \tilde{\mathbf{u}})) : \epsilon(\eta_u^j)) + \int_{\Omega_2} b(\tilde{p} - p) \nabla \cdot \eta_u^j \\ = \int_{\Omega} (e^{\tilde{\Upsilon}_1} (\nabla \cdot \tilde{\mathbf{u}})(\nabla \cdot \eta_u^j) - (e^{\Upsilon_1} (\nabla \cdot \mathbf{u}))(\nabla \cdot \eta_u^j)). \end{aligned} \quad (179)$$

We combine (178)–(179) with (176)–(177) to find

$$\begin{aligned} D_1^j &= - \int_{\Omega} (W(\tilde{\Upsilon}_1, \Upsilon_1) e^{\Upsilon_1} (\nabla \cdot (\tilde{\mathbf{u}} - \mathbf{u}))(\nabla \cdot \mathbf{w}_u^j) + \int_{\Omega} (2\mu \epsilon((\mathbf{u} - \tilde{\mathbf{u}})) : \epsilon(\eta_u^j)) \\ &\quad + \int_{\Omega_2} b(\tilde{p} - p) \nabla \cdot \eta_u^j + \int_{\Omega} (\Upsilon_1 - \tilde{\Upsilon}_1) e^{\Upsilon_1} (\nabla \cdot (\tilde{\mathbf{u}} - \mathbf{u}))(\nabla \cdot \mathbf{w}_u^j), \end{aligned} \quad (180)$$

$$\begin{aligned} D_2^j &\equiv \int_{\Omega_2} \nabla \tilde{p} \cdot v^{-1} W(\tilde{\Upsilon}_2, \Upsilon_2)(e^{\tilde{\Upsilon}_2} - e^{\Upsilon_2}) \nabla w_p^j + \int_{\Omega_2} (v^{-1} e^{\Upsilon_2} (\Upsilon_2 - \tilde{\Upsilon}_2) \nabla(p - \tilde{p}) \cdot \nabla w_p^j) \\ &= - \int_{\Omega_2} \frac{1}{M} \frac{\partial(\tilde{p} - p)}{\partial t} \eta_p^j \\ &\quad - \int_{\Omega_2} b \frac{\partial \nabla \cdot (\tilde{\mathbf{u}} - \mathbf{u})}{\partial t} \eta_p^j - \int_{\Omega_2} \nabla(\tilde{p} - p) \cdot v^{-1} W(\tilde{\Upsilon}_2, \Upsilon_2) e^{\Upsilon_2} \nabla w_p^j \\ &\quad + \int_{\Omega_2} (v^{-1} e^{\Upsilon_2} (\Upsilon_2 - \tilde{\Upsilon}_2) \nabla(p - \tilde{p}) \cdot \nabla w_p^j). \end{aligned}$$

After integration by parts, the previous expression becomes

$$D_2^j = \int_{\Omega_2} \frac{1}{M} (\tilde{p} - p) \frac{\partial \eta_p^j}{\partial t} + \int_{\Omega_2} b \nabla \cdot (\tilde{\mathbf{u}} - \mathbf{u}) \frac{\partial \eta_p^j}{\partial t} + \int_{\Omega_2} (\tilde{p} - p) \nabla \cdot (v^{-1} W(\tilde{\Upsilon}_2, \Upsilon_2) e^{\Upsilon_2} \nabla w_p^j) - \int_{\Omega_2} (p - \tilde{p}) \nabla \cdot (v^{-1} e^{\Upsilon_2} (\Upsilon_2 - \tilde{\Upsilon}_2) \nabla w_p^j).$$

Note that we have used the fact that $\nabla w_p^j \cdot \mathbf{n} = 0$ which follows from the variational formulation (72)–(73). We now apply standard inequalities and use (152)–(153) to obtain

$$D_2^j \leq C \left(\|\tilde{p} - p\|_{L^2} \left\| \frac{\partial \eta_p^j}{\partial t} \right\|_{L^2} + \|\tilde{\mathbf{u}} - \mathbf{u}\|_{H^1} \left\| \frac{\partial \eta_p^j}{\partial t} \right\|_{L^2} + \|\Upsilon_2 - \tilde{\Upsilon}_2\|_{C^1} \|\tilde{p} - p\|_{L^2} \|e^{\Upsilon_2}\|_{C^1} \|w_p^j\|_{H^2} \right), \tag{181}$$

where C has the desired properties. From (175) it follows that

$$\int_0^T D_2^j \leq C \|\Upsilon - \tilde{\Upsilon}\|_{\mathcal{K}} (\|\tilde{p} - p\|_{L^2(L^2)} + \|\tilde{\mathbf{u}} - \mathbf{u}\|_{L^2(H^1)}) \times \left(\frac{1}{N\sigma_{\mathbf{u}}} \|\mathcal{M}_{\mathbf{u}}(\mathbf{r}_{\mathbf{u}})\|_{L^2(L^2(S))} + \frac{1}{\sigma_p} \|\delta(x - x^j)\|_{L^2} \|\mathcal{M}_p^j(r_p)\|_{L^2(0,T)} \right) \tag{182}$$

which from repeated applications of Cauchy inequality yields

$$\int_0^T D_2^j \leq \frac{1}{2N\sigma_{\mathbf{u}}} C^2 \|\Upsilon - \tilde{\Upsilon}\|_{\mathcal{K}}^2 (\|\tilde{p} - p\|_{L^2(L^2)}^2 + \|\tilde{\mathbf{u}} - \mathbf{u}\|_{L^2(H^1)}^2) + \frac{1}{2N\sigma_{\mathbf{u}}} \|\mathcal{M}_{\mathbf{u}}(\mathbf{r}_{\mathbf{u}})\|_{L^2(L^2(S))}^2 + \frac{1}{2\sigma_p} C^2 \|\Upsilon - \tilde{\Upsilon}\|_{\mathcal{K}}^2 (\|\tilde{p} - p\|_{L^2(L^2)}^2 + \|\tilde{\mathbf{u}} - \mathbf{u}\|_{L^2(H^1)}^2) \|\delta(x - x^j)\|_{L^2}^2 + \frac{1}{2\sigma_p} \|\mathcal{M}_p^j(r_p)\|_{L^2(0,T)}^2. \tag{183}$$

Therefore,

$$\sum_{j=1}^N \int_0^T D_2^j \leq \left[\frac{1}{2\sigma_{\mathbf{u}}} + \frac{1}{2\sigma_p} \sum_{j=1}^N \|\delta(x - x^j)\|_{L^2}^2 \right] \times C^2 \|\Upsilon - \tilde{\Upsilon}\|_{\mathcal{K}}^2 (\|\tilde{p} - p\|_{L^2(L^2)}^2 + \|\tilde{\mathbf{u}} - \mathbf{u}\|_{L^2(H^1)}^2) + \frac{1}{2\sigma_{\mathbf{u}}} \|\mathcal{M}_{\mathbf{u}}(\mathbf{r}_{\mathbf{u}})\|_{L^2(L^2(S))}^2 + \frac{1}{2\sigma_p} \|\mathcal{M}_p(r_p)\|_{L^2(0,T)}^2. \tag{184}$$

From similar arguments, we find an analogous estimate for D_1^j defined in (165). Therefore, from (162) it follows that

$$\sum_{j=1}^N \int_0^T (D_1^j + D_2^j) dt \leq \left[\frac{1}{2\sigma_{\mathbf{u}}} + \frac{1}{2\sigma_p} \sum_{j=1}^N \|\delta(x - x^j)\|_{L^2}^2 \right] \times C^2 \|\Upsilon - \tilde{\Upsilon}\|_{\mathcal{K}}^2 (\|\tilde{p} - p\|_{L^2(L^2)}^2 + \|\tilde{\mathbf{u}} - \mathbf{u}\|_{L^2(H^1)}^2) + \frac{1}{2} \|F(\tilde{\Upsilon}) - F(\Upsilon) - DF(\Upsilon)(\tilde{\Upsilon} - \Upsilon)\|_{\mathcal{O}}^2 \tag{185}$$

which combined with (168) yields

$$\|F(\tilde{\Upsilon}) - F(\Upsilon) - DF(\Upsilon)(\tilde{\Upsilon} - \Upsilon)\|_{\mathcal{O}}^2 \leq C^2 \|\Upsilon - \tilde{\Upsilon}\|_{\mathcal{K}}^2 (\|\tilde{p} - p\|_{L^2(L^2)}^2 + \|\tilde{\mathbf{u}} - \mathbf{u}\|_{L^2(H^1)}^2), \tag{186}$$

where C has the desired properties. Finally, we use (69)–(70) to arrive at

$$\begin{aligned} & \|F(\tilde{\Upsilon}) - F(\Upsilon) - DF(\Upsilon)(\tilde{\Upsilon} - \Upsilon)\|_{\mathcal{O}}^2 \\ & \leq C^2 \|\tilde{\Upsilon} - \Upsilon\|_{C^1(\bar{\Omega})}^2 \left(\int_0^T \int_S |\mathcal{M}_u(\tilde{\mathbf{u}} - \mathbf{u})|^2 + \int_0^T |\mathcal{M}_p(p - \tilde{p})|^2 dt \right) \\ & \leq C^2 \|\tilde{\Upsilon} - \Upsilon\|_{C^1(\bar{\Omega})}^2 \|F(\tilde{\Upsilon}) - F(\Upsilon)\|_{\mathcal{O}}^2 \end{aligned}$$

where C has the desired properties. □

5.5. Proof of lemma 3.1

Let $\hat{\Upsilon} \in \mathcal{K}$ and $r > 0$. Let $(\mathbf{A}_1, A_2) \in L^2(0, T; L^2(S)) \times L^2(0, T; L^2(\Omega_2))$ and $\Upsilon = (\Upsilon_1, \Upsilon_2) \in B(\hat{\Upsilon}, r)$. Consider the following problem: for a.e. $t \in (0, T]$ find $\mathbf{v}(\cdot, t) \in \mathbf{H}_0$ such that

$$\int_{\Omega} \left(e^{\Upsilon_1} (\nabla \cdot \mathbf{h}_1) (\nabla \cdot \bar{\mathbf{v}}) + 2\mu \epsilon(\mathbf{h}_1) : \epsilon(\bar{\mathbf{v}}) \right) = \int_S \mathbf{A}_1 \cdot \boldsymbol{\gamma}_S(\mathbf{h}_1), \tag{187}$$

for all $\mathbf{h}_1 \in \mathbf{H}_0$. From standard elasticity theory it is possible to prove that, for almost all $t \in (0, T]$, there exists a unique $\bar{\mathbf{v}}(\cdot, t) \in \mathbf{H}_0$ that satisfies (187). Then, from (187) with $\mathbf{h}_1 = \bar{\mathbf{v}}$ and (84), it follows that

$$\|\bar{\mathbf{v}}(\cdot, t)\|_{H^1(\Omega_1)^3}^2 \leq C \int_S \mathbf{A}_1(\cdot, t) \cdot \boldsymbol{\gamma}_S(\bar{\mathbf{v}}(\cdot, t)), \tag{188}$$

a.e. in $(0, T]$ where C may depend on μ and Ω_1 . From (19) we find

$$\|\bar{\mathbf{v}}(\cdot, t)\|_{H^1(\Omega_1)^3} \leq C \|\mathbf{A}_1(\cdot, t)\|_{L^2(S)}, \tag{189}$$

where C may depend on μ and Ω_1 . It is also possible to show that $t \rightarrow \bar{\mathbf{v}}(\cdot, t)$ is strongly measurable which from (189) yields $\bar{\mathbf{v}} \in L^2(0, T; \mathbf{H}_0)$ with

$$\|\bar{\mathbf{v}}\|_{L^2(0, T; H^1(\Omega_1)^3)} \leq C \|\mathbf{A}_1\|_{L^2(0, T; L^2(S))}, \tag{190}$$

where C may depend on μ and Ω_1 and T . We now consider the problem. Find $(\mathbf{z}, \rho) \in \mathcal{H}$ such that $(\mathbf{z}(\cdot, 0), \rho(\cdot, 0)) = (0, 0)$ and the following equations are satisfied

$$\int_{\Omega} [e^{\Upsilon_1} (\nabla \cdot \mathbf{h}_1) (\nabla \cdot \mathbf{z}) + 2\mu \epsilon(\mathbf{h}_1) : \epsilon(\mathbf{z})] + \int_{\Omega_2} b\rho \nabla \cdot \mathbf{h}_1 = 0, \tag{191}$$

$$\int_{\Omega_2} \left[b\nabla \cdot \frac{\partial \mathbf{z}}{\partial t} h_2 + \frac{1}{M} \frac{\partial \rho}{\partial t} h_2 + v^{-1} e^{\Upsilon_2} \nabla \rho \cdot \nabla h_2 \right] = \int_{\Omega_2} (A_2(\cdot, T - t) - b\nabla \cdot \bar{\mathbf{v}}(\cdot, T - t)) h_2, \tag{192}$$

a.e. in $[0, T]$ for all $(\mathbf{h}_1, h_2) \in \mathcal{W}$ and for. Existence and uniqueness of a solution to (191)–(192) in \mathcal{H} is established in proposition 2.1. Moreover, from that proposition we may choose $\tilde{C} > 0$ such that

$$\|(\mathbf{z}, \rho)\|_{\mathcal{H}} \leq \tilde{C} \|A_2 - b\nabla \cdot \bar{\mathbf{v}}\|_{L^2(0, T; L^2(\Omega_2))}, \tag{193}$$

uniformly in $B(\hat{\Upsilon}, r)$, where \tilde{C} is a constant that may depend on \mathcal{A} defined in (86). Let us define

$$(\mathbf{v}(\cdot, t), w_p(\cdot, t)) = \left(\frac{\partial \mathbf{z}}{\partial t}(\cdot, T - t), \rho(\cdot, T - t) \right), \tag{194}$$

and note that $(\mathbf{v}, w_p) \in L^2(0, T; \mathbf{H}_0) \times [H^{2,1}(\Omega_2 \times [0, T]) \cap L^\infty(0, T; H^1(\Omega_2))]$ satisfies

$$\int_{\Omega} [e^{\Upsilon_1} (\nabla \cdot \mathbf{h}_1) (\nabla \cdot \mathbf{v}) + 2\mu \epsilon(\mathbf{h}_1) : \epsilon(\mathbf{v})] - \int_{\Omega_2} b \frac{\partial w_p}{\partial t} \nabla \cdot \mathbf{h}_1 = 0, \tag{195}$$

$$\int_{\Omega_2} \left[b \nabla \cdot \mathbf{v} h_2 - \frac{1}{M} \frac{\partial w_p}{\partial t} h_2 + v^{-1} e^{\Upsilon_2} \nabla w_p \cdot \nabla h_2 \right] - \int_{\Omega_2} (A_2 - b \nabla \cdot \bar{\mathbf{v}}) h_2 = 0. \tag{196}$$

Then,

$$(\mathbf{w}_u, w_p) \equiv (\mathbf{v} + \bar{\mathbf{v}}, w_p) \in L^2(0, T; \mathbf{H}_0) \times H^{2,1}(\Omega_2 \times [0, T]) \cap L^\infty(0, T; H^1(\Omega_2)) \tag{197}$$

satisfies (72)–(73). From (190) and (193) it follows easily that

$$\max\{\|\mathbf{w}_u\|_{L^2(0,T;H^1(\Omega_1)^3)}, \|w\|_{H^{2,1}(\Omega_2 \times [0,T])}\} \leq C(\|\mathbf{A}_1\|_{L^2(L^2(S))} + \|A_2\|_{L^2(L^2)}), \tag{198}$$

where the constant C may depend only on \mathcal{A} . Uniqueness now follows from the energy estimate (198).

5.6. Proof of proposition 3.1

Let $\mathbf{d} = (\mathbf{d}_u, \mathbf{d}_p) \in \mathcal{O}$ and $\Upsilon \in \mathcal{K}$ be arbitrary but fixed. Let $\tilde{\Upsilon} \in \mathcal{K}$ be arbitrary. We have from (52) and (50) that

$$\langle \mathbf{d}, DF(\Upsilon) \tilde{\Upsilon} \rangle_{L^2(\Omega_T)} = \frac{1}{\sigma_p} \int_0^T \mathbf{d}_p^T \cdot \mathcal{M}_p(\tilde{p}) dt + \frac{1}{\sigma_u} \int_0^T \int_S \mathbf{d}_u \cdot \mathcal{M}_u(\tilde{\mathbf{u}}) d\sigma d, \tag{199}$$

where $\tilde{\mathbf{h}} = (\tilde{\mathbf{u}}, \tilde{p})$ is the solution to (53)–(54), i.e.

$$L(\Upsilon_1, \tilde{\mathbf{u}}, \mathbf{w}) - \int_{\Omega_2} b \tilde{p} \nabla \cdot \mathbf{w} + \int_{\Omega_1} \tilde{\Upsilon}_1 e^{\Upsilon_1} (\nabla \cdot \mathbf{u})(\nabla \cdot \mathbf{w}) = 0, \tag{200}$$

$$\int_{\Omega_2} \frac{1}{M} \frac{\partial \tilde{p}}{\partial t} w + \int_{\Omega_2} v^{-1} e^{\Upsilon_2} \nabla \tilde{p} \cdot \nabla w + \int_{\Omega_2} b \frac{\partial \nabla \cdot \tilde{\mathbf{u}}}{\partial t} w + \int_{\Omega_2} v^{-1} \tilde{\Upsilon}_2 e^{\Upsilon_2} \nabla p \cdot \nabla w = 0 \tag{201}$$

for all $(\mathbf{w}, w) \in \mathcal{W}$. From lemma 3.1, let (\mathbf{w}_u, w_p) be the solution to (72)–(73) for \mathbf{A}_1 and A_2 defined in (78). Then, we integrate (in $(0, T)$) expressions in (200)–(201) for $(\mathbf{w}, w) = (\mathbf{w}_u, w_p)$ whose regularity enables us to integrate by parts. Then, we add the resulting equation and find

$$\begin{aligned} & \int_0^T L(\Upsilon_1, \tilde{\mathbf{u}}, \mathbf{w}_u) - \int_0^T \int_{\Omega_2} b \frac{\partial w_p}{\partial t} \nabla \cdot \tilde{\mathbf{u}} \\ & + \int_0^T \int_{\Omega_2} \left[-b \nabla \cdot \mathbf{w}_u \tilde{p} - \frac{1}{M} \frac{\partial w_p}{\partial t} \tilde{p} + v^{-1} e^{\Upsilon_2} \nabla w_p \cdot \nabla \tilde{p} \right] \\ & + \int_{\Omega_2} \left[\left(\frac{1}{M} \tilde{p} + b \nabla \cdot \tilde{\mathbf{u}} \right) w_p \right]_{t=0}^T + \int_0^T \int_{\Omega_2} v^{-1} \tilde{\Upsilon}_2 e^{\Upsilon_2} \nabla p \cdot \nabla w_p \\ & + \int_0^T \int_{\Omega_1} \tilde{\Upsilon}_1 e^{\Upsilon_1} (\nabla \cdot \mathbf{u})(\nabla \cdot \mathbf{w}) = 0. \end{aligned} \tag{202}$$

On the other hand, for a.e. $t \in [0, T]$ we choose $(\mathbf{h}_1, h_2) = (\tilde{\mathbf{u}}(\cdot, t), \tilde{p}(\cdot, t))$ in (72)–(73) and the result is substituted in (202) to find

$$\begin{aligned} & \frac{1}{\sigma_p} \sum_{j=1}^N \int_0^T \int_{\Omega_2} \mathbf{d}_p^j(t) \tilde{p}(x, t) \delta(x - x^j) dx dt + \frac{1}{\sigma_u} \int_0^T \int_S \mathbf{d}_u \cdot \boldsymbol{\gamma}(\tilde{\mathbf{u}}) \\ & = - \int_0^T \int_{\Omega_2} v^{-1} \tilde{\Upsilon}_2 e^{-\Upsilon_2} \nabla p \cdot \nabla w - \int_0^T \int_{\Omega_1} \tilde{\Upsilon}_1 e^{\Upsilon_1} (\nabla \cdot \mathbf{u})(\nabla \cdot \mathbf{w}). \end{aligned} \tag{203}$$

Then, from (199) and (46)–(48)

$$\langle \mathbf{d}, DF(\Upsilon) \tilde{\Upsilon} \rangle_{L^2(\Omega_T)} = - \int_0^T \int_{\Omega_2} v^{-1} \tilde{\Upsilon}_2 e^{-\Upsilon_2} \nabla p \cdot \nabla w - \int_0^T \int_{\Omega_1} \tilde{\Upsilon}_1 e^{\Upsilon_1} (\nabla \cdot \mathbf{u})(\nabla \cdot \mathbf{w}).$$

From (29) and the definitions for f_1 and f_2 (76)–(77), the previous expression becomes

$$\begin{aligned} \langle \mathbf{d}, DF(\mathbf{Y})\tilde{\mathbf{Y}} \rangle_{L^2(\Omega_T)} &= \int_{\Omega_2} \int_{\Omega_2} f_2(x) C_2^{-1}(x, x') \tilde{\mathbf{Y}}_2(x') + \int_{\Omega_1} \int_{\Omega_1} f_1(x) C_1^{-1}(x, x') \tilde{\mathbf{Y}}_1(x') \\ &= \langle (\tilde{\mathbf{Y}}_1, \tilde{\mathbf{Y}}_2), (f_1, f_2) \rangle_{\mathcal{K}}. \end{aligned}$$

Since \mathbf{d} and $\tilde{\mathbf{Y}}$ were arbitrary, expression (75) follows.

Acknowledgments

Funding for this research was provided in part by the ENI Multi-scale Reservoir Science Project within the ENI-MIT Energy Initiative Founding Member Program. The authors thank Professor Bradford Hager and Professor Ruben Juanes for helpful discussions related to the applied aspects of coupling subsurface flow with geomechanics.

References

- [1] Adams R A 1975 *Sobolev Spaces* (New York, NY: Academic)
- [2] Albery J, Carstensen C, Funken S A and Klose R 2000 Matlab-implementation of the finite element method in elasticity *Computing* **69** 2002
- [3] Biot M A 1941 General theory of three-dimensional consolidation *J. Appl. Phys.* **12** (2) 155–64
- [4] Ciarlet P G 1988 *Mathematical Elasticity: Three-Dimensional Elasticity* vol 1 (Amsterdam: North-Holland)
- [5] Colton D and Kress R 1992 *Inverse Acoustic and Electromagnetic Scattering Theory* (Berlin: Springer)
- [6] Deutsch C V 2002 *Geostatistical Reservoir Modeling* (Oxford: Oxford University Press)
- [7] Engl H W, Kunisch K and Neubauer A 1989 Convergence rates for Tikhonov regularization of non-linear ill-posed problems *Inverse Problems* **5** 523
- [8] Evans L C 1998 *Partial Differential Equations* 1st edn (Providence, RI: American Mathematical Society)
- [9] Gambolati G, Ferronato M, Teatini P, Deidda R and Lecca G 2001 Finite element analysis of land subsidence above depleted reservoirs with pore pressure gradient and total stress formulations *Int. J. Numer. Anal. Methods Geomech.* **25** 307–27
- [10] Gambolati G and Freeze R A 1973 Mathematical simulation of the subsidence of Venice: 1. Theory *Water Resources Res.* **9** 721–33
- [11] Gambolati G, Gatto P and Freeze R A 1974 Mathematical simulation of the subsidence of Venice: 2. Results *Water Resources Res.* **10** 563–77
- [12] Geertsma J 1973 Land subsidence above compacting oil and gas reservoirs *J. Pet. Technol.* **25** 734–44
- [13] Girault V, Pencheva G, Wheeler M F and Wildey T 2011 Domain decomposition for poroelasticity and elasticity with DG jumps and mortars *Math. Models Methods Appl. Sci.* **21** 169–213
- [14] Gunzburger M D 2003 *Perspectives in Flow Control and Optimization* 1st edn (Philadelphia, PA: SIAM)
- [15] Hanke M 1997 Regularizing properties of a truncated Newton-CG algorithm for nonlinear inverse problems *Numer. Funct. Anal. Optim.* **18** 18–971
- [16] Hille E and Phillips R S 1957 *Functional Analysis and Semi-Groups* (American Mathematical Society Colloquium Publications vol 31) (Providence, RI: American Mathematical Society) (revised edition)
- [17] Iglesias M A and Dawson C 2009 An iterative representer-based scheme for data inversion in reservoir modeling *Inverse Problems* **25** 035006
- [18] Iglesias M A and McLaughlin D 2011 Level-set techniques for facies identification in reservoir modeling *Inverse Problems* **27** 035008
- [19] Kaltenbacher B, Neubauer A and Scherzer O 2008 *Iterative Regularization Methods for Nonlinear Ill-Posed Problems* 1st edn (Berlin: de Gruyter & Co)
- [20] Kim J, Tchelepi H A and Juanes R 2011 Stability and convergence of sequential methods for coupled flow and geomechanics: drained and undrained splits *Comput. Methods Appl. Mech. Eng.* **200** 2094–116
- [21] Kim J, Tchelepi H A and Juanes R 2011 Stability and convergence of sequential methods for coupled flow and geomechanics: fixed-stress and fixed-strain splits *Comput. Methods Appl. Mech. Eng.* **200** 1591–1606
- [22] Kufner A, John O and Fucik S 1977 *Function Spaces* (Leyden: Noordhoff International Publishing)
- [23] Lewis R W and Sukirman Y 1994 Finite element modelling for simulating the surface subsidence above a compacting hydrocarbon reservoir *Int. J. Numer. Anal. Methods Geomech.* **18** (9) 619–39
- [24] Lions J L and Magenes E 1972 *Non-Homogeneous Boundary Value Problems and Applications* vol I 1st edn (Berlin: Springer)

- [25] Minkoff S E, Stone C M, Arguello J G, Bryant S, Eaton J and Peszynska M Wheeler M 1999 Staggered in time coupling of reservoir flow simulation and geomechanical deformation: step 1, a one-way coupling *SPE Paper 51920:SPE Reservoir Simulation Symp.* pp 14–17
- [26] Oliver D S and Chen Y 2011 Recent progress on reservoir history matching: a review *Comput. Geosci.* **15** 185–221
- [27] Remy N, Boucher A and Wu J 2009 *Applied Geostatistics With SGeMS: A User's Guide* (Cambridge: Cambridge University Press)
- [28] Russell T F and Wheeler M F 1983 Finite element and finite difference methods for continuous flows in porous media *Mathematics of Reservoir Simulation* ed R E Ewing (Philadelphia, PA: SIAM)
- [29] Segall P 1985 Stress and subsidence resulting from subsurface fluid withdrawal in the epicentral region of the 1983 Coalinga earthquake *J. Geophys. Res.* **90** 6801–16
- [30] Showalter R E 1997 *Monotone Operators in Banach Space and Nonlinear Partial Differential Equations* (Providence, RI: American Mathematical Society)
- [31] Simon J 1987 Compact sets in the $L^p(0, t; b)$ *Ann. Mat. Pura Appl.* **146** 65–96
- [32] Tarantola A 1987 *Inverse Problems Theory: Methods for Data Fitting and Model Parameter Estimation* 1st edn (New York: Elsevier)
- [33] Teatini P *et al* 2011 Geomechanical response to seasonal gas storage in depleted reservoirs: a case study in the Po River basin, Italy *J. Geophys. Res.* **116** F02002
- [34] Vasco D W, Ferretti A and Novali F 2008 Estimating permeability from quasi-static deformation: temporal variations and arrival time inversion *Geophysics* **73** O37–52
- [35] Vasco D W, Ferretti A and Novali F 2008 Reservoir monitoring and characterization using satellite geodetic data: interferometric synthetic aperture radar observations from the Krechba field, Algeria *Geophysics* **73** WA113–22
- [36] Vasco D W, Karasaki K and Doughty C 2000 Using surface deformation to image reservoir dynamics *Geophysics* **65** 132–47
- [37] Vasco D W, Karasaki K and Kishida K 2001 A coupled inversion of pressure and surface displacement *Water Resources Res.* **37** 3071–89
- [38] von Terzaghi K 1943 *Theoretical Soil Mechanics* (New York: Wiley)
- [39] Xu Q 2005 Representation of inverse covariance by differential operators *Adv. Atmos. Sci.* **22** 181–98